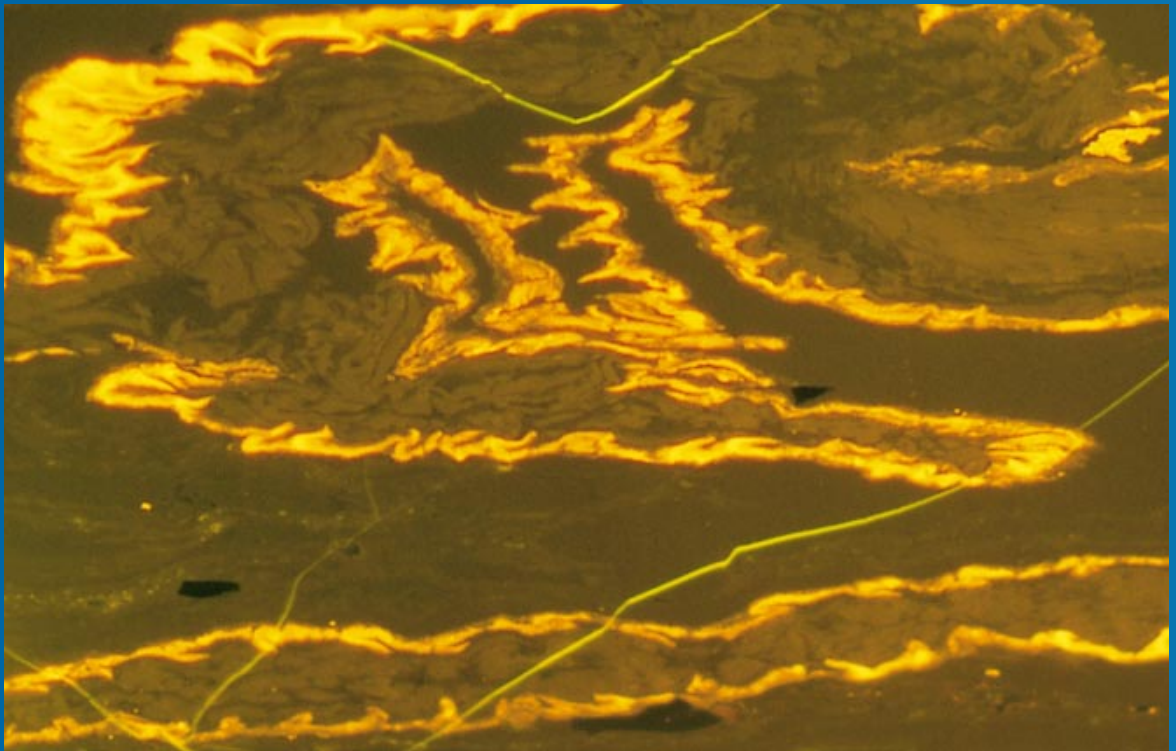


**Petroleum potential and depositional environments of Middle Jurassic coals and non-marine deposits, Danish Central Graben, with special reference to the Søgne Basin**

H. I. Petersen, J. Andsbjerg,  
J. A. Bojesen-Koefoed,  
H. P. Nytoft and P. Rosenberg



**Petroleum potential and depositional environments of Middle Jurassic coals and non-marine deposits, Danish Central Graben, with special reference to the Søgne Basin**

Henrik I. Petersen, Jan Andsbjerg,  
Jørgen A. Bojesen-Koefoed,  
Hans P. Nytoft and Per Rosenberg

## Geology of Denmark Survey Bulletin 36

### Keywords

Organic petrography and geochemistry, facies, non-marine deposits, mire environments, organic maturity, source rock, petroleum, coal, kerogen, Danish Central Graben, Søgne Basin, Middle Jurassic.

### Cover

Photomicrograph of yellowish-orange fluorescing folded cutinites derived from the outer layer of leaves (cuticle) in a groundmass of vitrinite. Sample 4473A, West Lulu-1 well, Middle Jurassic Bryne Formation, seam T3, 17.78–25.40 cm; reflected blue-light, water immersion. The section is c. 300 µm across.

*Henrik I. Petersen, Jan Andsbjerg, Jørgen A. Bojesen-Koefoed, Hans P. Nytoft and Per Rosenberg*

Geological Survey of Denmark and Greenland  
Thoravej 8, DK-2400 Copenhagen NV, Denmark

*Chief editor of this series:* Peter R. Dawes

*Scientific editor:* Svend Stouge

*Copy editor:* Peter R. Dawes

*Editorial secretary:* Esben W. Glendal

*Critical readers:* Walter Pickel (Germany) and Ger van Graas (Norway)

*Drawing work:* Stefan Sølberg

*Photographic work:* Jakob Lautrup and Benny Scharck

*Lay-out and graphic production:* Carsten E. Thuesen

*Printers:* From & Co. A/S, Copenhagen

*Manuscript submitted:* 2nd December, 1997

*Final version approved:* 25th May, 1998

*Printed:* 18th August, 1998

ISBN 87-7871-028-6

ISSN 1397-1891

## Geology of Denmark Survey Bulletin

The series *Geology of Denmark Survey Bulletin* is a continuation of *Danmarks Geologiske Undersøgelse Serie A* and incorporates *Danmarks Geologiske Undersøgelse Serie B*.

### Citation of the name of this series

It is recommended that the name of this series is cited in full, viz. *Geology of Denmark Survey Bulletin*

If abbreviation of this volume is necessary the following form is suggested: *Geology Denmark Surv. Bull.* 36, 78 pp.

### Available from:

Geological Survey of Denmark and Greenland  
Thoravej 8, DK-2400 Copenhagen NV, Denmark  
Phone: +45 38 14 20 00, fax: +45 38 14 20 50, e-mail: geus@geus.dk

or

Geografforlaget ApS  
Fruehøjvej 43, DK-5464 Brenderup, Denmark  
Phone: +45 64 44 26 83, fax: +45 64 44 16 97, e-mail: go@geografforlaget.dk

# Contents

Abstract . . . . .	5
Introduction . . . . .	7
Petroleum generation from coal and terrestrial kerogen . . . . .	8
Structural setting . . . . .	10
Middle Jurassic lithostratigraphy . . . . .	11
The Bryne Formation . . . . .	12
The Central Graben Group . . . . .	12
Biostratigraphic datings . . . . .	12
Samples, analytical methods and data processing . . . . .	13
Samples . . . . .	13
Organic petrographic analyses . . . . .	13
Vitrinite reflectance measurements . . . . .	14
Organic petrography . . . . .	14
Screening analyses . . . . .	15
Organic geochemical analyses . . . . .	15
Extraction . . . . .	15
Gas chromatography and gas chromatography/mass spectrometry . . . . .	15
Pyrolysis-gas chromatography . . . . .	15
Multivariate regression analysis . . . . .	16
The coals of the Bryne Formation in the Søgne Basin . . . . .	16
Sedimentological description and interpretation of the coal-bearing intervals . . . . .	16
West Lulu-3 well . . . . .	16
West Lulu-1 well . . . . .	18
Lulu-1 well . . . . .	19
Amalie-1 well . . . . .	19
Cleo-1 well . . . . .	23
Sequence stratigraphic framework and spatial coal seam distribution . . . . .	24
Organic petrographic and geochemical results . . . . .	29
Vitrinite reflectances . . . . .	29
Organic petrographic composition . . . . .	29
Screening data . . . . .	38
Extracts . . . . .	41
Gas chromatography . . . . .	43
Gas chromatography/mass spectrometry . . . . .	43
Pyrolysis-gas chromatography . . . . .	45
Results of the multivariate regression analysis . . . . .	46
Discussion . . . . .	48
Peat-forming mires and depositional development of the coal-bearing succession . . . . .	48
Influence of relative sea-level changes on coal composition . . . . .	52
Organic maturity . . . . .	52
Petroleum generative potential . . . . .	54
Middle Jurassic (Central Graben Group) strata outside the Søgne Basin . . . . .	58
Sedimentological description and interpretation of the measured core-intervals . . . . .	58
Alma-1x well . . . . .	58
Anne-3a well . . . . .	58
Elly-3 well . . . . .	58

Falk-1 well	58
M-8 well	60
Skjold Flank-1 well	60
Organic petrographic and geochemical results	65
Alma-1x well	65
Anne-3a well	66
Elly-3 well	66
Falk-1 well	68
M-8 well	69
Skjold Flank-1 well	69
Discussion	71
Organic maturity	71
Petroleum generative potential	71
Conclusions	72
The coal seams of the Bryne Formation in the Søgne Basin	72
Central Graben Group deposits	74
Acknowledgements	75
References	75

# Abstract

Petersen, H.I., Andsbjerg, J., Bojesen-Koefoed, J.A., Nytoft, H.P. & Rosenberg, P. 1998: Petroleum potential and depositional environments of Middle Jurassic coals and non-marine deposits, Danish Central Graben, with special reference to the Søgne Basin. *Geology of Denmark Survey Bulletin* 36, 78 pp.

New data from five wells in the Søgne Basin, Danish Central Graben of the North Sea – West Lulu-1, West Lulu-3, Lulu-1, Amalie-1 and Cleo-1 – together with previously released data from the West Lulu-2 well, show that the cumulative thickness of the Bryne Formation coal seams decreases towards the palaeo-shoreline from 5.05 m to 0.60 m, and that the seams have varying extents. Their overall organic petrographic and geochemical composition reflects the palaeoenvironmental conditions in the precursor mires, in particular the rate of rise in the watertable, principally related to the relative rise in sea level, and the degree of marine influence. Laterally towards the palaeo-shoreline, all coal seams have increased proportions of  $C_{27}$  steranes and higher  $C_{35}$ -homohopane indices suggesting stronger marine influence on the coastal reaches of the ancient mires. In each well it is also observed that coal seams formed during accelerated relative sea-level rise (T-seams) are characterised by higher contents of sterane  $C_{27}$  and higher  $C_{35}$ -homohopane indices than seams formed during slower rates of base-level rise (R-seams). The most landward and freshwater-influenced parts of the seams have higher proportions of sterane  $C_{29}$  and the highest Pr/Ph ratios.

The coals, with respect to thermal maturity, are well within the oil window, except in the Amalie-1 well where they are more mature. The largest average hydrogen indices and thermally extracted and generated bitumen yields are obtained from the T-seams. However, generally an increase in the hydrogen index is recorded in a seaward direction for all seams. Multivariate regression analysis demonstrates that collotelinite, telinite, the vitrinite maceral group, vitrinite-rich microlithotypes and the TOC content have a significant positive influence on the remaining generative potential represented by  $S_2$ . Pyrolysis-gas chromatography reveals that during maturation the coals will generate from 72.4 to 82.0% oil-like components and only 18.0 to 27.6% gas. However, this does not necessarily imply that all of these oil-like components can be expelled to form a crude oil accumulation. Distribution of  $C_{27-29}$  regular steranes shows good correlation between extracts of Bryne Formation coals and oils/condensates present in Bryne Formation sandstones.

The sum of evidence indicates that the coals in the Søgne Basin have generated and are still capable of generating liquid and gaseous petroleum, but with respect to petroleum generation potential, they are not as good as the documented oil-prone Middle Jurassic coals from North-East Greenland and Tertiary coals from Asia. Mudstones intercalated with the Bryne Formation coals have a similar or lower generative potential as the coals.

In areas outside the Søgne Basin, the coastal plain deposits of the Central Graben Group contain predominantly terrestrial-derived kerogen type III or IIb. The thermal maturity of the organic matter ranges from close to or within the peak oil generation range in the oil window (Alma-1x, Anne-3a and M-8 well) to the late oil window (Elly-3 and Falk-1 wells) or close to the end of the oil window (Skjold Flank-1 well). Only a limited generative potential remains in Elly-3, but the kerogen may initially have possessed a good petroleum potential. In the Falk-1 well, a good generative capacity still remains. The kerogen in Skjold Flank-1 may possess the capability to generate condensate and gas, whereas the organic matter in the Alma-1x, Anne-3a and M-8 wells generally exhibits a poor petroleum generative potential.

---

*Authors' address:*

Geological Survey of Denmark and Greenland, Thoravej 8, DK-2400 Copenhagen NV, Denmark.

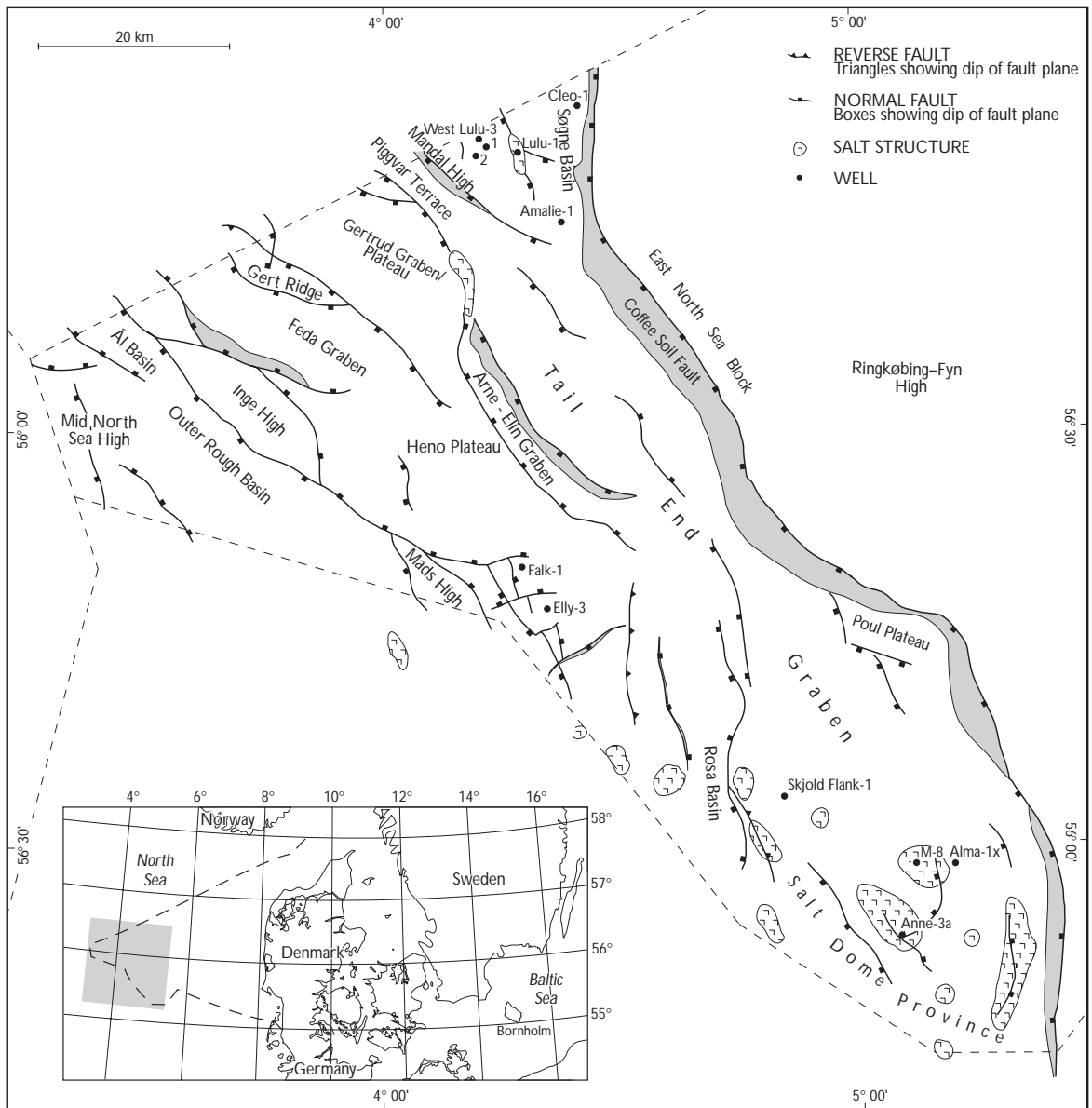


Fig. 1. Structural and location map of the Danish Central Graben showing the distribution of the wells investigated in this study and the West Lulu-2 well reported on by Pedersen & Andsbjerg (1996) and Petersen *et al.* (1996). The Harald Field is located in the north-western part of the Søgne Basin and includes the wells West Lulu-1, -2, -3 and Lulu-1. The dashed line on both main and inset maps outlines the Danish North Sea sector; for other national sectors of the North Sea, see Fig. 3. Modified from Andsbjerg (1997).

# Introduction

Hydrocarbons in the Danish Central Graben of the North Sea mainly have their source in the Upper Jurassic marine shales and are primarily produced from Upper Cretaceous – Paleogene chalk reservoirs, but exploration efforts are increasingly directed towards Middle Jurassic sandstone reservoirs (Damtoft *et al.* 1992). One of the Middle Jurassic target areas has been the Søgne Basin in the northern part of the Danish Central Graben where the commercial Harald Field consists of two gas accumulations and minor reserves of oil and condensate (Fig. 1). Oil tests from the field show typical terrestrial geochemical signatures very similar to extracts from the coals in the Middle Jurassic Bryne Formation (Petersen *et al.* 1995, 1996). This could imply that the gas also had a terrestrial source. In addition, a test from the Elly-2 well, close to the Elly-3 well on the Heno Plateau (Fig. 1), revealed typical terrestrial signatures (Geological Survey of Denmark and Greenland – GEUS, unpublished data). These observations and the increasing evidence for petroleum generation from coals and non-marine strata (see p. 8) make the search for terrestrial source rocks in the Danish Central Graben an intriguing question. Terrestrial Middle Jurassic strata, in particular the coal-bearing Bryne Formation, are obvious possibilities.

The general objective of this study is to provide organic petrographic and geochemical data on the petroleum generative potential of Middle Jurassic terrestrial deposits in the Danish Central Graben. Emphasis is placed on the coals in the Bryne Formation in the Søgne Basin since these constitute a highly interesting source rock candidate, strongly supported by the evidence for terrestrially sourced petroleum in the Harald Field and the evidence for petroleum potential of the time-equivalent Brent Formation coals in the Norwegian part of the North Sea (Bertrand 1989; for the national sectors,

see Fig. 3). A detailed interpretation of the depositional environments of the coal-bearing strata and the coal seams, including the areal extent and spatial distribution of the coals, are integrated into the present study. This is done in order to relate organic petrographic and geochemical variations in the coals to the precursor mire environments and to assess the influence of relative sea-level changes on coal composition, which may have direct impact on the petroleum generative potential. Outside the Søgne Basin, emphasis is likewise placed on non-marine Middle Jurassic strata dominated by terrestrially dominated kerogen.

To obtain a well-defined control on the depositional environment and the composition of the associated organic matter deposited in that environment, and accordingly the petroleum generative potential, sampling was preferentially confined to the Middle Jurassic well-cores. However, cuttings and sidewall cores from the Middle Jurassic interval have occasionally been included, in particular outside the Søgne Basin where limited coring of the Middle Jurassic interval may be a problem. From the wells M-8 and Anne-3a in the Salt Dome Province (Fig. 1) only cuttings have been investigated in this study.

The distribution of the investigated wells is shown on the main map in Figure 1. The Søgne Basin is represented by the West Lulu-1 and West Lulu-3 wells and the Lulu-1, Amalie-1 and Cleo-1 wells. Outside the Søgne Basin, the Heno Plateau is represented by the Falk-1 and Elly-3 wells, whereas the Salt Dome Province in the southern part of the Danish Central Graben is represented by the Skjold Flank-1, Alma-1x, M-8 and Anne-3a wells.

In addition, some data from the West Lulu-2 well taken from Petersen *et al.* (1996) are included in this presentation; this well is also shown in Figure 1.



# Petroleum generation from coal and terrestrial kerogen

The role of coal and terrestrial kerogen as a source for commercial petroleum other than gas has been extensively discussed over the last few decades. The dismissal of coal and terrestrial organic matter as a good source rock has mainly been related to the supposed incapability of coal to generate oil and, if generated, to expel the oil. However, the well-documented demonstration of crude oil derived from non-marine coal-bearing strata strongly suggests that coals and non-marine successions are capable of producing commercial amounts of liquid petroleum (Table 1). In addition, other investigations have revealed Middle Jurassic highly oil-prone coals in Hochstetter Forland, North-East Greenland (Bojesen-Koefoed *et al.* 1996), the petroleum potential of Middle Jurassic coals in the Danish Central Graben, North Sea (Petersen *et al.* 1996), Upper Cretaceous oil-generating coals of the San Juan Basin, USA (Clayton *et al.* 1991), while oil shows on Nuussuaq, West Greenland, have several terrestrial organic geochemical characteristics pointing to a non-marine source rock (Christiansen *et al.* 1996). Thus, any objection against the capability of coals and non-marine strata dominated by terrestrial organic matter should be reconsidered on the basis of the available evidence. In the following some of the more important objections against coal and terrestrial kerogen as an important contribu-

tor to significant oil generation will be discussed in detail.

The classical grouping of terrestrial organic matter into kerogen types I, II, III and IV is based on H/C and O/C ratios ('van Kevelen diagram'; van Krevelen 1961). The petroleum generation capability is related to the hydrogen content of the organic matter, and kerogen type I is initially hydrogen-rich ( $H/C > 1.5$ ) while type IV has the lowest H/C ratios ( $H/C < 0.6$ ). In the 'van Krevelen diagram' the kerogen types I-IV generally plot in the fields of lacustrine alginite, higher land plant liptinite/marine organic matter, humic organic matter and inertinite organic matter respectively. The entities of kerogen are thus similar to the macerals of coals (e.g. Mukhopadhyay *et al.* 1985; Hutton *et al.* 1994). Most kerogen and coals are heterogeneous and contain mixtures of the different types of organic matter and the bulk chemical analysis reflects the relative abundance of the constituents. Due to the typical dominance of humic organic material (vitrinite) in most coals these will commonly plot as kerogen type III ( $H/C = 0.6-0.9$ ), although the coals may contain significant proportions of oil-prone hydrogen-rich components like alginite, resinite, cutinite and per-hydrous vitrinite. A similar problem arises during chemical kerogen-typing, where a mixture of two quite different kerogen types may mimic a third type

Table 1. Areas with petroleum generated from terrestrial rocks

Country Area/Basin	Age of source rock	References
China Turpan Basin	Early-Middle Jurassic	Huang <i>et al.</i> 1991
Australia Surat/Bowen Basin	Permian-Jurassic	Khorasani 1987; Murchison 1987
Australia Eromanga Basin	Jurassic-Cretaceous	Thomas 1982; Murchison 1987
USA Greater Green River Basin	Late Cretaceous	García-González <i>et al.</i> 1997
Australia Gippsland Basin	Late Cretaceous-Tertiary	Shibaoka <i>et al.</i> 1978; Shanmugam 1985
New Zealand Taranaki Basin	Tertiary	Johnston <i>et al.</i> 1991
Canada Beaufort-Mackenzie Basin	Tertiary	Snowdon 1980; Snowdon & Powell 1982; Issler & Snowdon 1990
Indonesia Ardjuna sub-basin & Mahakam Delta	Tertiary	Durand & Oudin 1979; Noble <i>et al.</i> 1991
Nigeria Niger Delta	Tertiary	Bustin 1988

(Murchison 1987; Hutton *et al.* 1994). Thus, although kerogen and coal may be composed of similar complex mixtures of precursor material, common opinion has regarded humic coals in general as gas-prone kerogen type III. This consensus and the presumed ability of coal to absorb generated liquid petroleum due to the small pore diameters and large pore volumes within coal are often considered to be the critical factors which prevent migration out of a coal bed (e.g. Hunt 1991). This may imply that hydrocarbons are only released when increased thermal maturation lead to cracking of liquid petroleum to gas (Radke *et al.* 1980a).

Snowdon (1991) suggested that generated hydrocarbons (HC/g TOC) should exceed a saturation threshold value before expulsion occurs, and further stated that type III organic matter within the oil window generally contains less than the critical 30–50 mg HC/g TOC. Based on a two-phase migration theory, Huc *et al.* (1986) suggested the contrary that hydrocarbon migration is favoured in coals when compared to adjacent shales. For instance, the Talang Akar delta plain coals, offshore north-west Java, Indonesia, were shown to effectively expel crude oil (Noble *et al.* 1991). These coals contain mainly oil-prone macerals, of which *c.* 70% react to form hydrocarbons in the temperature range of oil stability. Also, Stout (1994) reported that the migration of petroleum in coals is strongly dependent on maceral associations (microlithotypes), and the transmission of lithostatic pressure to the liquid petroleum in the coal may increase the release of oil (Bertrand 1989). In particular the alternation between relatively incompress-

ible inertinite-rich microlithotypes and compressible microlithotypes may favour expulsion (Durand & Paratte 1983), and the natural fracture system of coals may be of importance for hydrocarbon flow (Close 1993). Most important is indication of a continuous evolution and destruction of the micropore system during organic matter maturation which eliminates the absorption capacity of the coal (Durand & Paratte 1983; Katz *et al.* 1991). For example, it is suggested from pyrolysis data from Middle Jurassic coals of North-East Greenland that part of the coals will be able to generate up to 50% liquid petroleum by weight during maturation (Bojesen-Koefoed *et al.* 1996), which will dramatically change the micropore system. Cook & Struckmeyer (1986) note that if coal seams absorb liquid petroleum, generated oil pool occurrences in coal-bearing strata should have a negative correlation with coal seam thickness; however, this does not appear to be the case. These authors further suggest that at low ranks ( $< 0.65 \%R_{max}$ ) migration of liquid petroleum out of coal is an efficient process. This is important in relation to the different maturity levels during which different macerals, due to a wide range of activation energies, are effective petroleum generators (Fig. 2; e.g. Boreham & Powell 1993). Early, incipient petroleum generation from vitrinitic substances has been suggested by Cook & Struckmeyer (1986) and Liu & Taylor (1991), and Khorasani (1987) observed petroleum generation from suberinite and terpene resinite in the reflectance range  $\%R_{max} = 0.34\text{--}0.45$  and  $\%R_{max} = 0.45\text{--}0.60$  of the associated vitrinite, respectively. Similar low maturity levels for petroleum generation

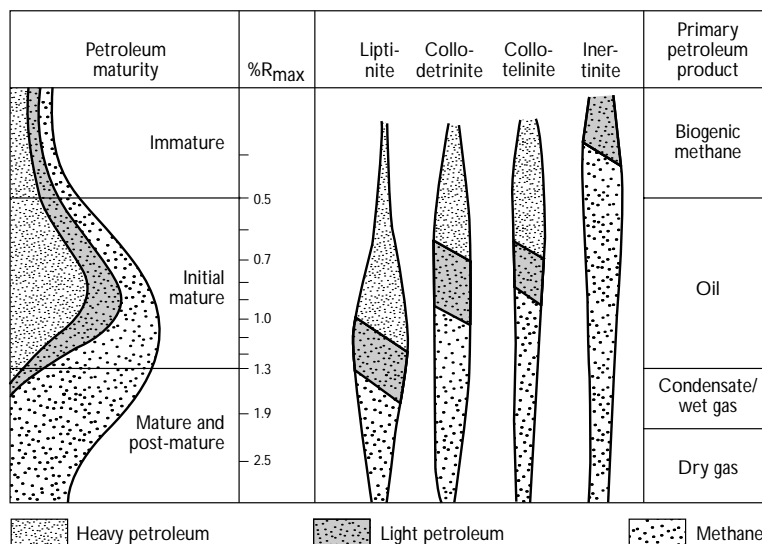


Fig. 2. The primary petroleum products derived from the liptinite and inertinite maceral groups and the macerals collodetrinite and collotelinite during maturation. Modified from Murchison (1987).

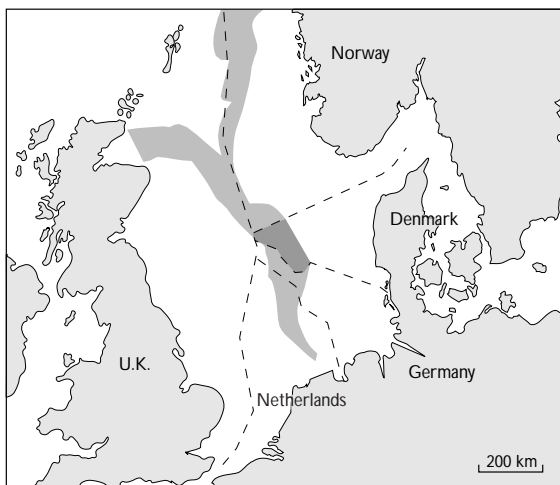
from resinite has been observed in the Beaufort–MacKenzie Basin (0.40–0.60 %R<sub>o</sub> vitrinite), Canada (Snowdon & Powell 1982) and in the Gippsland Basin (0.50 %R<sub>o</sub> vitrinite), Australia (Shanmugam 1985).

According to Hunt (1991) a potential coal source rock must exhibit Hydrogen Index (HI) values of 200 and H/C ratios greater than *c.* 0.9, and the coal should contain more than 15% liptinite. Both the HI and the H/C ratio are averages of a commonly heterogeneous maceral composition of the coal, and may mask the presence of a significant proportion of oil-prone components. This justifies detailed petrographic investigations of coals and kerogen. According to Bertrand (1989) the influence of the liptinite content on HI is only evident when it is over 10%, and the vitrinite macerals are regarded as an important source for petroleum. Likewise, a complex relationship between coal petrography and hydrocarbon generative potential, expressed as pyrolysis derived S<sub>1</sub>+S<sub>2</sub>, was found in a study on Middle Jurassic coals in the West Lulu-2 well in the Søgne Basin, Danish Central Graben (Petersen *et al.* 1996). The microlithotypes vitrite and clarite, the macerals telinite and collotelinite, the maceral group liptinite in general, and the TOC appeared to be favourable for high S<sub>1</sub>+S<sub>2</sub> contents. Fluorescent vitrinite suggests that this may be partly related to liptinitic material incorporated

into the vitrinite or the presence of per-hydrous vitrinite, i.e. the vitrinitic precursor material had an initial higher hydrogen content owing to deposition under anoxic conditions (e.g. Hunt 1991). A similar explanation was suggested by Bagge & Keeley (1994) in a study on the oil generating potential of Middle Jurassic coals in northern Egypt. They were not able to demonstrate a correlation between liptinite content and source rock potential, and suggested that hydrogen-rich vitrinites were partly responsible for the petroleum generative capacity. In a transmission electron microscope (TEM) study Liu & Taylor (1991) also concluded that type III kerogen associated with minor amounts of sub-microscopic lipid-rich material may provide an excellent source rock independent of whether organic material occurs as coal or as dispersed coaly matter in sedimentary rocks.

Obviously high contents of microscopic visible liptinite macerals favour the petroleum generative potential, but the importance of the vitrinitic components, particularly the nature of the vitrinite, and submicroscopic lipid-rich material should not be underestimated. The oil generative potential of coal and dispersed organic matter in non-marine sediments thus depends on the depositional environment and the composition of the parent vegetation (e.g. Collinson *et al.* 1994).

## Structural setting



The Danish Central Graben is part of the Central Graben (Fig. 3), a complex N–S trending Mesozoic intracratonic rift basin. It was initiated in the Triassic and was most active during the Middle and Late Jurassic (Møller 1986). The Central Graben separates the Mid North Sea High to the west from the East North Sea Block of the Ringkøbing–Fyn High to the east in the Danish Sector (Fig. 1). The development of the Danish Central Graben was determined by differential subsidence of grabens and basins along N–S and NW–SE trending faults.

Fig. 3. Map showing the location of the Central Graben in the North Sea with, in darker shading, the Danish part. For details and structural elements see Fig. 1. The dashed lines outline the national sectors of the North Sea.

Subsidence of the Danish Central Graben started in the north-eastern part of the area, where the Søgne Basin and Tail End Graben (Fig. 1) began to subside as separate half-grabens during the Middle Jurassic (Gowers & Sæbøe 1985; Møller 1986). Initiation of rift-associated subsidence was probably related to domal uplift and subsequent dome collapse in the North Sea area (Ziegler 1982, 1990; Underhill & Partington 1993). Most authors (e.g. Gowers & Sæbøe 1985; Møller 1986; Cartwright 1991; Korstgård *et al.* 1993) agree that asymmetric sub-

sidence was initiated in the Søgne Basin in connection with boundary fault activity during the Middle Jurassic. Middle Jurassic subsidence occurred mainly along N-S trending faults inherited from the pre-Jurassic, especially along segments of the Coffee Soil Fault (Fig. 1).

According to Mogensen *et al.* (1992) salt structures were generated in the Søgne Basin in the Triassic. Subsidence and faulting in Middle Jurassic times initiated the development of boundary fault salt pillows and up-dip salt structures in the southern Søgne Basin.

## Middle Jurassic lithostratigraphy

A formal lithostratigraphy for the Middle Jurassic of the North Sea was published by Jensen *et al.* (1986). All Middle Jurassic deposits of the Søgne Basin in the north-eastern part of the Danish Central Graben are referred to as the Bryne Formation, which has previously been

established in the Norwegian Central Graben by Vollset & Doré (1984). In the southern part of the Danish Central Graben, the Middle Jurassic deposits are referred to as the Central Graben Group of NAM & RGD (1980) (see Fig. 4).

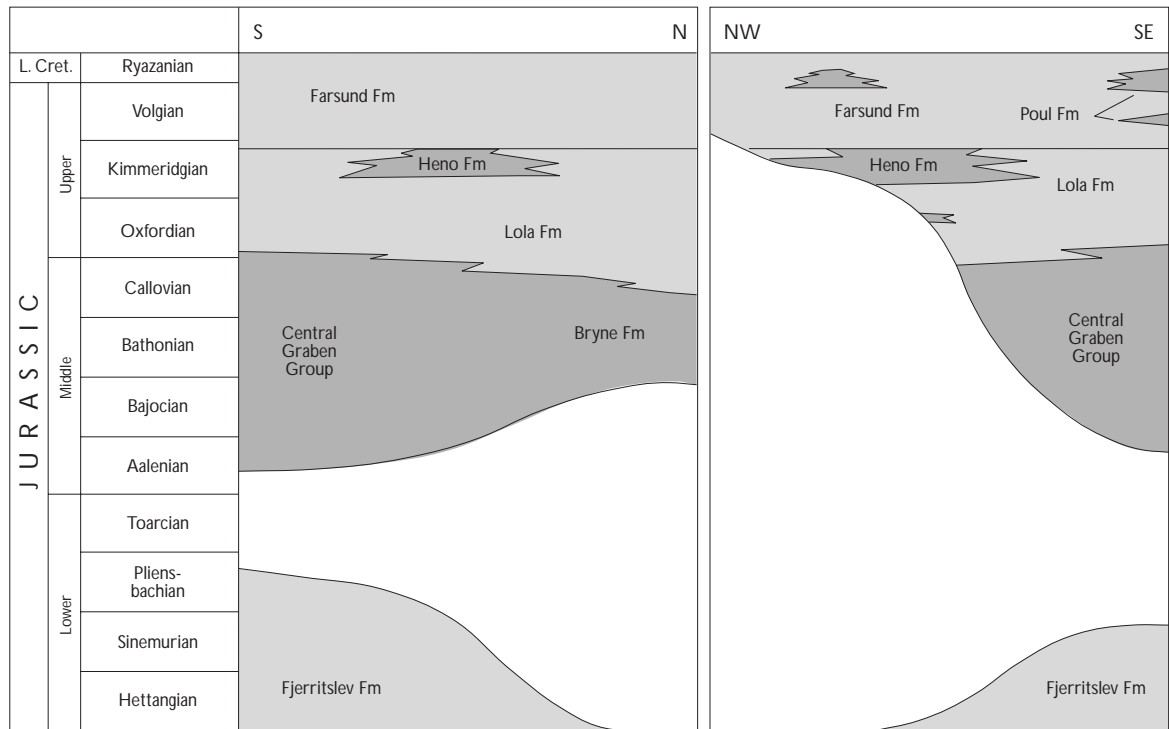


Fig. 4. The Jurassic lithostratigraphy of the Danish Central Graben showing the Middle Jurassic Central Graben Group and the Bryne Formation. From Andsbjerg (1997).

## The Bryne Formation

Middle Jurassic sandstones with interbedded mudstones and coals were encountered by the first exploration well, Lulu-1, in the Danish part of the Søgne Basin (Fig. 1). Similar deposits encountered in the Norwegian part of the Central Graben were included in the Bryne Formation, and Jensen *et al.* (1986) extended the Bryne Formation to include the Middle Jurassic deposits of the northern part of the Danish Central Graben (Fig. 4).

In the Søgne Basin the Bryne Formation is separated from Triassic and Permian deposits by a major unconformity. The Bryne Formation is conformably overlain by marine mudstones of the Upper Jurassic Lola Formation (Jensen *et al.* 1986) and unconformably by Cretaceous deposits on structural highs. The Bryne Formation shows thicknesses from 130 to 300 metres in wells in the Danish part of the Søgne Basin. It wedges out on structural highs, but may possibly attain larger thicknesses in the deepest parts of the basin.

A detailed sedimentological analysis of cores from the Lulu-1 well was published by Frandsen (1986) who interpreted the sediments as deposits of a deltaic inter-distributary bay overlain by coastal sediments. Middle Jurassic deposits further south in the Danish Central Graben had previously been interpreted as alluvial plain

and delta plain deposits by Koch (1983). Damtoft *et al.* (1992) suggested a fluvial channel and floodplain environment for the Bryne Formation, whereas Johannessen & Andsbjerg (1993) interpreted the sediments as alluvial plain deposits overlain by tidal and shallow marine deposits.

## The Central Graben Group

The Central Graben Group was named by NAM & RGD (1980) with the Dutch Central Graben as the type area, and was extended to include the Salt Dome Province in the southern part of the Danish Central Graben by Jensen *et al.* (1986). In the Danish part of the Central Graben the Central Graben Group consists of the sand prone Lower Graben Sand Formation overlain by the mudstone dominated Middle Graben Shale Formation (Jensen *et al.* 1986; Fig. 4). The maximum drilled thickness of the Central Graben Group is 237 m (O-1 well), but more commonly the thickness ranges between 50 and 150 m.

The deposits of the Central Graben Group have been interpreted as alluvial plain sediments overlain by deposits of a delta plain dominated by swamps and inter-distributary bays (Koch 1983; Jensen *et al.* 1986).

## Biostratigraphic datings

The Middle Jurassic of the central and southern North Sea generally has a poor biostratigraphy. This is due to the predominance of non-marine facies, and to the large depth at which Middle Jurassic deposits are encountered in the Central Graben.

A major sequence boundary separates the Bryne Formation into a fluvial dominated lower part and an upper part composed of predominantly paralic and marginal marine deposits (Andsbjerg & Dybkjær 1997). In the uppermost part of the fluvial dominated succession the presence of the dinocyst *Adnatosphaeridium caulleryi* suggests an age not older than Bathonian. This evidence, in combination with Late Bathonian ages above the sequence boundary, indicate that sequence boundary incision took place during the Bathonian, probably during the later part of the Bathonian. The

occurrence of *Scrinocassis* sp. in the lowermost part of the Bryne Formation indicates an age not younger than the Late Bajocian for that interval.

The upper part of the Bryne Formation is reasonably well dated in a few wells due to dinoflagellate cysts found in marine and estuarine deposits (Andsbjerg & Dybkjær 1997). Above the major sequence boundary the Bryne Formation seems to be of Late Bathonian to Late Callovian age. The occurrence of the dinoflagellate cysts *Cleistosphaeridium varispinosum* and *Nannoceratopsis gracilis* in incised valley-fill deposits right above the sequence boundary suggests that the valley fill ranges from Late Bathonian to earliest Callovian. The presence of *Dissilodinium willei* in the succession above the incised valley-fill deposits suggests a Middle Callovian age for that interval, and the occurrence of

*Ctenidodinium continuum*, *Liesbergia scarburghensis* and *Meiourogonyaulax* cf. *M. caytonensis* near the top of the Bryne Formation indicates a latest Callovian to earliest Oxfordian age.

In the southern part of the Danish Central Graben wells with deposits of the Central Graben Group are not as closely spaced as the wells with Bryne Formation sediments, and the Central Graben Group deposits exhibit fewer biostratigraphic datings. As is the case for the Bryne Formation, the lower part of the Central Graben Group succession yields poor biostratigraphic datings. A few good datings are supplied by age diagnostic spores. *Krauselisporites hyalina* in the upper part of the Lower Graben Sand Formation suggests a Bathonian age, and *Kekryphalospora distincta* lower in that formation indicates an age not younger than Early

Bajocian. A few dinoflagellate cysts have been found in the Lower Graben Sand Formation. In the upper part of the formation the Late Bajocian – Early Callovian *Pareodynia evitii* has been found below an erosive channel base, which may correlate to the major sequence boundary separating the upper and lower parts of the Bryne Formation.

In the uppermost part of the succession, in the coal-bearing Middle Graben Shale Formation, *Chytroisphaeridia hyalina* and *Ctenidodinium sellwoodii* indicate ages not younger than Mid and Late Callovian respectively; however, the presence of *Energlynia acollaris* and *Wanaea thyssanota* may indicate an age up to Early Oxfordian. *Pareodinia prolongata* and *Rigaudella aemula*, which may range up to the Middle Oxfordian, are also found within this succession.

## Samples, analytical methods and data processing

### Samples

The material in this study is mainly taken from drill-cores as this procedure enables a precise correlation between sample lithology, depositional environment and organic petrography and geochemistry of the sample. If considered necessary, other sample types (sidewall cores, cuttings, extracted cuttings) were included. All core samples are indicated on the sedimentological logs presented in this bulletin.

The coal seams in the well-cores in the Søgne Basin were sampled from floor to roof (channel samples) such that, if possible, the samples represent the total thickness of the seams and also cover macroscopically visible changes in coal layering (coal facies change). A few samples were likewise collected from coaly mudstones associated with the coal seams. In the Søgne Basin a total of 110 core samples were collected, viz. 44 from West Lulu-1, 29 from West Lulu-3, 18 from Lulu-1, 13 from Amalie-1 and 6 from Cleo-1. The 6 core samples from the Cleo-1 well were supplemented with 13 sidewall core samples, 18 cuttings and 5 extracted cuttings from the Middle Jurassic interval.

Outside the Søgne Basin samples were likewise preferentially taken from drill-cores. However, due to lim-

ited coring in the Middle Jurassic interval, cuttings were also used. Core samples were collected from levels in the cores with visible disseminated organic matter or from black mudstones presumed to be rich in organic material. A total of 105 samples have been investigated, viz. 10 core samples and 20 cuttings from Alma-1x, 11 cuttings from Anne-3a, 10 core samples from Elly-3, 12 core samples and 5 cuttings from Falk-1, 12 cuttings from M-8, and 10 core samples, 13 cuttings and 2 extracted cuttings from the Skjold Flank-1 well (Fig. 1).

### Organic petrographic analyses

Particulate pellets suitable for optical analyses were prepared by crushing the samples to a grain size between 63 µm and 1 mm. Approximately 20 ml of a dried (24 hrs at 60°C) homogenised sample split was embedded in epoxy. Following hardening the sample was cut vertically into two pieces and the 'new' face was ground and polished using 1/4 µm diamond powder for the final polish to obtain a smooth surface. The preparation procedure thus takes into account the grain size and density induced separation during embedding in epoxy resin.

Table 2. Macerals and minerals identified in the coal seams

Maceral group	Macerals
Vitrinite	Telinite Collotelinite Collodetrinite Gelinite Corpogelinite
Liptinite	Sporinite Cutinite Liptodetrinite Resinite Exsudatinite
Inertinite	Fusinite Semifusinite Inertodetrinite Macrinite (Char)* (Pyrolytic carbon)*
Mineral matter	Pyrite Other minerals

\* detected but not counted

### Vitrinite reflectance measurements

The organic maturity (rank) of the organic matter was petrographically determined by random reflectance

measurements on the vitrinite maceral collotelinite. The equipment used was a Leitz MPV-SP system, which was calibrated against a standard of 0.893 %R<sub>o</sub>. A total of 100 measurements per sample conducted in monochromatic light and oil immersion was the optimum; however, commonly this was not possible. The reflectance measurement procedure is in accordance with the standards outlined by Stach *et al.* (1982). A total of 25 samples have been measured.

### Organic petrography

*Maceral and kerogen analyses.* Each sample was analysed in reflected white light and fluorescence-inducing blue light in oil immersion using a Zeiss incident light microscope and a Swift point counter. A total of 500 points (macerals, minerals) were counted in each sample. In the coal samples 14 different macerals plus pyrite and 'other minerals' were recorded (Table 2). The presence of char and pyrolytic carbon was qualitatively noted. Hard coal maceral identification follows the standards in Stach *et al.* (1982) and ICCP (1998). Maceral analyses of the coals were carried out contemporaneously with the microlithotype analysis (see below), and a total of 57 samples were investigated.

Table 3. Kerogen classification

Kerogen type	Maceral composition		Fluorescence properties	Range of Hydrogen Index (mg HC/g C <sub>org</sub> )	H/C atomic ratio	Peak generation (%R <sub>o</sub> )	Generated hydrocarbons
	Major	Minor					
1	Alginite Algodetrinite Sapropelinite 1	Bacterial remnants Sapropelinite 11	Greenish yellow for alginite	> 700	> 1.5	0.6–0.9	Mainly oil
11a	Sapropelinite 11 Liptodetrinite Resinite (A+B)	Particulate liptinite (A+B) Alginite Corpogelinite	Orange to orange brown for sapropelinite 11 Yellow for resinite (A+B)	400–700	1.1–1.5	0.6–0.9 0.3–0.7 (for resinite)	Mainly oil; major gas in higher maturation (> 1.3%R <sub>o</sub> )
11b	Particulate liptinite (mainly B) Liptodetrinite	Alginite Sapropelinite 11 Collodetrinite Humosapropelinite	Yellow for sporinite, cutinite etc.	150–400	0.8–1.3	0.7–1.1	Oil and gas
111	Vitrinite (Collotelinite, Humosapropelinite)	Resinite Inertinite Sporinite	Dark brown for resinite	25–150	0.5–0.8	0.8–1.0 (oil) 1.0–1.5 (gas)	Mainly gas
1V	Inertinite	Vitrinite		< 25	0.5	No source of hydrocarbons	Minor gas (no source for liquid hydrocarbons)

From Mukhopadhyay *et al.* 1985

The kerogen analyses were likewise carried out by means of point-counting. The coal maceral group terminology was used to type the organic material (e.g. Hutton *et al.* 1994), and the following entities were recorded: liptinitic terrestrial organic matter (OM) and terrestrial OM, the latter divided if possible into vitrinitic OM and inertinitic OM. Intimately associated organic and mineral matter were counted as organomineral matrix. Pyrite and mineral matrix were also recorded.

Kerogen classification was based on the scheme developed by Mukhopadhyay *et al.* (1985), where each kerogen type among other things is characterised by a specific maceral composition and hydrogen index range (Table 3). A total of 12 kerogen analyses were carried out.

*Microolithotype analyses.* The same equipment described above was used for the microolithotype analysis. The analysis was only performed on the coal samples, and 500 microolithotypes were recorded in each sample. Analysis procedure and microolithotype identification follow the standards described in Stach *et al.* (1982) (Table 4), and 57 samples were investigated.

## Screening analyses

A portion of all 215 samples were crushed to a grain size < 250 µm for total organic carbon (TOC) determination and Rock-Eval pyrolysis. A LECO IR-212 induction furnace was used to estimate the TOC (wt%). The samples for TOC determination were treated with HCl at 60°C to remove carbonate-bonded carbon before combustion. An untreated sample (about 10 mg) was used for Rock-Eval pyrolysis on a Delsi Rock-Eval II or Vinci Rock-Eval 5 equipment. In addition, 15 extracted coal samples from the Søgne Basin were analysed by Rock-Eval pyrolysis.

## Organic geochemical analyses

### Extraction

Solvent extracts were prepared by means of a Soxhlet instrument using CH<sub>2</sub>Cl<sub>2</sub>/CH<sub>3</sub>OH (93 vol./7 vol.) as solvent. Asphaltenes were precipitated by addition of 40-fold *n*-pentane. The maltene fractions were separated into saturated, aromatic and heteroatomic compounds by medium performance liquid chromatography (MPLC)

Table 4. Microolithotype classification

Microolithotype	Maceral Group Composition
Vitrinite	vitrinite > 95%
Liptite	liptinite > 95%
Inertite	inertinite > 95%
Clarite	vitrinite+liptinite > 95%
Vitrinertite	vitrinite+inertinite > 95%
Durite	inertinite+liptinite > 95%
Trimacerite	vitrinite, inertinite, liptinite > 5%
Duroclarite	vitrinite > inertinite, liptinite
Clarodurite	inertinite > vitrinite, liptinite
Vitrinertoliptite	liptinite > vitrinite, inertinite

using a method modified from Radke *et al.* (1980b). A total of 64 samples were extracted.

### Gas chromatography and gas chromatography/mass spectrometry

Saturate fractions of 64 extracts were analysed by splitless injection gas chromatography (GC) on a Hewlett Packard 5890 gas chromatograph fitted with a 25 m HP-1 WCOT column and FID. In addition the saturate fractions were analysed by coupled gas chromatography/mass spectrometry (GC/MS) using splitless injection and a Hewlett Packard 5890 series II gas chromatograph equipped with a 25 m HP-5 WCOT column and coupled to a Hewlett Packard 5971A quadrupole mass spectrometer. The components emerging from the GC were scanned for preselected fragment ions (Selected Ion Monitoring, SIM), and special attention was paid to the *m/z* 191 fragment ion of hopanes and the *m/z* 217 and *m/z* 218 fragment ions of steranes.

### Pyrolysis-gas chromatography

Temperature programmed pyrolysis-gas chromatography (Py-GC) was carried out on 15 solvent-extracted samples using a custom-made stainless steel pyrolysis unit coupled to a Hewlett-Packard 5890A gas chromatograph, furnished with a 50 m Chrompack CP-Sil-8CB WCOT column and FID, using direct on-column injection. The pyrolysis unit and the column were joined by 1 m precolumn, which was used for cold trapping of pyrolysis products in liquid nitrogen prior to chro-



matography. The pyrolysis temperature program (300–550°C at 20°C/min followed by 2.5 minutes at 550°C) was controlled by a custom made unit. The GC temperature program was: initial time 27 minutes at 30°C, ramp from 30–300°C at 4.5°C/min, hold at 300°C for 20 minutes.

Data analysis was carried out using HP-chemstation software. Determination of the proportions of gas-range ( $C_{1-5}$ ) and oil-range ( $C_{6+}$ ) components was carried out by construction of a horizontal baseline on blank-subtracted pyrograms at the zero-level before elution of the  $C_1$  peak, and splitting the integrated chromatogram into a  $C_{1-5}$  (gas) and a  $C_{6+}$  (oil) fraction (Pepper & Corvi 1995).

### Multivariate regression analysis

Multivariate regression analysis was used to evaluate the data obtained from the petrographic and screening analyses (Rock-Eval, LECO) carried out on 54 samples from the coal seams in the Søgne Basin. Data from the previously investigated West Lulu-2 well (Petersen *et al.* 1996) were included ending up with a total of 94 samples. The variables (macerals, maceral groups, microlithotypes, TOC values) used in the multivariate calibration were the normalised data from the maceral group, maceral and microlithotype analyses together with the TOC and  $T_{max}$  values. The target parameter to which correlation was performed was the  $S_2$  value. In a study by

Petersen *et al.* (1996) the hydrocarbon generative potential represented by  $S_1+S_2$  was used as target parameter. However, as  $S_1$  may vary in a way that is not entirely related to the composition of the organic material, but probably also due to primary migration, it was decided in this study only to correlate to  $S_2$ , which is taken to represent the remaining hydrocarbon generative potential. The scope of the correlation is to obtain information on the relation between the remaining generative potential and the composition of the organic matter, and thus to identify the petrographic constituents which are likely to be responsible for petroleum generation in the coal seams.

The correlation was performed with the PC software Sirius (Kvalheim & Karstang 1987) using partial least squares (PLS) regression analyses (Martens & Næs 1991). The latent variables were verified by cross validation proposed by Wold (1978), and the group memberships were calculated using the so-called 'Soft Independent Modeling of Class Analogies' (SIMCA) algorithms (Wold 1976; Kvalheim & Karstang 1992). Prior to modeling the variables were scaled to unit variances in order to avoid dominance from variables high in variance over variables low in variance but yet with significant influence on the target parameter. By doing this all variables are equally weighted with respect to variance prior to the estimation of their importance on the model, however, care must be taken not to model 'noise' from variables with very low values.

## The coals of the Bryne Formation in the Søgne Basin

### Sedimentological description and interpretation of the coal-bearing intervals

#### *West Lulu-3 well*

Below the carbonaceous succession there are fining upward, very fine-grained to fine-grained sandstones with small-scale trough cross-lamination and ripple cross-lamination (Figs 5, 6). Bioturbation may be present in the uppermost part of the interval. The sandstones are interpreted as fluvial channel deposits (Johannessen & Andsbjerg 1993).

The sandstones are overlain by a succession c. 8 m thick that is dominated by carbonaceous shales and characterised by thin coal layers or laminae, coaly debris, rootlets with occasionally coalified leaves and twigs, as well as three coal seams, named from below, seams R1, R1a and T2. Rootlets are also abundant in thin silty intercalations and in flaser-bedded heterolithic siltstone, which shows bioturbation. Seam R1 is c. 0.56 m thick and it appears as bright and banded coal with pyrite filling vertical cleats. The seam is gradually followed by black, carbonaceous shale. Seam R1a is only c. 0.30 m thick. Coal seam T2 is c. 0.71 m thick and contains vertical pyrite veinlets.

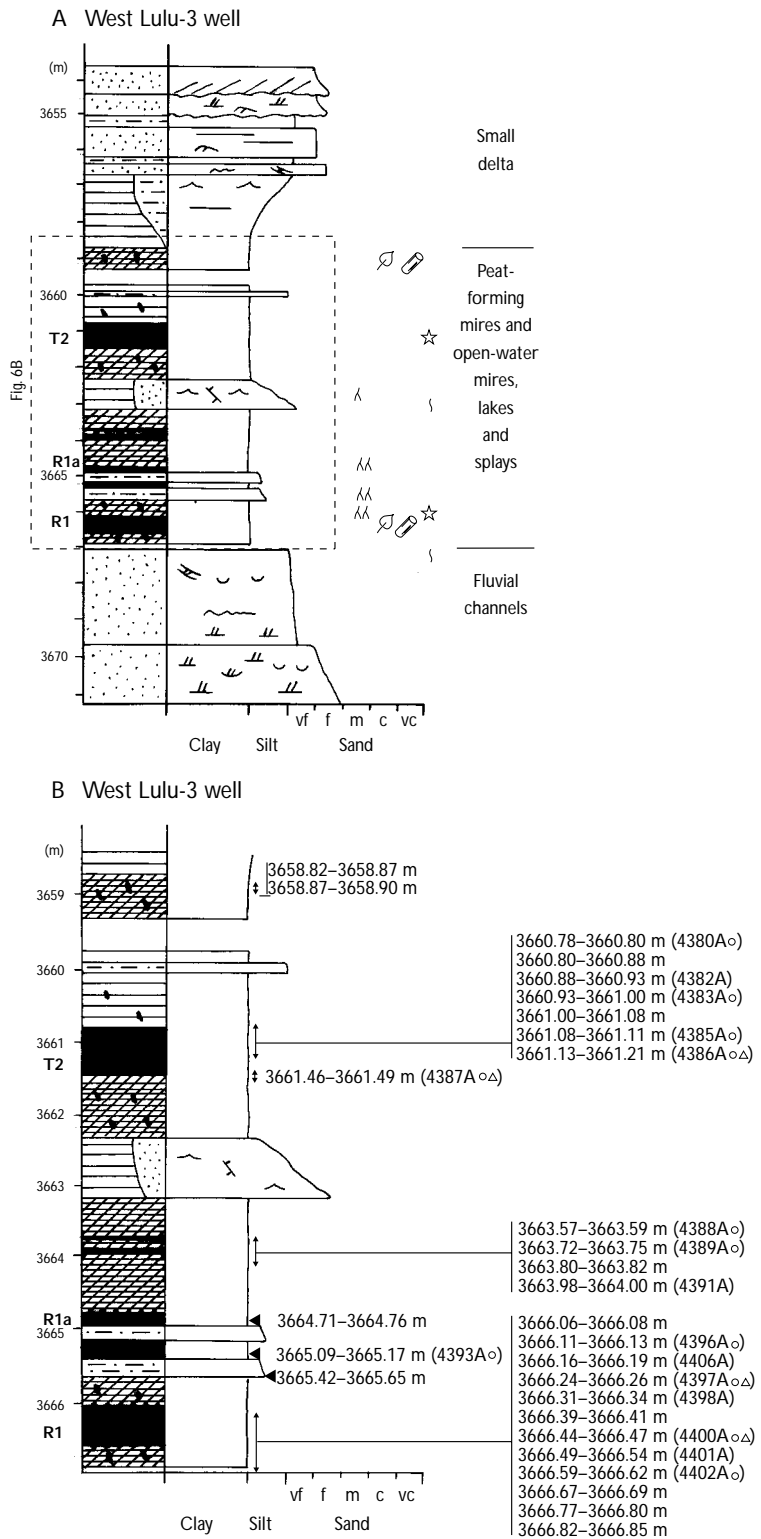
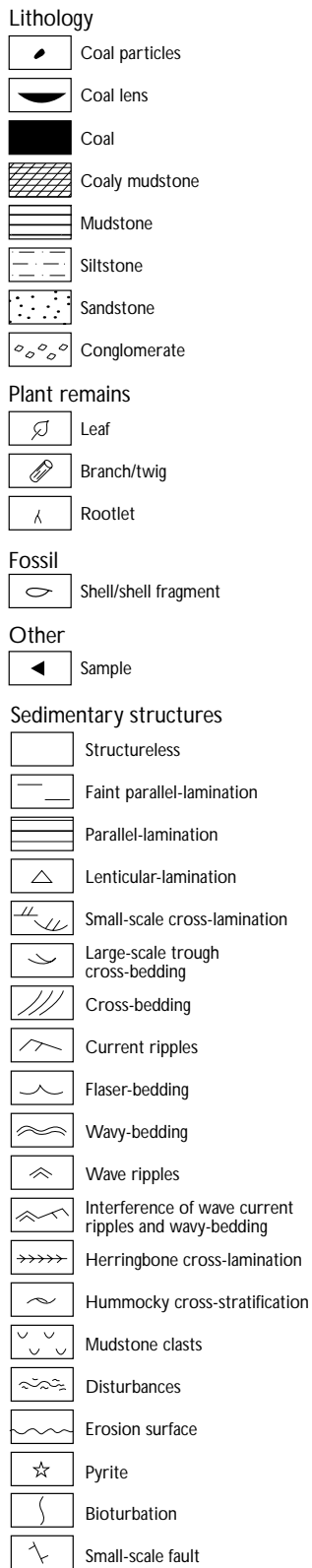


Fig. 5. Explanation of symbols used in the measured well-sections.

Fig. 6. **A:** The coal-bearing section of the West Lulu-3 well showing the position of seams R1, R1a and T2, and the interpreted depositional environments. **B:** Enlargement of the coal-bearing unit with indication of the sampled intervals. Sample numbers of petrographically analysed samples shown; o: sample analysed by GC and GC/MS; Δ: sample analysed by Py-GC. For well location, see Fig. 1.

The carbonaceous succession is followed by a coarsening upward succession of heterolithic clay- and siltstone, and sandstone showing mainly faintly parallel-lamination, current ripples and ripple cross-lamination. The sediments were deposited in a lagoon or bay-head delta (Andsbjerg 1997).

### West Lulu-1 well

Lowermost in the investigated interval are well-sorted, fine-grained, grey, sandstone beds showing trough

cross-bedding, current- and wave-ripple cross-lamination, occasionally hummocky cross-stratification, and bioturbation structures (Fig. 7). The sediments are interpreted to have been deposited in a wave-influenced minor mouth bar.

The sandstone beds are overlain by a complex succession of carbonaceous mudstones and three coal seams, named from below, R1, R1a and T2. Seam R1 is c. 0.89 m thick. It starts with mainly bright-dull, banded coal but becomes more bright towards a c. 0.11 m thick vitrinite-rich, clayey coal layer in the upper part of the seam (Table 5). Seam R1 ends with bright and dull coal.

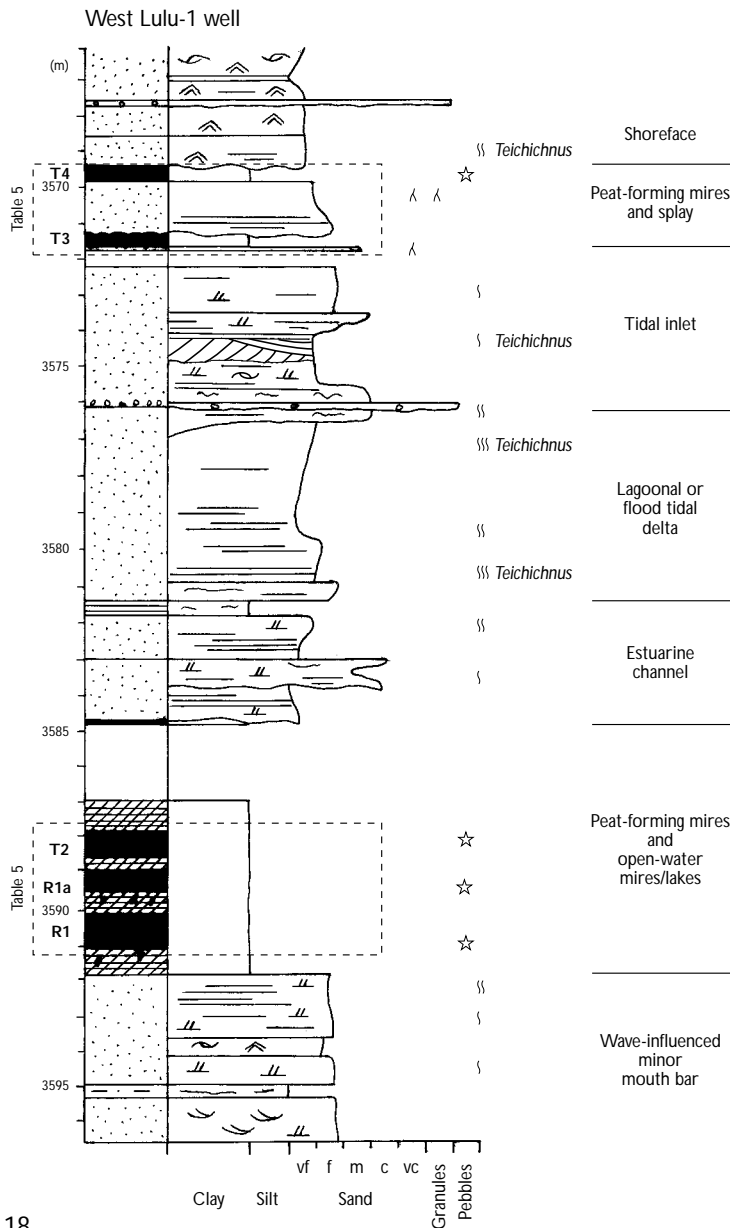


Fig. 7. The coal-bearing section of the West Lulu-1 well showing the position of seams R1, R1a, T2, T3 and T4, and the interpreted depositional environments. See Fig. 5 for legend, Table 5 for detailed description of the sampled intervals, and Fig. 1 for well location.

Small pyrite crystals and horizontal and nearly vertical pyrite veinlets are observed throughout the seam. Clayey coal and black, hard carbonaceous mudstone with vitrinite laminae or lenses and fusinite particles overlie seam R1. The following approximately 0.58 m thick seam R1a shows a trend from bright coal in the lower part to banded coal and clayey coal with vitrinite laminae in the upper part (Table 5). Pyrite has been observed as vertical laminae. Carbonaceous mudstone with vitrinite lenses and an increasing content of clay overlies seam R1a. The c. 0.66 m thick seam T2 consists in the basal part of mainly dull coal, where pyrite may be present (Table 5). The middle part is brighter and contains pyrite, while the upper part is composed of hard, dull coal, probably with pyrite.

A 13 m thick succession of poorly sorted, mainly fine-grained sandstone with coarser-grained intervals overlies the organic-rich complex (Fig. 7). The sandstone beds in the lowermost part of the succession have erosional bases and contain ripple cross-lamination and current ripple structures. The sandstones are interpreted to represent estuary channel deposits. Approximately 5 m of mainly upward coarsening, faintly parallel laminated, *Teichichnus* bioturbated sandstone is interpreted to represent lagoonal or flood tidal delta deposits. Uppermost in the sandstone succession is a 4 m thick, erosionally based sandstone unit, that shows a stepwise upward coarsening profile. The unit consists of heterolithic sandstone dominated by hummocky cross-stratification and sandstone showing swaley cross-stratification and low angle cross-bedding. This unit is interpreted as wave-dominated mouth bar and tidal inlet deposits.

The uppermost rooted sandstone is overlain by seam T3, c. 0.66 m thick. The lower part of the seam is hard and dull, but it becomes more banded and bright in the upper part (Table 5). An erosional boundary separates it from the overlying sandstone and the c. 0.48 m thick seam T4 composed of banded coal, possibly containing pyrite. Seam T4 is erosionally overlain by mainly very fine-grained to fine-grained sandstone beds showing wave ripple, hummocky cross-stratification, current ripple and ripple cross-lamination structures. The sediments were deposited in a shoreface environment.

### *Lulu-1 well*

The investigated interval constitutes part of the Inter-distributary Bay Association of Frandsen (1986) and the

sediments were mainly interpreted to represent crevasse splays. However, they have more recently been re-interpreted by Johannessen & Andsbjerg (1993) and Andsbjerg (1997).

The siliciclastic sediments underlying the coal seam R1 consist primarily of light to dark grey, mainly structureless, bioturbated silt- and sandstone beds (Fig. 8). The sediments contain small pyrite concretions, organic debris and coalified leaves and twigs. The sediments are interpreted to represent estuary channel and lagoonal deposits (Andsbjerg 1997).

The overlying coaly interval contains grey to black siltstone layers and thin coal layers with rootlets descending into the underlying siltstones. Seam R1 between 3599.43–3599.49 m is composed of banded to dull coal with visible pyrite. A siltstone to very fine-grained sandstone with current ripples and trough cross-bedding is overlying the coaly interval. Rootlets penetrate the sediments from the overlying coal seam T2. The seam is c. 0.56 m thick and contains a c. 0.08 m thick silt layer approximately in the middle part. The coal below the silt layer is bright in the basal part, and becomes dull towards the top, whereas the coal above the silt layer generally is dull and banded. Immediately above and below the silt layer small pyrite concretions are present in the coal.

Seam T2 is overlain by a siltstone, followed by a thin coal layer, which is erosively overlain by a bioturbated siltstone bed. Above that is a 8 m thick coarsening upward succession. Above a basal mudstone follow well-sorted, very fine- to fine-grained, light to grey and bioturbated sandstones that show wave ripples, trough cross-bedding, current ripples and hummocky cross-stratification. Towards the top the sandstone becomes parallel laminated, and rootlets descend from the overlying seam T4. The sediments represent a prograding shoreface and beach (Johannessen & Andsbjerg 1993). Seam T4 is c. 0.36 m thick and consists of banded-bright coal and dull coal with vitrinite laminae. A succession of mainly fine-grained sandstone beds with bioturbation and predominately current ripples, hummocky cross-stratification and faintly parallel lamination overlies seam T4.

### *Amalie-1 well*

The coaly interval between 5070.75 m and 5071.72 m overlies a homogeneous mudstone, interpreted to represent a lagoonal environment, which towards the coaly interval is black and carbonaceous with coal lenses and

Table 5. Macroscopic description of samples from West Lulu-1

<b>Seam T4, 0.48 m (3569.39–3569.87 m):</b>	
3569.39–3569.41 m, (4468A oΔ):	Dull-bright banded coal, possibly with pyrite
3569.54–3569.59 m, (4469A oΔ):	As above
3569.66–3569.72 m, (4470A):	Dull-bright banded to dull coal; pyrite possibly present
<b>Seam T3, 0.43 m (3571.32–3571.75 m):</b>	
3571.32–3571.44 m:	Dull-bright banded coal, mainly dull
3571.44–3571.49 m, (4472A o):	Hard and black bright to dull coal
3571.49–3571.57 m, (4473A oΔ):	Mainly bright coal
3571.62–3571.70 m:	Hard, dull coal with vitrinite particles or laminae
3571.70–3571.75 m, (4475A oΔ):	Hard, dull coal
<b>Seam T2, 0.66 m (3587.98–3588.64 m):</b>	
3587.98–3588.08 m, (4476A):	Hard, dull coal with pyrite(?) and vitrinite lenses
3588.08–3588.11 m:	Hard, dull coal
3588.21–3588.28 m, (4478A oΔ):	Dull (to bright) coal, probably with pyrite
3588.28–3588.33 m:	Mainly bright coal with pyrite
3588.33–3588.46 m, (4480A o):	Mainly bright coal
3588.46–3588.54 m, (4481A):	Hard, clayey dull coal or coaly mudstone
3588.54–3588.59 m:	Dull coal with vitrinite particles and lenses
3588.59–3588.64 m, (4483A):	Bright to dull coal with pyrite
<b>(3588.64–3589.05 m, carbonaceous mudstone with vitrinite lenses; not sampled)</b>	
<b>Seam R1a, 0.58 m (3589.05–3589.63 m):</b>	
3589.05–3589.07 m:	Carbonaceous mudstone or clayey coal with vitrinite laminae
3589.07–3589.12 m, (4485A o):	Bright-dull banded coal
3589.12–3589.17 m:	Dull coal with vitrinite laminae; pyrite present
3589.17–3589.22 m, (4487A o):	Mainly bright coal
3589.22–3589.35 m:	Mainly bright coal with duller layers; pyrite present in vertical cleats
3589.35–3589.40 m, (4489A):	Mainly bright coal
3589.40–3589.48 m:	As above
3589.58–3589.63 m, (4491A o):	Bright coal
<b>3589.63–3590.29 m, hard, dark grey-black carbonaceous mudstone and clayey coal with vitrinite lenses and laminae:</b>	
3589.68–3589.71 m:	Hard, black and dull with vitrinite laminae
3589.76–3589.78 m:	Hard and black with vitrinite laminae; fusinite particles observed
3589.96–3589.99 m:	As above
3590.21–3590.29 m, (4495A o):	Carbonaceous mudstone or clayey coal with vitrinite laminae
<b>Seam R1, 0.89 m (3590.29–3591.18 m):</b>	
3590.29–3590.39 m:	Dull and bright coal with clay laminae, fusinite particles present
3590.52–3590.57 m, (4497A):	Dull coal with vitrinite laminae, pyrite present
3590.57–3590.59 m, (4498A o):	Mainly bright coal, small pyrite crystals present
3590.59–3590.65 m, (o):	Carbonaceous mudstone with vitrinite laminae or particles
3590.65–3590.70 m:	Vitrinite-rich carbonaceous mudstone or clayey coal
3590.70–3590.75 m, (4501A o):	Hard, dull coal
3590.75–3590.80 m:	Mainly bright coal; horizontal pyrite lens and small pyrite crystals
3590.80–3590.82 m, (4503A o):	Mainly bright coal
3590.82–3590.87 m, (4504A):	Mainly bright coal with pyrite in almost vertical cleats
3590.87–3590.93 m:	Hard mainly dull coal
3590.93–3590.98 m, (4506A o):	Mainly bright coal
3590.98–3591.08 m, (4507A o):	Bright-dull banded coal; pyrite present
3591.08–3591.13 m:	Bright-dull banded coal
3591.13–3591.18 m, (4509A):	Mainly bright coal with dull laminae
<b>3591.18–3591.92 m, carbonaceous mudstone:</b>	
3591.18–3591.23 m, (o):	Dull carbonaceous mudstone, top more coaly
3591.23–3591.31 m:	Dull carbonaceous mudstone with vitrinite lenses

Samples analysed petrographically are indicated by sample number in brackets. o: sample extracted, fractionated and analysed by means of GC and GC/MS; Δ: sample analysed by means of Py-GC.

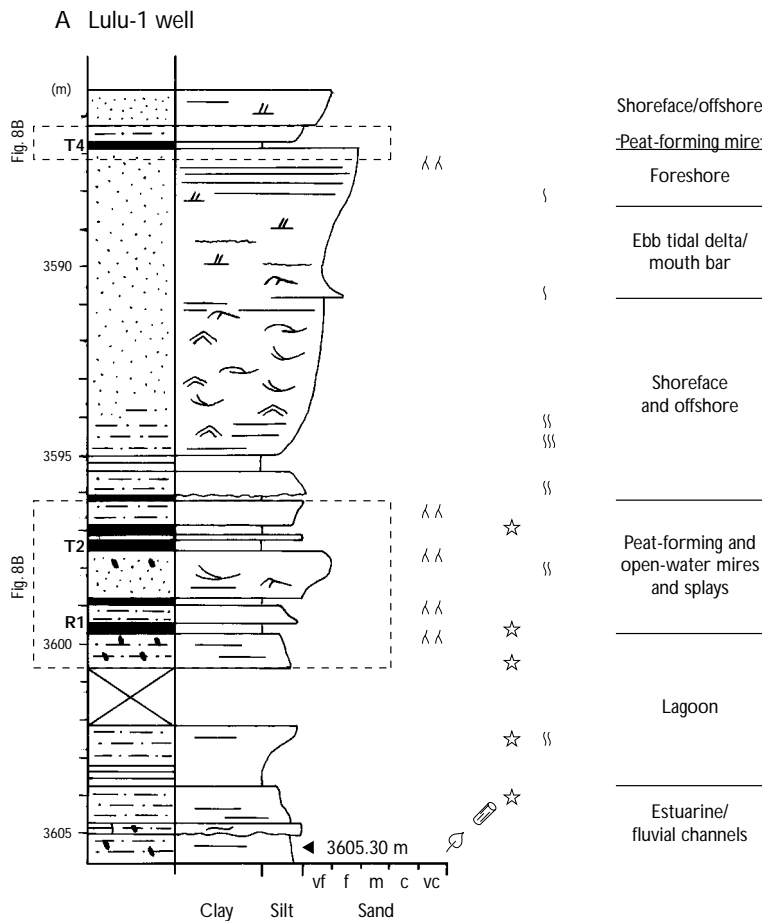
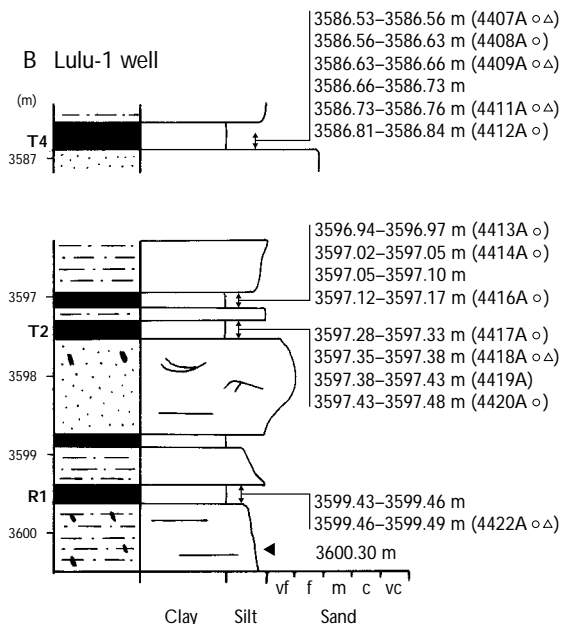


Fig. 8. **A**: The coal-bearing section of the Lulu-1 well showing the position of seams R1, T2, and T4, and the interpreted depositional environments.

**B**: Enlargement of the coal-bearing units with indication of the sampled intervals. Sample numbers of petrographically analysed samples shown; o: sample analysed by GC and GC/MS;  $\Delta$ : sample analysed by Py-GC.

See Fig. 5 for legend and Fig. 1 for well location.



laminae (Fig. 9). The coaly interval consists of only an 0.08 m thick coal layer composed of dull coal with vitrinite laminae. The seam is overlain by a 0.22 m thick coaly mudstone layer, and finally the 0.25 m thick coal seam R1 of mainly dull coal with vitrinite laminae. A 23 m thick succession separates seam R1 from seam T4. Immediately above seam R1 is a 0.5 m thick bed of heterolithic clay- and siltstone interpreted as deposited in a lagoon. Above that the lower part of the succession consists of two erosionally based, fining upward sandstone units that show cross-bedding, ripple cross-lamination, bidirectional ripple cross-lamination, flaser-bedding and wavy-bedding. Rip-up mudstone clasts are present above basal erosion surfaces. On top of the lowermost fining upward unit (5067.7 m) is a structureless mudstone and a 0.15 m thick coaly mudstone, and on top of the second unit (5063.5 m) a 0.4 m thick coaly mudstone. The fining upward sandstone units are interpreted as tidal creek or tidally-influenced fluvial channel deposits, possibly with interbedded tidal

A Amalie-1 well

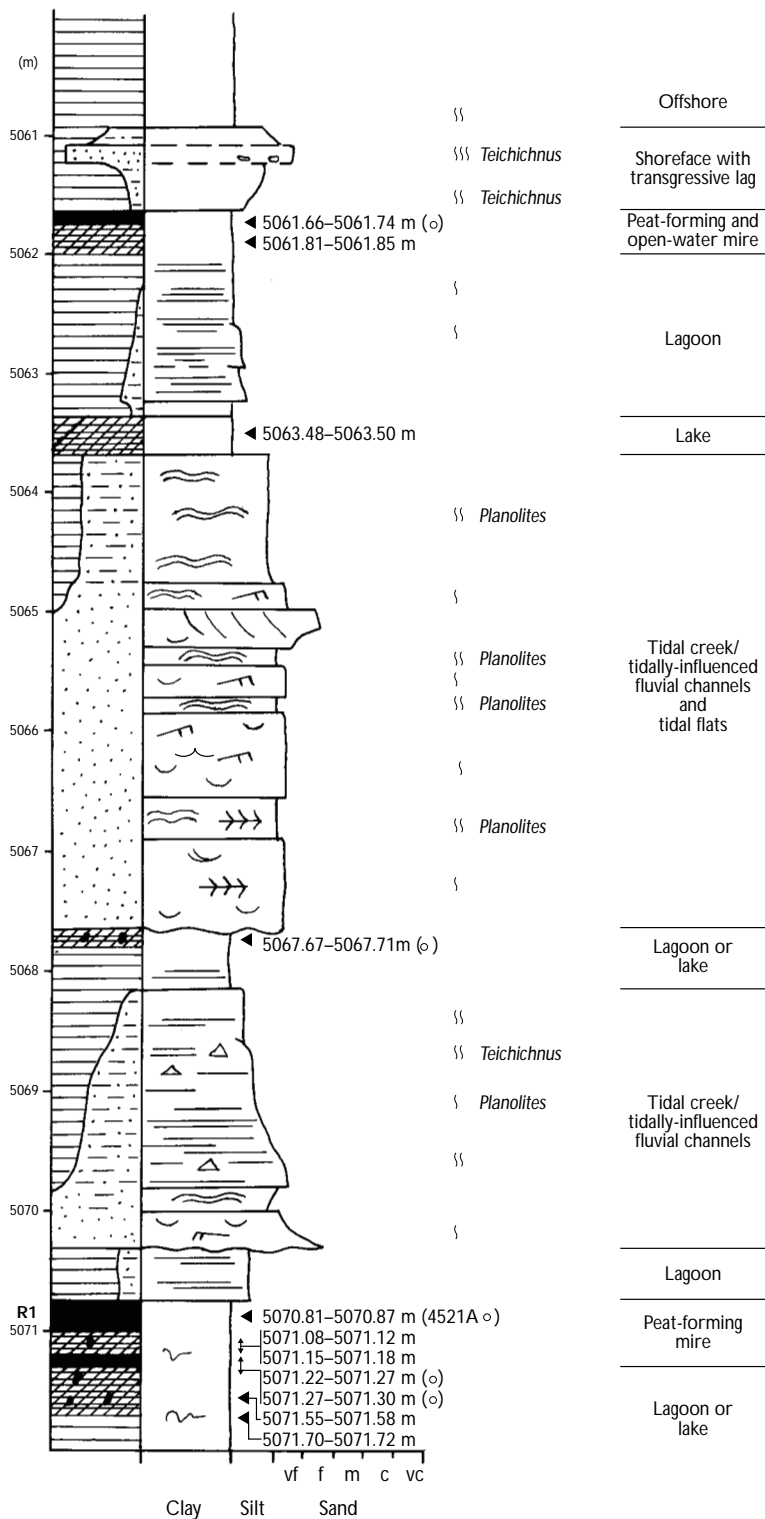


Fig. 9. **A** and **B**: The coal-bearing sections of the Amalie-1 well showing the position of seams R1 and T4, and the interpreted depositional environments. Sample numbers of petrographically analysed samples shown; o: sample analysed by GC and GC/MS; Δ: sample analysed by Py-GC. See Fig. 5 for legend and Fig. 1 for well location.

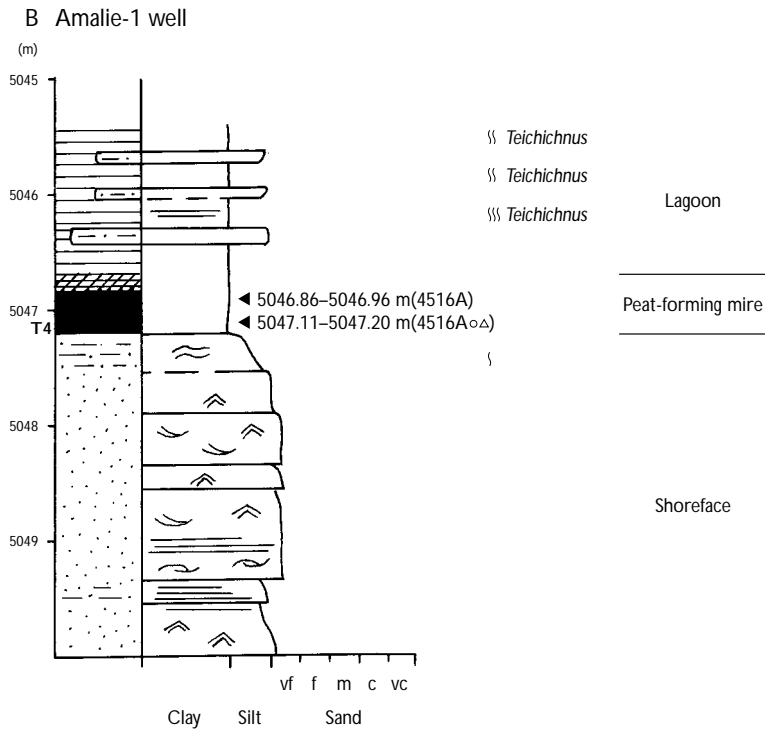


Fig. 9. cont.

flat sediments in the upper unit (Andsbjerg 1997). *Teichichnus* and *Planolites* burrows have been recognised in the channel deposits. Above the fining upward units is a 2.5 m thick succession of heterolithic siltstone and mudstone, which at the top coarsens upward to a 0.3 m thick sandstone bed. A carbonaceous mudstone with a 0.08 m thick layer of bright coal is present at the base of the coarsening upward unit. This succession is interpreted to be interbedded lagoon and wash-over deposits. The uppermost sandstone bed may represent a transgressive shelf deposit. This succession (Fig. 9A) is separated from the succession shown in Figure 9B by an approximately 10 m thick generally coarsening upward mudstone to sandstone succession interpreted as shoreface deposits. A 2.5 m thick erosionally based unit of very fine- and fine-grained sandstone dominated by wave ripple cross-lamination, hummocky cross-stratification, swaley cross-stratification and possibly low-angle cross-bedding underlies seam T4 (Fig. 9B). This uppermost coarsening upward part of the shoreface succession is interpreted to be progradational shelf and shoreface deposits (Andsbjerg 1997).

The c. 0.35 m thick coal seam T4 composed of hard and bright coal overlies the shoreface sandstones. The

seam is overlain by highly *Teichichnus* bioturbated clay- and siltstone deposited in a lagoonal environment.

### *Cleo-1 well*

The lowermost part of the succession consists of a siltstone to very fine-grained sandstone. However the crushed core interval hinders recognition of sedimentary structures (Fig. 10). It is overlain by a generally homogeneous, light grey, grey and dark grey mudstone, with common coal particles. Occasional sediment disruption may be related to bioturbation. Rootlets occur in a narrow horizon characterised by coal streaks. The mudstone is overlain by a faintly parallel-laminated, but generally very disturbed, silt- to very fine-grained sandstone with abundant coal particles, streaks and lenses, and coalified wood. Rootlets are also present. The succession is topped by a more sandy, but also very coaly interval. The mudstones with evidence of vegetation are interpreted to represent distal floodplain to shallow lake or pond deposits, while the overlying sandstones were deposited in fluvial, possibly tidally influenced, channels.



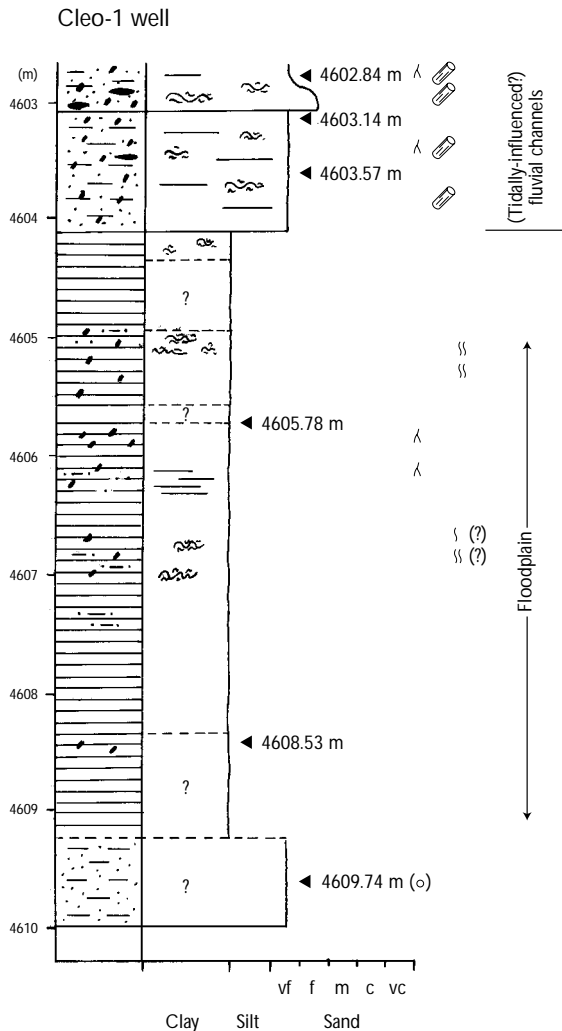


Fig. 10. Sedimentological log of the measured part of the Cleo-1 well showing the interpreted depositional environments. Collected samples shown; o: sample analysed by GC and GC/MS. See Fig. 5 for legend and Fig. 1 for well location.

## Sequence stratigraphic framework and spatial coal seam distribution

A sequence stratigraphic interpretation of the coal-bearing interval in the West Lulu-2 well and correlation of the coal-bearing strata between wells within the Søgne Basin has been presented by Petersen & Andsbjerg (1996) and Petersen *et al.* (1996). These studies focused on a detailed organic petrographic and geochemical investigation of the six coal seams and their relationship to sequence stratigraphic key surfaces and sys-

tems tracts. This sequence stratigraphic framework was revised somewhat in the more detailed sequence stratigraphic and sedimentological study by Andsbjerg (1997). In the studies by Petersen & Andsbjerg (1996) and Petersen *et al.* (1996) two sequences, A and B, were recognised in the coal-bearing unit of the West Lulu-2 well, with only seam T1 situated in sequence A and the remaining five coal seams situated in the transgressive systems tract (TST) of sequence B (Fig. 11). Seam R1 was situated at the base of the TST and separates the lowstand systems tract (LST) from the TST, and it was thus correlatable to the transgressive surface (TS1). Seam T2 was situated closely above R1 at the very basal part of the TST, whereas seams R2, T3 and T4 were situated close to or include the correlative level to the maximum flooding surface (MFS). In the revised sequence stratigraphic model of Andsbjerg (1997) sequence Bat-1A is equivalent to sequence A of Petersen & Andsbjerg (1996), whereas sequence B of Petersen & Andsbjerg (1996) is subdivided into two sequences, Cal-1A and Cal-1B. The regional sequence boundary (SB) Cal-1A subdivides the Middle Jurassic succession into a lower part dominated by fluvial deposits and an upper part dominated by paralic and shallow marine deposits (Andsbjerg 1997). Only the T1 seam, identified in the West Lulu-2 well, is located below the Cal-1A SB in sequence Bat-1A. The Middle Jurassic sediments above the Cal-1A SB represent sequences Cal-1A, Cal-1B and Cal-1C. The Cal-1B SB separates seams R1 and T2 from seams R2, T3 and T4. However, the five seams R1 to T4 are all located in transgressive systems tracts of their respective sequences. Therefore, coal seams R1–R2 and T2–T4 treated herein are located in sequences Cal-1A and Cal-1B.

In most wells the Cal-1A SB is located at the base of stacked massive channel sandstones. The missing section below the unconformity may amount to up to c. 40 m, and the unconformity is interpreted as bounding an incised valley with a relief amounting to at least 40 m. The stacked fluvial and estuarine channel sandstones and interbedded tidal channel and low-energy estuary deposits that constitute the incised valley fill represent the LST and lower TST of the Cal-1A sequence. The valley fill succession is capped by the R1 coal seam, which is also found overlying an interfluvial bypass surface or a very thin (0.5 m) valley-fill unit in the West Lulu-4 well. The upper part of the Cal-1A TST is present above seams R1 and T2 as a thin transgressive shoreface sandstone in the easternmost wells and as a succession of mainly estuarine deposits in the wells to the west. A coarsening upward succession of shelf and

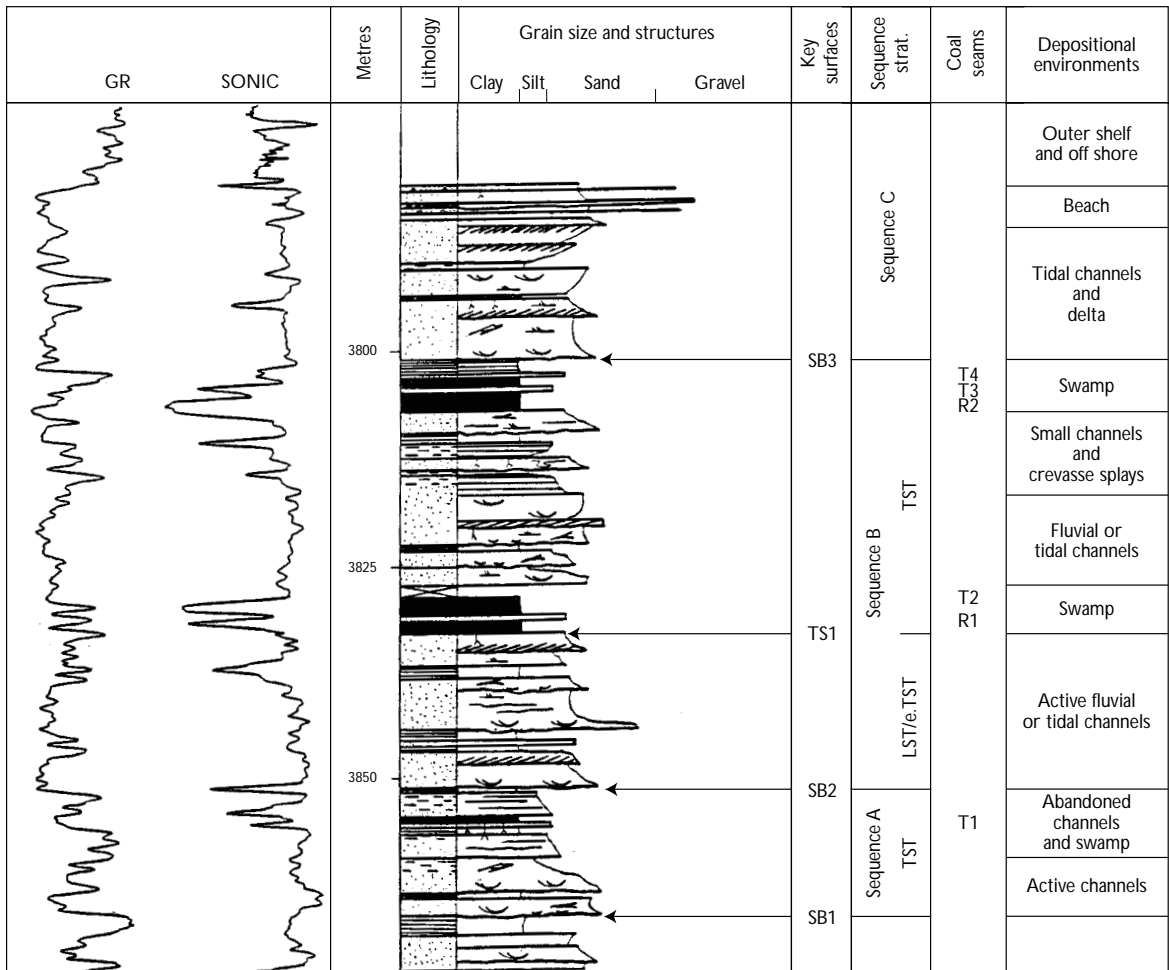


Fig. 11. The coal-bearing section of the West Lulu-2 well showing the position of seams T1, R1, T2, R2, T3 and T4, and the interpreted depositional environments. The coal-bearing unit is bounded by two sequence boundaries (SB1 and SB3) and consists of sequence A, which contains a transgressive systems tract (TST), and sequence B, which contains a lowstand systems tract/early TST and a TST. A transgressive surface (TS) is situated below seam R1. After Petersen *et al.* (1996).

shoreface deposits represents the highstand systems tract (HST) and forced regression systems tract (FRST) of Cal-1A in the easternmost wells (Andsbjerg 1997). In wells in an intermediate position there is a somewhat thinner succession of bay-head or tidal delta deposits, whereas the HST/FRST is missing from the westernmost wells due to erosion at the Cal-1B SB. The Cal-1B SB is located in beach deposits overlying the coarsening upward shoreface succession in the easternmost wells and at the base of tidally influenced channel sandstones in the wells to the west. The beach deposits and lowermost channel sandstones may represent the LST or lowermost TST of Cal-1B. Seams R2, T3 and T4 in

the wells to the west and seam T4 seam in the wells to the east are situated on top of these LST/lowermost TST deposits and are thus incorporated in the TST of the Cal-1B sequence.

The sequence stratigraphic framework together with the excellent lateral control provided by the characteristic gamma ray signals of the coal seams helped correlation of the coal intervals. A more detailed coal seam-to-coal seam correlation in the Søgne Basin is possible due to the organic petrographic and geochemical data obtained in the present study (see p. 29). The cored succession in the Cleo-1 well is not included in this correlation; coal seams are absent and the succession prob-

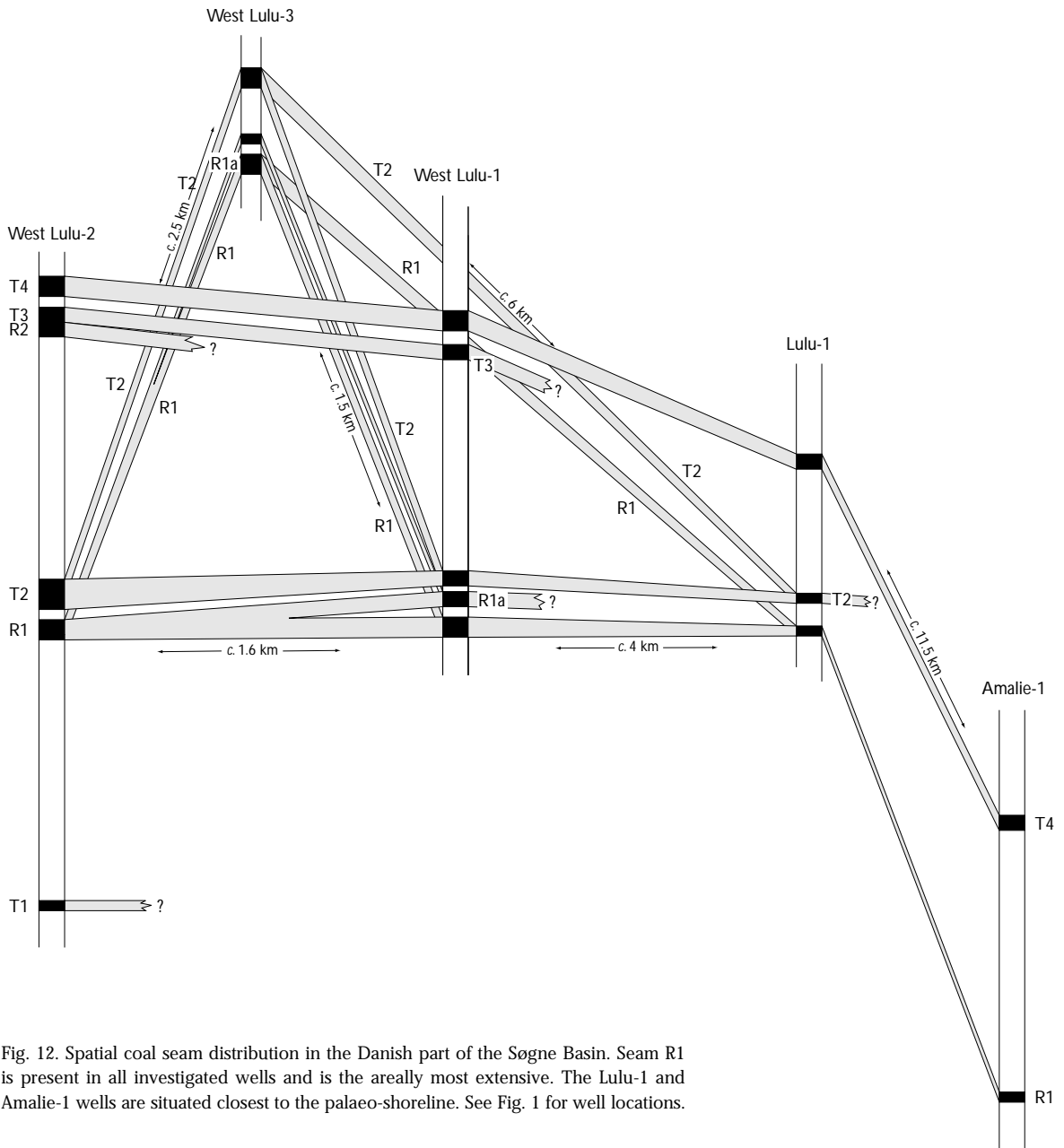


Fig. 12. Spatial coal seam distribution in the Danish part of the Søgne Basin. Seam R1 is present in all investigated wells and is the areally most extensive. The Lulu-1 and Amalie-1 wells are situated closest to the palaeo-shoreline. See Fig. 1 for well locations.

ably belongs to the LST of sequence Cal-1A (Andsbjerg 1997).

The spatial distribution of the coal seams is shown in the fence diagram in Figure 12. Seam T1 in sequence Bat-1A has been observed in West Lulu-2, West Lulu-4 and possibly in Lulu-1. A coal seam is not present at that level in West Lulu-1 and the Norwegian 3/7-4 well and the Bat-1A sequence has been erosionally removed in West Lulu-3. In contrast seam R1 is areally extensive

and is present in all wells, which is in accordance with correlation of the seam with a transgressive surface (Fig. 13). In a landward position relative to the palaeo-coastline (West Lulu-2 and West Lulu-1 wells) seam R1 is between *c.* 0.85 and 0.89 m thick (Table 6). In West Lulu-3 the seam is *c.* 0.56 m thick, but basinwards it thins to about *c.* 0.06 m and *c.* 0.25 m in the Lulu-1 and Amalie-1 wells respectively. At 0.66 m above seam R1 in both the West Lulu-3 and West Lulu-1 wells a coal

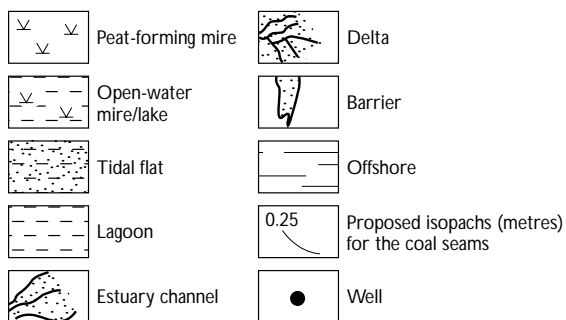
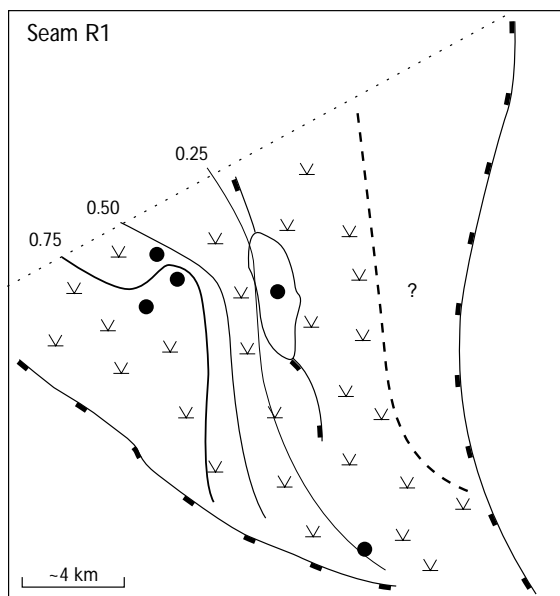


Fig. 13. Palaeogeographic map showing the areal extent of the precursor mire of seam R1 in the Danish part of the Søgne Basin. Isopach-lines show the thickness of coal seam R1 and suggest that the precursor peat deposit thinned towards the palaeo-shoreline and that it had a rather uniform thickness parallel to the ancient coastline. For names and location of the wells, see Fig. 1.

Table 6. Thickness of Bryne Formation coal seams

Well	W. Lulu-2	W. Lulu-3	W. Lulu-1	Lulu-1	Amalie-1
Seam	(m)				
T4	0.50	(0.35?)*	0.48	0.36	0.35
T3	0.94	-	0.66	-	-
R2	1.06	-	-	-	-
T2	1.30	0.71	0.66	0.56	-
R1a	(R1, 0.85)	0.30	0.58	-	-
R1	0.85	0.56	0.89	0.06	0.25
T1	0.40	-	-	-	-
Total	5.05	1.57	3.27	0.98	0.60

\*estimated from sonic log

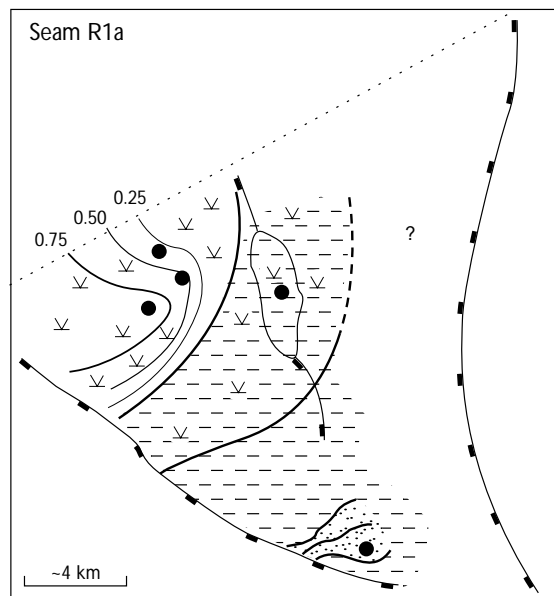


Fig. 14. Palaeogeographic map showing the limited areal extent of the precursor mire of seam R1a. The mire was probably separated from a lagoonal environment towards the south-south-east by an open-water mire or lacustrine environment. For legend, see Fig. 13.

seam named R1a occurs. It is 0.30 m thick in West Lulu-3 and 0.58 m in West Lulu-1. Its organic petrographic and geochemical composition (see below) is intermediate between seam R1 and the overlying seam T2, and it is interpreted to be a split of seam R1. The areal extent of the original peat mire which formed seam R1a was limited (Fig. 14).

Seam T2, situated close to TS1 in the basal part of the TST of sequence Cal-1A, is also laterally extensive. The seam is *c.* 1.30 m thick in West Lulu-2 and thins to *c.* 0.71 m in West Lulu-3 and in a basinwards direction to *c.* 0.66 m in West Lulu-1 and 0.56 m, including a *c.* 0.08 m thick silt layer, in Lulu-1 (Table 6). In contrast to the immediately underlying seam R1, seam T2 is no longer recognisable as coal in the Amalie-1 well, and is probably developed as carbonaceous mudstone. This corroborates the interpretation that the precursor peat of seam R1 formed during relatively slow watertable (base-level) rise related to initial relative sea-level rise allowing peat accumulation to occur over a large area, whereas the T2 peat accumulated during accelerated watertable rise which hindered peat formation at the position of Amalie-1 (Fig. 15; Petersen & Andsbjerg 1996).

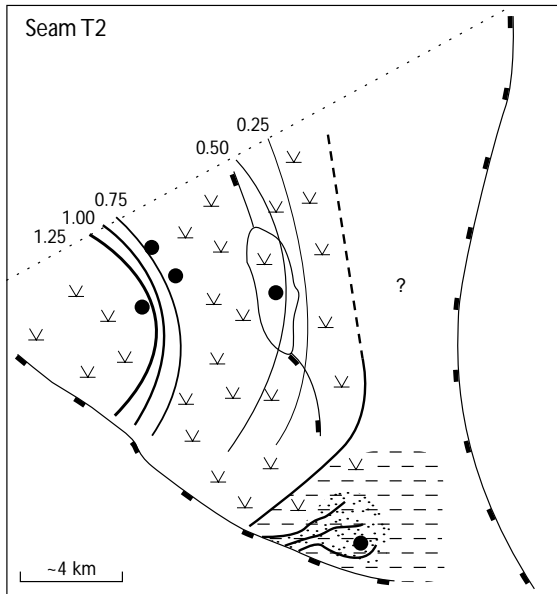


Fig. 15. Palaeogeographic map showing the areal extent of the precursor mire of seam T2. The coal seam thickens towards the north-east where it attains a thickness of 1.3 m. For legend, see Fig. 13.

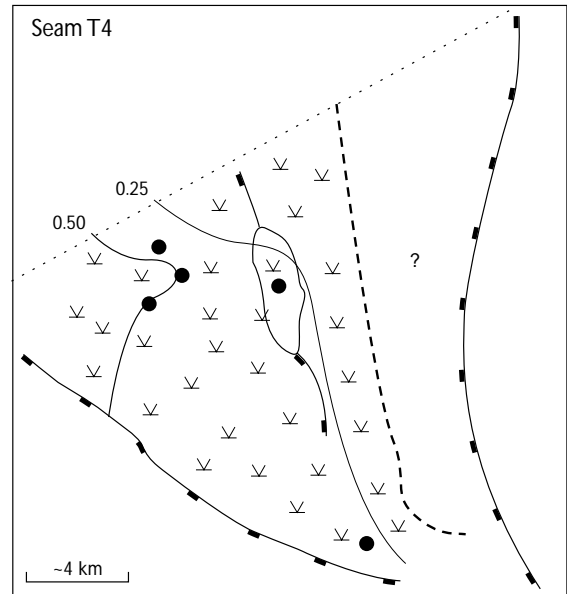


Fig. 17. Palaeogeographic map showing the areally extensive precursor mire of seam T4. Coal isopach-lines suggest that the thickness of the original peat deposit was relatively uniform. For legend, see Fig. 13.

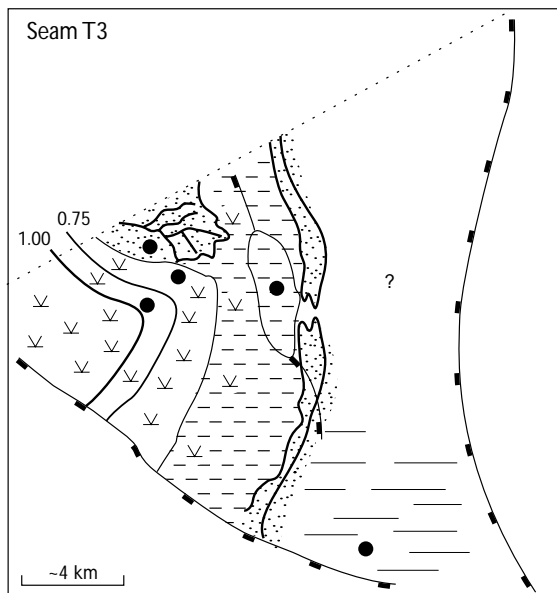


Fig. 16. Palaeogeographic map showing the areal extent of the precursor mire of seam T3. The areally restricted precursor mire of seam T3 was probably protected from the offshore marine environment to the east by barrier islands behind which lagoonal and open-water mire environments prevailed. For legend, see Fig. 13.

In West Lulu-2 a thick coal bed was interpreted to be a composite of two seams, R2 and T3 (Fig. 11; Petersen & Andsbjerg 1996; Petersen *et al.* 1996). This division is no longer recognisable in West Lulu-1 where only seam T3, 0.66 m thick, seems to be present. The areal extent of seam T3 is limited, and during deposition lagoonal, barrier and offshore environments prevailed east of the T3 mire (Fig. 16).

The overlying seam T4 can be followed laterally from West Lulu-2 to Amalie-1. In the most landward position (West Lulu-2) relative to the palaeo-shoreline the seam is c. 0.50 m thick, but it thins to c. 0.35 m in both Lulu-1 and Amalie-1 (Table 6). Based on the sonic log motif of West Lulu-3, the seam may also be present in that well (Fig. 17).

This suggested spatial coal seam distribution in the Bryne Formation is restricted by the limited number of drilled and cored wells in the Danish part of the Søgne Basin, but wells in the Norwegian part of the Søgne Basin indicate a much larger areal extent of the coal seams. The fence diagram gives an idea of the distribution of the cumulative coal seam thickness in the Søgne Basin. The thickest cumulative seam thickness, 5.05 m, occurs in the West Lulu-2 well positioned most landward relative to the ancient sea, and the total coal seam thick-

ness diminishes in a seaward direction (Fig. 12; Table 6). The part of the ancient peat mires situated closest to the palaeo-shoreline should be favourable for the formation of petroleum-prone organic components due to a continuously high watertable and anoxic conditions (Petersen *et al.* 1996). However, this may be compensated for by the greater total amount of organic matter in the more landward parts of the palaeomires.

## Organic petrographic and geochemical results

### Vitrinite reflectances

The 16 vitrinite reflectance measurements from the coals in the West Lulu-1, West Lulu-3 and Lulu-1 wells fall in the range 0.75–0.89 %R<sub>m</sub> with the lowest reflectance value measured in seam T4 in West Lulu-1 and the highest value measured in Lulu-1 (Tables 7–9). Twelve vitrinite reflectance values of the West Lulu-2 well coals are within the same range, 0.78–0.89 %R<sub>m</sub> (Petersen *et al.* 1996). The majority (22) of the 28 reflectance values, however, lie between 0.81 %R<sub>m</sub> and 0.89 %R<sub>m</sub>. These reflectance values indicate that the coals within the four wells are of high volatile bituminous B/A rank. The 2 vitrinite reflectance values from the Amalie-1 well are significantly higher, both 1.3 %R<sub>m</sub>, indicating a medium volatile bituminous rank (Table 10). Vitrinite reflectance measurements on vitrinitic material in Cleo-1 give values of 0.90 %R<sub>m</sub> and 0.95 %R<sub>m</sub> inferring a high volatile bituminous A rank.

### Organic petrographic composition

In the following the organic petrographic composition and lateral development of the seams is presented. With respect to seams T1 and R2, which only occur in the West Lulu-2 well, the reader is referred to Petersen & Andsbjerg (1996) and Petersen *et al.* (1996).

*Seam R1.* In West Lulu-3 the seam is composed of comparatively high contents of vitrinite and varying amounts of inertinite, vitrite+clarite and the inertinite-rich microlithotypes vitrinite+durite+clarodurite (Figs 18, 19). Detrovitrinite, including fluorescent collodetrinite, dominates over telovitrinite.

Pyrolytic carbon occurs throughout the seam (see Petersen 1998), and in the interval 28–31 cm oxidised cutinite and unsorted inertodetrinite and macrinite are present. Liptinite constitutes between 1.0 and 4.4 vol.% of the coal and it is composed of liptodetrinite, spornite, resinite and cutinite with a liptinite maceral only in a few cases exceeding 1.4 vol.%. Pyrite, mainly occurring as minute crystals, generally constitutes 1.0 vol.% or less.

Seam R1 is dominated by vitrinite in the West Lulu-1 well, but the content of vitrite+clarite decreases upwards through the seam while vitrinite+durite+clarodurite shows an increasing tendency (Figs 18, 19). Collotelinite is weakly fluorescent, and fine-grained allochthonous inertodetrinite occurs disseminated in vitrinite. The liptinite content ranges between 0.8 and 3.2 vol.% and is mainly composed of liptodetrinite, cutinite and spornite. Pyrite is only present in very small amounts.

Table 7. West Lulu-3 well: GC data, GC/MS data and vitrinite reflectance values

Seam	Sample number	Pr Ph	CPI	%R <sub>m</sub>	Steranes					
					29αααS		29αββ(S+R)		%αββ	
					29ααα(S+R)	29αββ(S+R)+29ααα(S+R)	C <sub>27</sub>	C <sub>28</sub>	C <sub>29</sub>	
T2	4380A	5.56	1.09	-	0.39	0.49	18.8	27.2	54.0	
	4383A	5.69	1.11	-	0.46	0.50	20.1	30.5	49.4	
	4385A	5.19	1.12	-	0.43	0.51	23.5	26.5	50.0	
	4386A	5.42	1.09	-	0.44	0.48	21.0	28.4	50.5	
	4387A	5.36	1.09	-	0.40	0.47	12.3	27.0	60.7	
R1a	4393A	6.17	1.12	-	0.41	0.48	14.6	25.8	59.5	
R1	4396A	5.84	1.11	0.88	0.40	0.47	10.0	24.2	65.7	
	4397A	5.69	1.11	0.87	0.42	0.51	10.0	23.9	66.2	
	4400A	5.81	1.12	0.87	0.43	0.48	10.1	24.2	65.7	
	4401A	-	-	0.88	-	-	-	-	-	
	4402A	5.74	1.11	-	0.45	0.48	9.1	23.7	67.2	
Mudstones	4388A	7.77	1.10	-	0.25	0.37	16.7	20.6	62.7	
	4389A	7.48	1.13	-	0.36	0.44	13.4	27.7	58.9	

Table 8. West Lulu-1 well: GC data, GC/MS data and vitrinite reflectance values

Seam	Sample number	Pr Ph	CPI	%R <sub>m</sub>	Steranes				
					29 $\alpha\alpha\alpha$ S	29 $\alpha\beta\beta$ (S+R)	% $\alpha\beta\beta$		
					29 $\alpha\alpha\alpha$ (S+R)	29 $\alpha\beta\beta$ (S+R)+29 $\alpha\alpha\alpha$ (S+R)	C <sub>27</sub>	C <sub>28</sub>	C <sub>29</sub>
T4	4468A	3.46	1.06	0.76	0.49	0.62	31.9	28.7	39.5
	4469A	3.01	1.05	0.75	0.47	0.59	31.2	28.6	40.2
T3	4472A	3.65	1.04	-	0.48	0.60	31.9	29.0	39.1
	4473A	3.35	1.06	0.78	0.46	0.63	31.9	29.3	38.8
	4475A	3.62	1.06	0.77	0.47	0.61	31.2	28.2	40.5
T2	4478A	3.26	1.05	-	0.46	0.57	29.7	28.4	41.9
	4480A	2.95	1.04	-	0.46	0.55	30.8	28.4	40.7
R1a	4485A	3.57	1.05	-	0.48	0.57	29.6	27.8	42.6
	4487A	3.45	1.04	-	0.48	0.57	31.0	27.7	41.3
	4491A	3.25	1.04	0.86	0.43	0.51	24.6	28.7	46.7
R1	4498A	3.94	1.04	-	0.46	0.49	17.3	25.5	57.2
	4499A	3.65	1.04	-	0.44	0.47	17.2	26.1	56.7
	4501A	3.10	1.04	-	0.46	0.51	22.5	26.6	50.9
	4503A	3.72	1.05	-	0.47	0.54	23.9	27.8	48.2
	4504A	-	-	0.86	-	-	-	-	-
	4506A	3.71	1.05	0.87	0.48	0.55	23.0	26.9	50.1
	4507A	3.77	1.06	-	0.47	0.52	23.6	27.9	48.5
Mudstones	4495A	3.50	1.03	-	0.45	0.50	20.7	25.8	53.5
	4510A	3.45	1.04	-	0.45	0.51	22.1	26.4	51.6

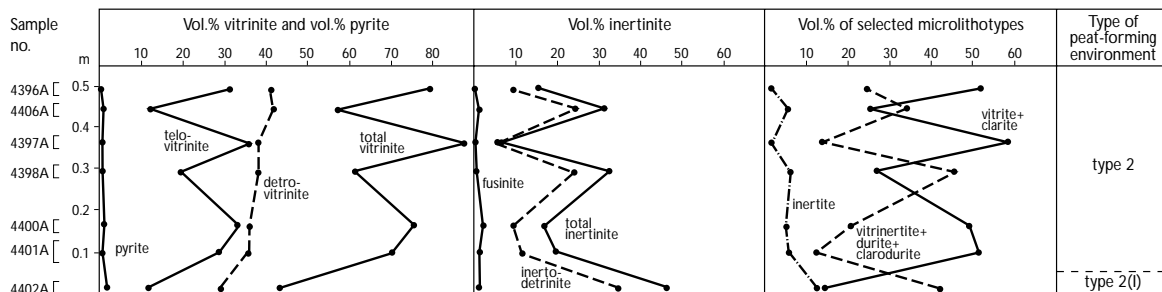
Table 9. Lulu-1 well: GC data, GC/MS data and vitrinite reflectance values

Seam	Sample number	Pr Ph	CPI	%R <sub>m</sub>	Steranes				
					29 $\alpha\alpha\alpha$ S	29 $\alpha\beta\beta$ (S+R)	% $\alpha\beta\beta$		
					29 $\alpha\alpha\alpha$ (S+R)	29 $\alpha\beta\beta$ (S+R)+29 $\alpha\alpha\alpha$ (S+R)	C <sub>27</sub>	C <sub>28</sub>	C <sub>29</sub>
T4	4407A	3.19	1.08	0.85	0.48	0.63	34.0	29.2	36.7
	4408A	2.58	1.05	-	0.51	0.64	32.7	28.0	39.3
	4409A	2.47	1.06	-	0.50	0.66	34.7	28.3	37.0
	4411A	2.82	1.06	-	0.50	0.62	36.7	27.4	35.9
	4412A	3.59	1.05	-	0.49	0.62	33.7	29.6	36.7
T2	4413A	2.46	1.07	-	0.50	0.64	33.1	28.6	38.2
	4414A	2.74	1.08	0.89	0.49	0.61	35.1	27.1	37.9
	4416A	3.17	1.07	0.77	0.48	0.62	33.9	28.4	37.8
	4417A	2.90	1.05	-	0.49	0.63	35.4	27.6	37.0
	4418A	2.67	1.07	-	0.48	0.62	33.8	29.8	36.4
	4419A	-	-	0.89	-	-	-	-	-
	4420A	2.84	1.07	-	0.50	0.60	36.5	28.4	35.1
R1	4422A	3.11	1.05	0.89	0.46	0.52	22.0	30.3	47.7

Table 10. Amalie-1 well: GC data, GC/MS data and vitrinite reflectance values

Seam	Sample number	Pr Ph	CPI	%R <sub>m</sub>	Steranes				
					29 $\alpha\alpha\alpha$ S	29 $\alpha\beta\beta$ (S+R)	% $\alpha\beta\beta$		
					29 $\alpha\alpha\alpha$ (S+R)	29 $\alpha\beta\beta$ (S+R)+29 $\alpha\alpha\alpha$ (S+R)	C <sub>27</sub>	C <sub>28</sub>	C <sub>29</sub>
T4	4515A	-	-	1.30	-	-	-	-	-
	4516A	2.56	1.15	1.30	0.41	0.49	34.6	29.6	35.8
R1	4521A	3.57	1.09	-	0.46	0.60	35.8	28.3	35.9
Mudstones	4517A	2.96	1.03	-	0.48	0.56	29.7	32.8	37.5
	4520A	1.26	1.13	-	0.49	0.58	23.9	31.8	44.3
	4524A	2.38	1.08	-	0.46	0.54	35.5	30.7	33.8
	4525A	2.56	1.11	-	0.44	0.55	36.9	30.1	32.9

West Lulu-3  
Seam R1



West Lulu-1  
Seam R1

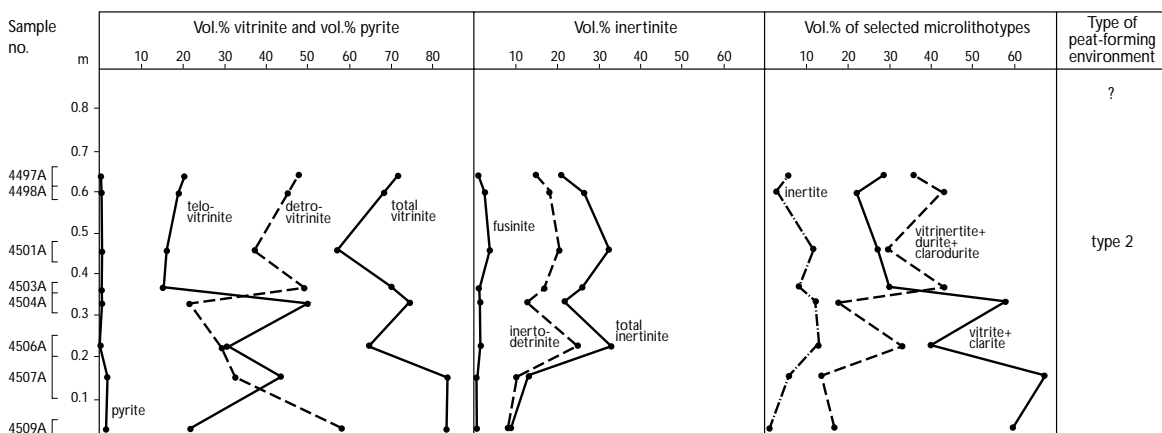


Fig. 18. Coal petrographic composition of seam R1 in the West Lulu-1 and West Lulu-3 wells.

In both Lulu-1 and Amalie-1 seam R1 is dominated by vitrinite (Fig. 19). In Lulu-1 the seam contains significant proportions of vitrite+clarite (65.6 vol.%), and in Amalie-1 vitrinertite (35.8 vol.%), vitrite (28.0 vol.%) and carbominerite (19.4 vol.%). Cutinite, sporinite, lipodetrinite and resinite are recognised in R1 in Lulu-1 whereas the high rank of the coal in Amalie-1 has only allowed the detection of a few lipodetrinites. The pyrite content is in both locations 0.8 vol.%.

**Seam R1a.** The sample from R1a in West Lulu-3 and the majority of seam R1a in West Lulu-1 is characterised by high contents of vitrinite and the microlithotypes vitrite+clarite (Figs 19, 20). A fusinite peak in the lower and upper part of R1a in West Lulu-1 accounts for coinciding inertite peaks. Char particles have been observed in both levels in the seam, and in R1a in West Lulu-3 pyrolytic carbon is present. The liptinite content ranges between 1.6 and 3.6 vol.% and is composed of lipodetrinite, cutinite, resinite and sporinite. Generally the content of a single liptinite maceral is less than 2.0

vol.%. The pyrite content does not exceed 1.0 vol.%, and except for 10.2 vol.% detrital minerals and 16.6 vol.% carbominerite in R1a in West Lulu-3 the microscopic visible inorganic fraction ranges between 0 and 2.0 vol.%.

**Seam T2.** In West Lulu-3 seam T2 is characterised by an increase in the contents of inertinite and inertinite-rich microlithotypes followed by a decrease (Figs 19, 21). Total vitrinite content shows also a weak increase but a marked decrease occurs in the level with peak inertinite content. Vitrite+clarite exhibits varying values, however increases in the upper part of T2. The colodetrinite and collotelinite macerals are fluorescent. Char (see Petersen 1998) and oxidised cutinite and resinite are present in several levels in the seam. The liptinite content ranges between 1.6 and 7.8 vol.% and consists of lipodetrinite, cutinite, sporinite, resinite and in the uppermost part of the seam also suberinite. In general the content of individual liptinite macerals does not exceed 1.6 vol.%. The basal part of T2 is rich in detri-



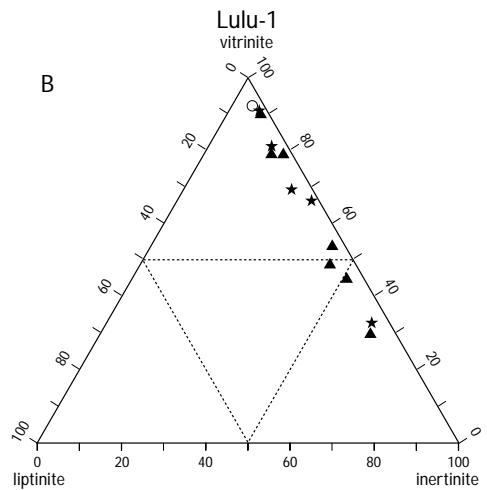
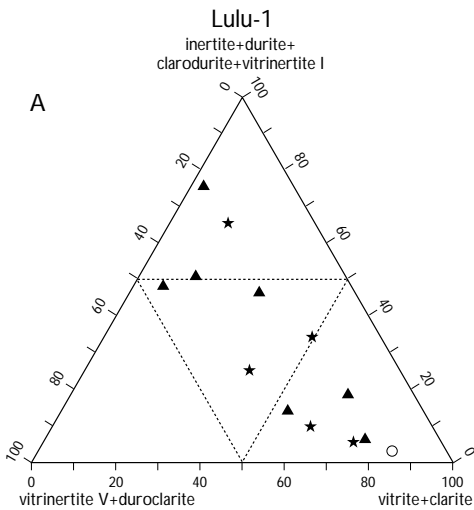
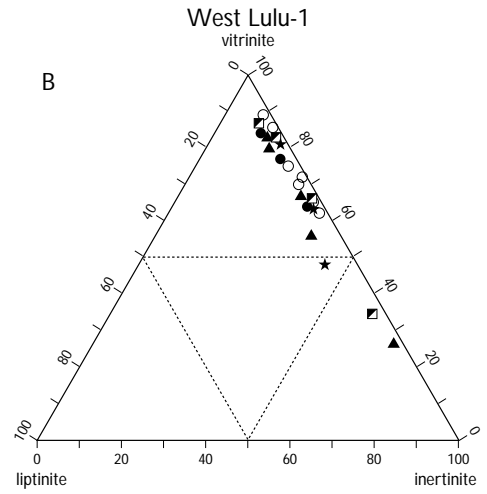
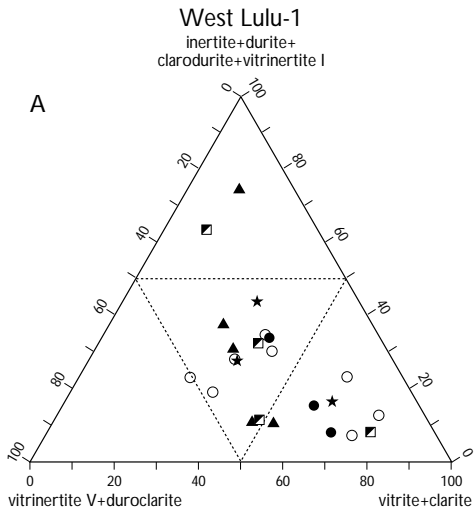
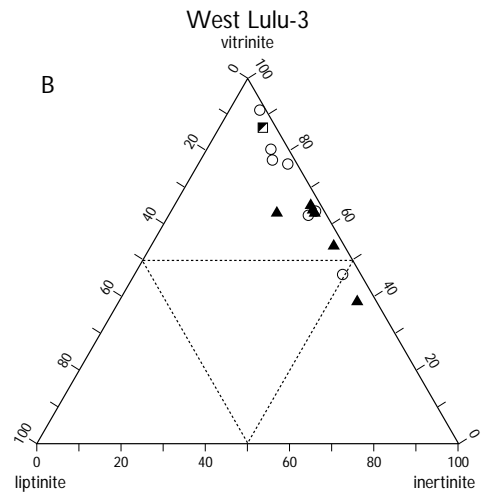
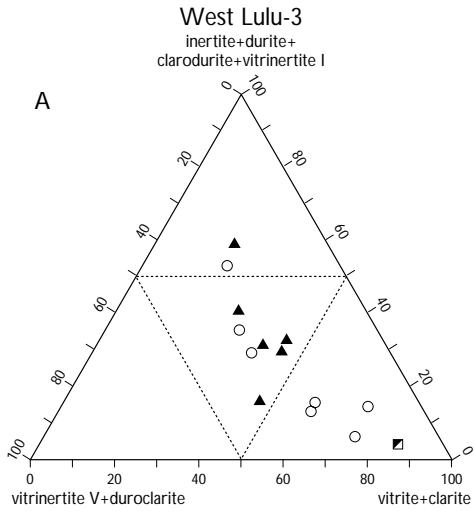


Fig. 19. Triangular plots showing the microlithotype and maceral group composition of seams R1, R1a, T2, T3 and T4 in the West Lulu-3, West Lulu-1, Lulu-1 and Amalie-1 wells.

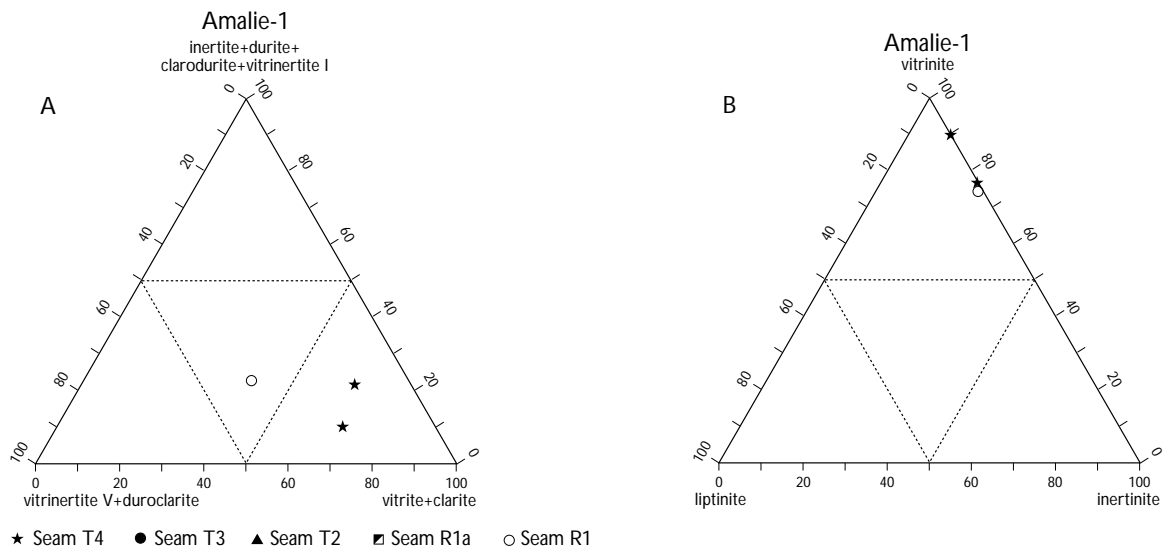


Fig. 19. cont.

tal mineral matter (26.0 vol.%) and carbominerite (41.4 vol.%), while the pyrite content is low or nil.

Seam T2 in West Lulu-1 shows a pronounced decrease in the contents of vitrinite, vitrite+clarite and pyrite up through the seam accompanied by a similar increase in the contents of inertinite and inertinite-rich microlithotypes, in particular inertite (Figs 19, 21). Within the lower part of the seam the inertinite commonly occurs as fine-grained and occasionally micrograded allochthonous inertodetrinite. The liptinite content lies between 2.4 and 6.8 vol.% and consists of liptodetrinite, resinite, sporinite and cutinite. The finely detrital liptodetrinite may occur in association with inertodetrinite. Pyrite varies between 0.2 and 2.0 vol.% and the content of detrital minerals through the seam is, except for one sample, very low (< 1.0 vol.%).

The lower and upper part of seam T2 in Lulu-1 has high proportions of vitrinite and vitrite+clarite while the middle portion is dominated by inertinite and inertinite-rich microlithotypes (Figs 19, 21). The vitrinite fluoresces during blue light irradiation. The inertodetrinite is generally very fine-grained, it may be well-sorted and rounded, and it shows microgradation and microlamination, commonly together with tiny liptodetrinite particles (Figs 22, 23). Groundmass-like macrinite occurs in the interval 33–38 cm, and in the uppermost part char and fusinite occur. Pyrolytic carbon has been observed in the interval c. 8–23 cm. Very small fluorescent particles are associated with micrinite-like particles and inertodetrinite. The liptinite content ranges between 1.6 and 5.8 vol.%, with the majority of the samples above 3.0 vol.%. The liptinite fraction consists of lip-

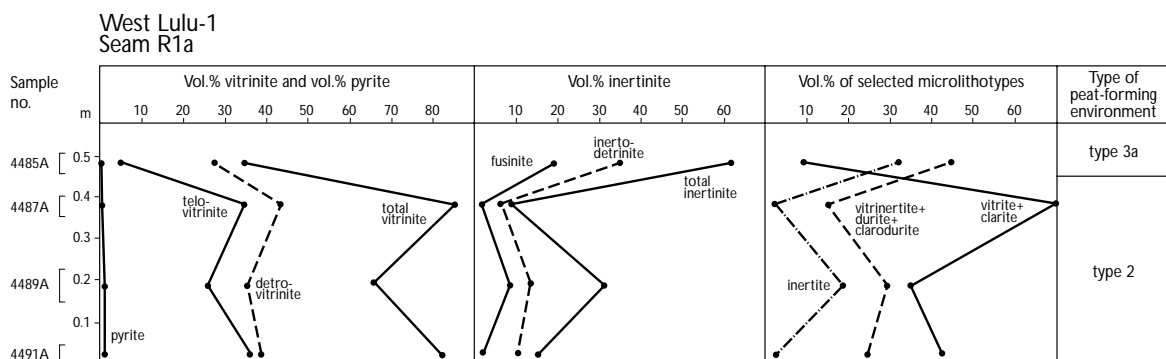
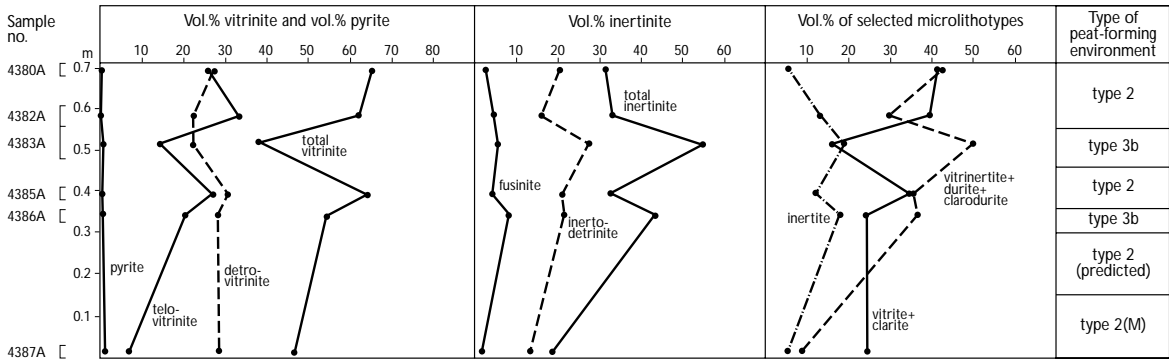
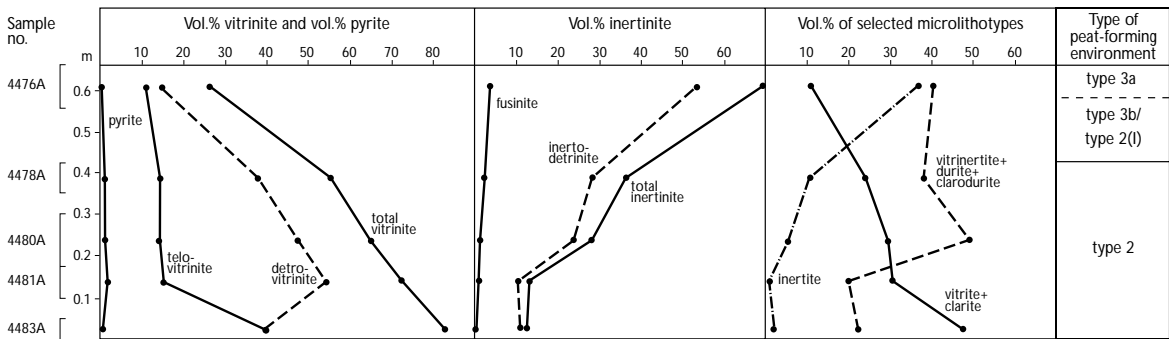


Fig. 20. Coal petrographic composition of seam R1a in the West Lulu-1 well.

West Lulu-3  
Seam T2



West Lulu-1  
Seam T2



Lulu-1  
Seam T2

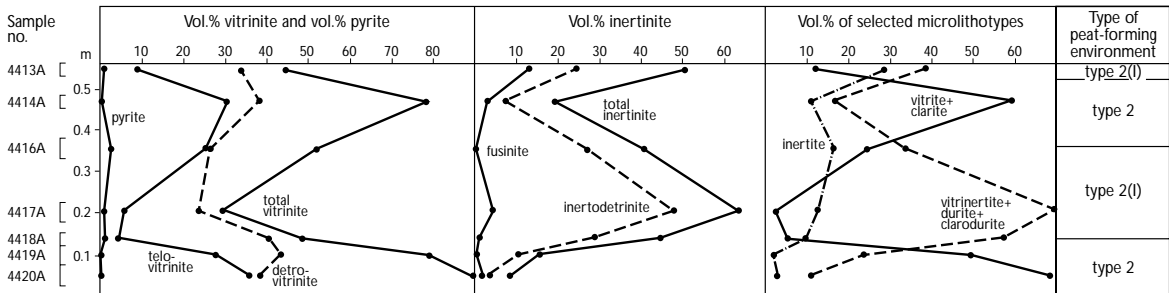


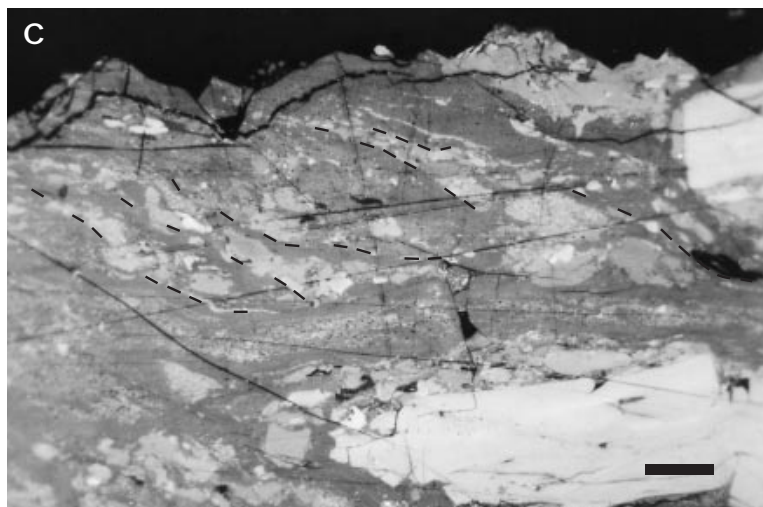
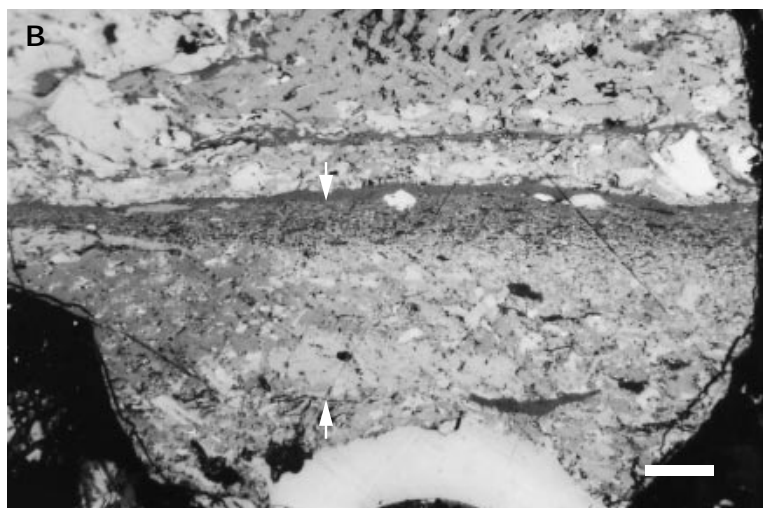
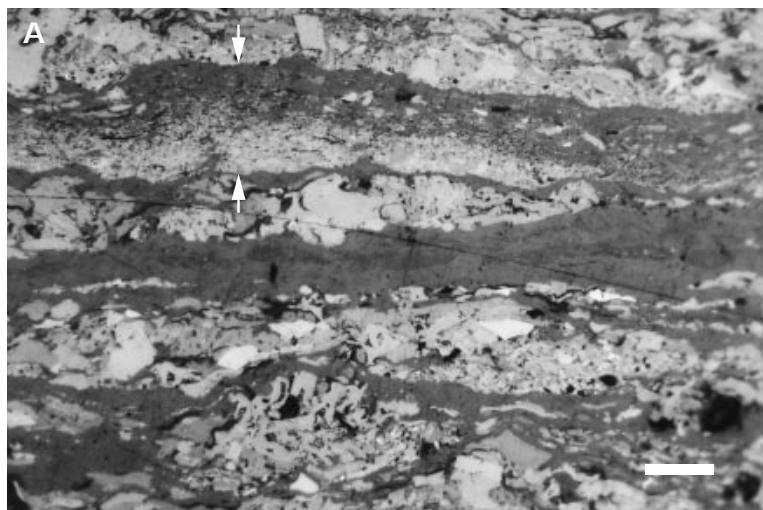
Fig. 21. Coal petrographic composition of seam T2 in the West Lulu-3, West Lulu-1 and Lulu-1 wells.

todetrinite, resinite, sporinite and cutinite. Pyrite, which may be framboidal, ranges between nil and 2.6 vol.%, while detrital minerals constitute less than 1.5 vol.% in all samples.

*Seam T3.* The seam occurs in West Lulu-1 and is characterised by high contents of vitrinite and vitrite+clarite, although the vitrite+clarite content decreases in the uppermost investigated sample (Figs 19, 24). Inertinite

and inertinite-rich microlithotypes show the opposite trend. Char is observed, in particular in the uppermost sample. The vitrinite, generally dominated by telovitrinite (telinite and collotelinite), is strongly fluorescent (Fig. 25), and bitumens are liberated from the vitrinite during blue-light illumination. The liptinite content, varying between 3.4 and 5.0 vol.%, is composed of lip-todetrinite, cutinite, sporinite and resinite (Fig. 25). Exsudatinite expelled into a small cleat has been

Fig. 22. Photomicrographs from seam T2 in the Lulu-1 well. **A** and **B**: Examples of microgradation starting with inertodetrinite and ending with increased amounts of liptodetrinite and vitrinite (sample 4417A, 17.78–22.86 cm). **C**: Micro-cross-lamination; approximate angle of cross-lamination is indicated by punctuated lines (sample 4418A, 12.70– 15.24 cm). All photographs in reflected white light and oil immersion. Scale bar ~ 30  $\mu$ m.



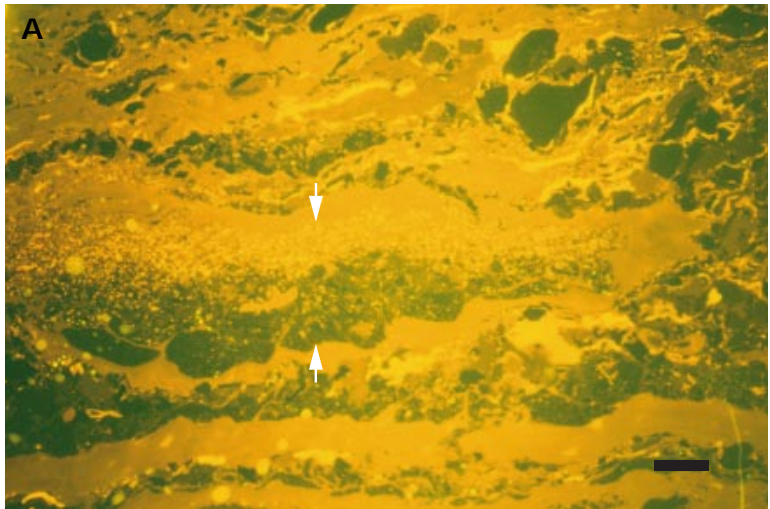


Fig. 23. Photographs from seam T2 in the Lulu-1 well. **A** and **B**: Microgradation shown between arrows; increased proportion of liptodetrinite towards the top of the micrograded lamina is evident from the abundance of tiny yellowish-fluorescent particles (sample 4417A, 17.28–22.86 cm). Note also the fluorescence of the vitrinite bands. Photographs in reflected light, blue-light irradiation and water immersion. Scale bar ~ 30  $\mu$ m.

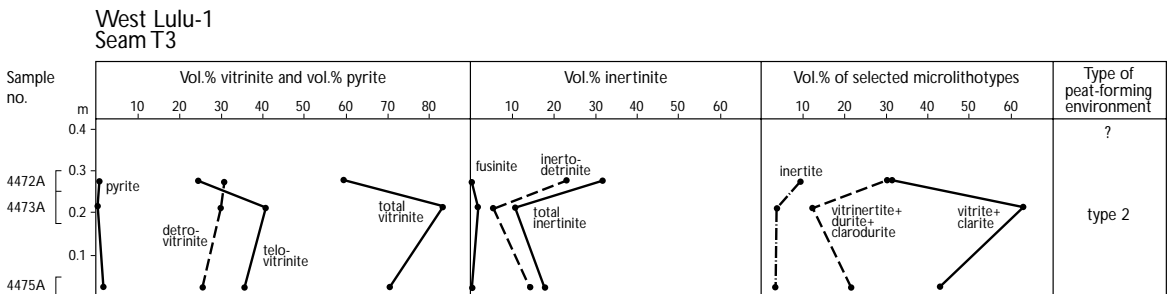
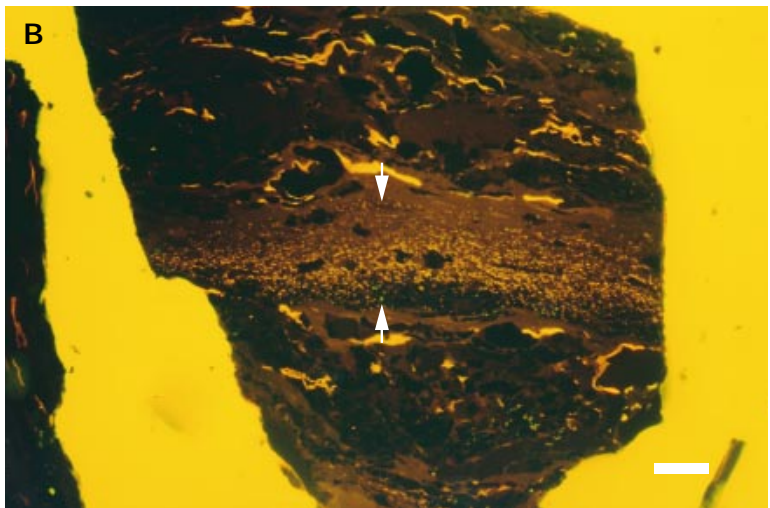


Fig. 24. Coal petrographic composition of seam T3 in the West Lulu-1 well.

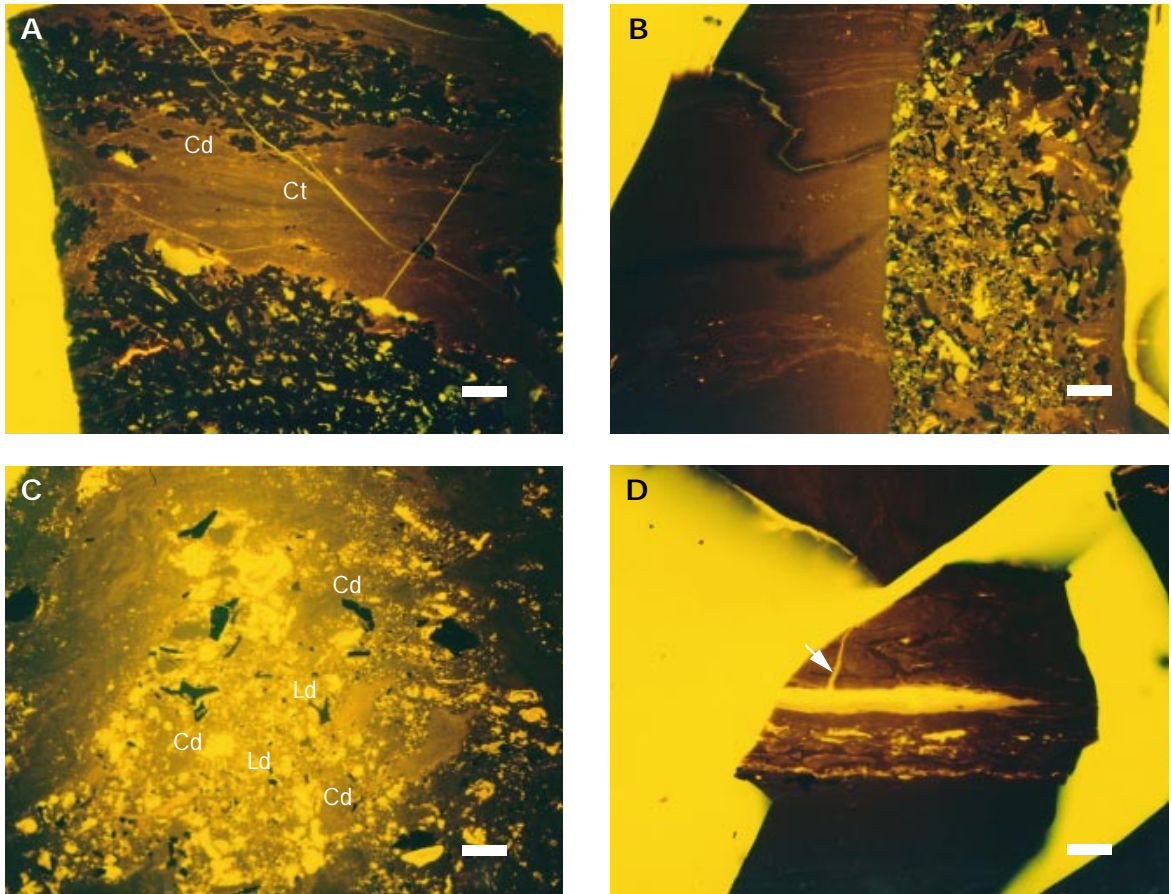


Fig. 25. Photomicrographs from seam T3 in the West Lulu-1 well. **A:** Contact between non-fluorescent inertodetrinite and macrinite (dark particles), and fluorescent collodetrinite (Cd) and collotelinite (Ct) (sample 4475A, 0–5.08 cm). **B:** Contact between fluorescent collotelinite with thin cutinites (left) and a mixture of fluorescent collodetrinite and liptodetrinite and non-fluorescent inertodetrinite (right). Note the lowered fluorescence intensity due to oxidation along cleats in the collotelinite (sample 4473A, 17.78–25.40 cm). **C:** Mainly liptodetrinite (Ld) in groundmass of fluorescent collodetrinite (Cd) (sample 4473A, 17.78–25.40 cm). **D:** Exsudatinites expelled into small cleat (arrow) (sample 4473A, sample 17.78–25.40 cm). All photographs in reflected light, blue-light irradiation and water immersion. Scale bar ~ 30 μm.

observed (Fig. 25). Pyrite varies between 0.2 and 1.8 vol.% and the content of detrital minerals amounts to 6.0 vol.% (carbominerite: 19.0 vol.%).

**Seam T4.** In West Lulu-1 the seam is characterised by an increasing content of vitrinite and vitrite+clarite and a contemporaneous decrease in inertinite and vitrinite+durite+clarodurite and inertite from base to top (Figs 19, 26). The vitrinite is strongly fluorescent, and the inertodetrinite is generally fine-grained and allochthonous. Minute and framboidal pyrite is present.

Except for an interval dominated by inertinite and inertinite-rich microlithotypes in approximately the mid-

dle part of T4 in Lulu-1, the seam is also in this well characterised by high contents of vitrinite, generally fluorescent, and vitrite+clarite (Figs 19, 26). The inertinite in the inertinite-rich interval is composed of high-reflecting pyrofusinite, semifusinite, macrinite and fine-grained, relatively well-sorted inertodetrinite commonly associated with liptinite. Char is observed in the uppermost part of the seam (see Petersen 1998). Detrital mineral matter does not exceed 1.6 vol.% in the majority of the seam. However, in the uppermost part it increases to 6.6 vol.% (carbominerite 29.0 vol.%). Likewise the pyrite content, part of which is framboidal, increases to 4.2 vol.%. Liptodetrinite, sporinite, cutinite and resi-

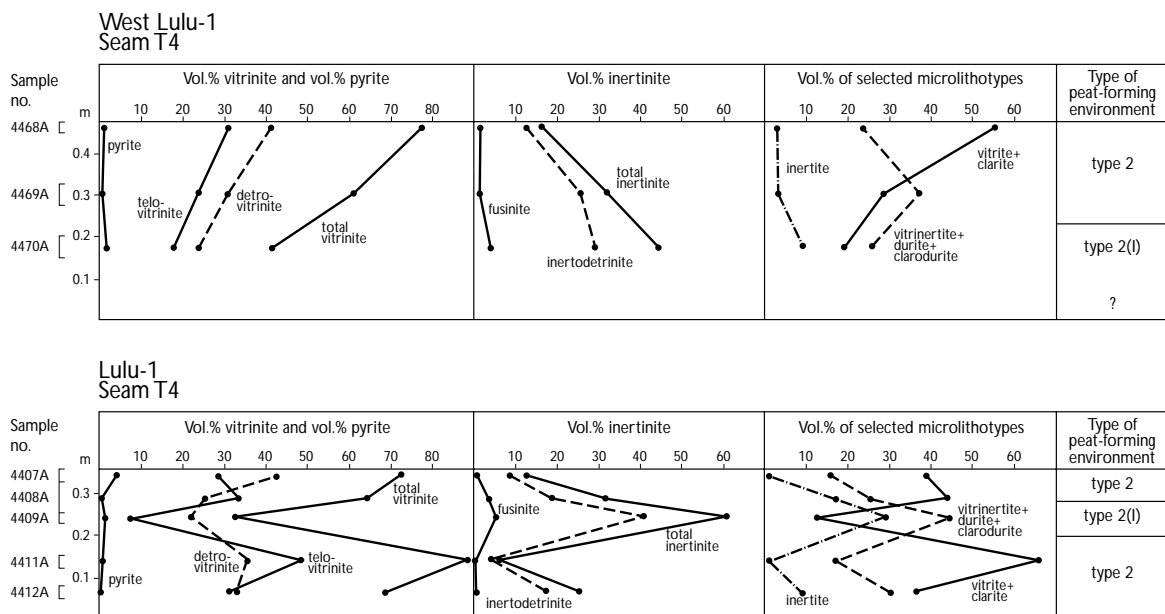


Fig. 26. Coal petrographic composition of seam T4 in the West Lulu-1 and Lulu-1 wells.

nite constitute the liptinite maceral group throughout the seam in both wells, and the content lies between 1.8 and 7.0 vol.%. The highest content of a single liptinite maceral is 4.2 vol.% (liptodetrinite, sample 4470, West Lulu-1), but in general individual liptinite macerals constitute not much more than 1 vol.%.

In Amalie-1 well T4 is again dominated by vitrinite (76.6–88.0 vol.%) and vitrinite+clarite (59.8–61.0 vol.%) (Fig. 19). Char and pyrolytic carbon have been observed. Due to the high rank of the coal in this well, and thus the absence or only very weak fluorescence of the liptinite macerals, the liptinites could only occasionally be distinguished.

**Mudstones.** Four coaly mudstone or thin coal laminae samples from the West Lulu-3 and West Lulu-1 wells reveal an organic petrographic composition very similar to the main coal seams. The vitrinite maceral group dominates (41–86 vol.%) followed by the inertinite maceral group (8–29 vol.%). The liptinite content varies from 5 to 11 vol.%. Carbominerite, vitrite, duroclarite and vitrinerite are the primary microolithotypes.

### Screening data

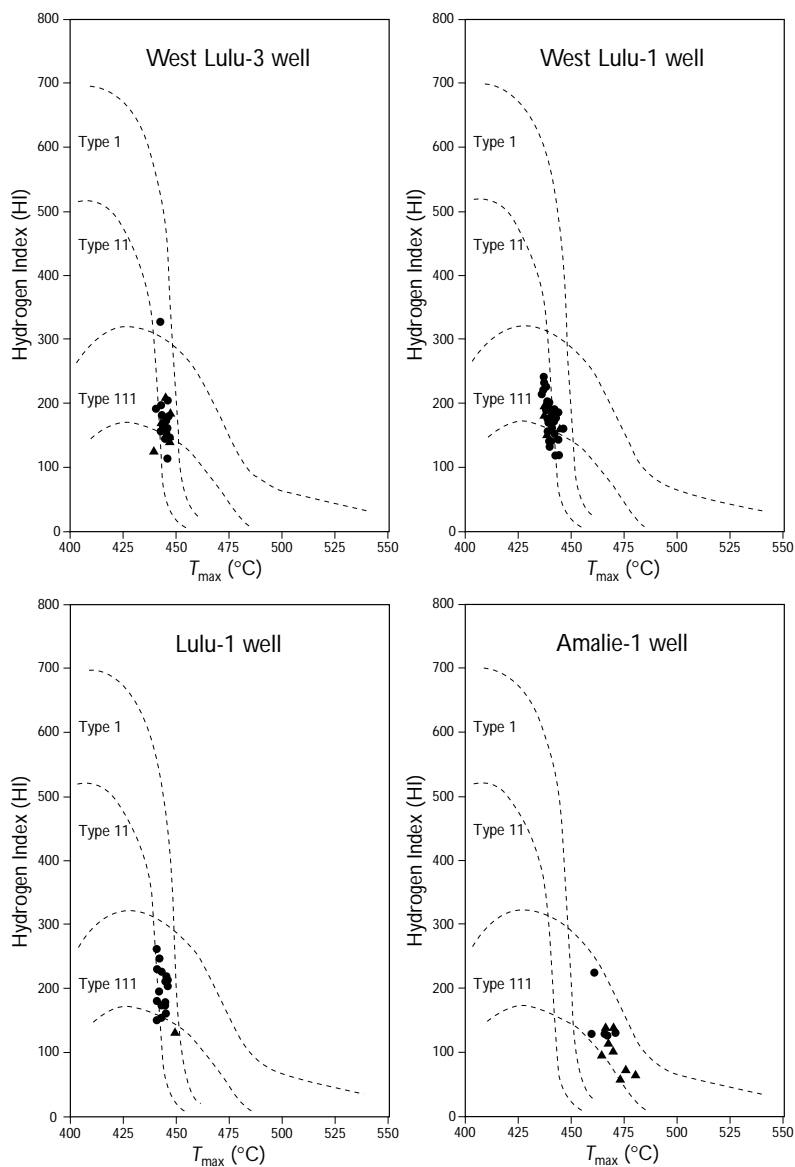
**West Lulu-3.** A total of 29 coal and coaly mudstone samples were analysed (Fig. 6).  $T_{max}$  values range between 439°C and 447°C and average 444°C (Fig. 27). Four extracted coal samples do not provide a change in the  $T_{max}$

values compared to the untreated counterparts. In the 20 coal samples hydrogen index (HI) values range between 118 and 331 (average: 178), but with the majority below 200 (Fig. 27). The HI values range between 128 and 211, average 172, in the coaly mudstone samples. In this well coal seam R1 has the highest average HI value and the highest average thermal extracted and generated petroleum content,  $S_1+S_2 = 140.45$  mg HC/g rock (Table 11). The sample with a HI = 331 has a  $S_1+S_2$  content of 253.84 mg HC/g rock, which is considerably above the average, and the content thus has a strong influence on the average  $S_1+S_2$  value of seam R1.

**West Lulu-1.** A total of 44 coal and coaly mudstone samples were analysed (Table 5). The  $T_{max}$  values range between 436°C and 446°C and average 440°C (Fig. 27). No change in the  $T_{max}$  values is observed during pyrolysis of extracted samples. The HI values range between 126 and 242 in 38 coal samples and between 142 and 195 in 6 coaly mudstone samples averaging 180 and 168 respectively (Fig. 27). The highest average HI values on the basis of individual seams is found in seams T2, T3 and T4, with an average HI of 222 in seam T3 as the maximum, and the lowest values in seams R1a and R1 (Table 11).

Average thermal extracted and generated petroleum contents,  $S_1+S_2$ , are likewise highest in seam T3 (164.11 mg HC/g rock) and lowest in seam R1 (122.85 mg HC/g rock) (Table 11).

Fig. 27. Hydrogen Index vs.  $T_{max}$  plot of coal and coaly mudstone samples from the West Lulu-3, West Lulu-1, Lulu-1 and Amalie-1 wells. The samples plot within the band of typical kerogen type III. Note a tendency to higher HI values from West Lulu-3, over West Lulu-1 to Lulu-1, and the overlap of the coal and coaly mudstone samples. The lower HI values obtained from the Amalie-1 samples are caused by the higher maturity of the organic matter ( $\%R_m = 1.3$ ).  
 ●: coal; ▲: coaly mudstone.



*Lulu-1 well.* A total of 16 coal samples and 2 coaly mudstone samples were analysed (Fig. 8). The  $T_{max}$  ranges between 440°C and 449°C with an average of 443°C (Fig. 27). Extracted samples and their untreated counterparts show more or less similar  $T_{max}$  values. In the coal samples HI varies between 152 and 263, averaging 200, and in the 2 coaly mudstones HI is 133 and 157. Seam T4 has the highest average HI (HI = 222) in this well (Table 11). Seam T2 gives the highest average thermal extracted and generated petroleum contents,  $S_1+S_2 = 163.19$  mg HC/g rock, and seam R1 the lowest value (143.24 mg HC/g rock) (Table 11).

*Amalie-1 well.* Five coal samples and 8 coaly mudstone samples were analysed in this well (Fig. 9). The  $T_{max}$  varies between 459°C and 480°C with an average of 468°C (Fig. 27). The  $T_{max}$  value of an extracted sample is very similar to the untreated counterpart. The HI lies between 129 and 225 in the coal samples and between 60 and 140 in the coaly mudstones, averaging 149 and 99 respectively (Fig. 27). The highest HI value of 225 is derived from a thin coal layer not related to one of the established seams. Seam T4 has the highest average thermal extracted and generated petroleum content of all seams in the Amalie-1 well (Table 11).



Table 11. Average Hydrogen Index and average  $S_1+S_2$  for the Bryne Formation coals

Well	Seam	Average Hydrogen Index (mg HC/g TOC)	Average $S_1+S_2$ (mg HC/g rock)
West Lulu-2*	T4	215	182.30
West Lulu-1	T4	217	152.59
Lulu-1	T4	222	159.62
Amalie-1	T4	131	110.84
West Lulu-2*	T3	203	181.49
West Lulu-1	T3	222	164.11
West Lulu-2*	R2	186	160.83
West Lulu-2*	T2	205	165.80
West Lulu-3	T2	167	129.94
West Lulu-1	T2	177	139.37
Lulu-1	T2	182	163.19
West Lulu-3	R1a	148	109.06
West Lulu-1	R1a	160	140.52
West Lulu-2*	R1	208	167.38
West Lulu-3	R1	194	140.45
West Lulu-1	R1	164	122.85
Lulu-1	R1	201	143.24
Amalie-1	R1	129	85.95

\*data from Petersen *et al.* (1996)

Table 12. Cleo-1 well: screening data

Sample type	Depth (m)	TOC (wt%)	$T_{max}$ (°C)	$S_1$ (mg HC/g rock)	$S_2$ (mg HC/g rock)	HI	PI	
Core	4602.84	72.16	443	6.33	186.68	259	0.03	
	4603.14	3.21	452	0.37	1.84	57	0.17	
	4603.57	72.06	447	6.90	165.40	230	0.04	
	4605.78	2.73	467	0.35	1.90	70	0.16	
	4608.53	2.57	456	0.26	2.40	93	0.10	
	4609.74	3.55	447	0.33	4.90	138	0.06	
SWC	4551	28.50	447	6.56	60.11	211	0.10	
	4553	62.90	437	19.14	147.81	235	0.11	
	4554	31.89	490	3.83	60.63	190	0.06	
	4563	0.73	437	0.14	0.55	75	0.20	
	4572	5.40	439	1.34	6.94	129	0.16	
	4579	0.60	440	0.11	0.37	62	0.23	
	4605	0.69	443	0.13	0.56	81	0.19	
	4607	0.43	453	0.33	0.79	184	0.29	
	4615	0.40	440	0.10	0.34	85	0.23	
	4639	1.30	455	0.14	0.76	58	0.16	
	4641	1.37	444	0.25	1.47	107	0.15	
	4654	11.63	455	2.40	13.03	112	0.16	
	4660	2.98	445	1.10	4.17	140	0.21	
	Cuttings	4563	1.37	444	0.15	0.69	50	0.18
		4572	2.20	446	0.47	1.89	86	0.20
4581		1.58	444	0.32	1.10	70	0.23	
4590		1.50	442	0.32	0.95	63	0.25	
4599		1.06	442	0.24	0.91	86	0.21	
4609		2.44	444	0.46	2.36	97	0.16	
4618		1.18	443	0.21	1.02	86	0.17	
4627		1.55	448	0.30	1.45	94	0.17	
4636		1.18	445	0.22	0.80	68	0.22	
4645		0.91	447	0.10	0.50	55	0.17	
4654		1.69	448	0.31	0.98	58	0.24	
4663		0.55	445	0.16	0.35	64	0.31	
4673		0.50	438	0.12	0.26	52	0.32	
4682	0.62	438	0.33	0.50	81	0.40		
4691	0.65	440	0.20	0.29	45	0.41		
4700	0.40	441	0.07	0.24	60	0.23		
4709	1.10	442	0.20	0.50	45	0.29		
Extracted cuttings	4554	3.05	448	0.12	2.65	87	0.04	
	4584	0.88	445	0.04	0.42	48	0.09	
	4621	2.15	445	0.12	1.77	82	0.06	
	4657	1.32	446	0.07	0.87	66	0.07	
	4694	1.25	435	0.06	0.74	59	0.07	

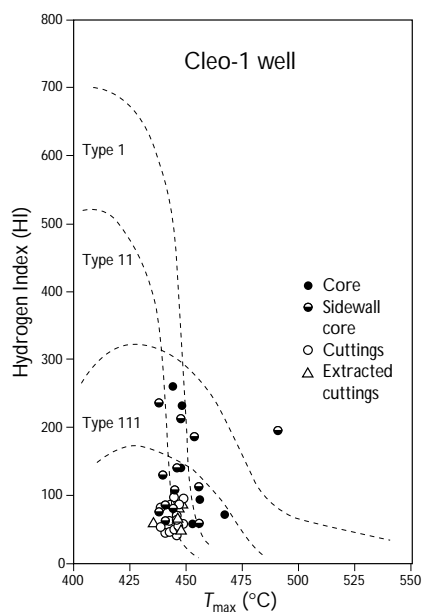


Fig. 28. Hydrogen Index vs.  $T_{max}$  plot of core samples, sidewall core samples, cuttings and extracted cuttings from the Cleo-1 well. The majority of the samples show low HI values corresponding to kerogen type IV.

*Cleo-1 well.* Two vitrinite lenses (twigs ?) and 4 coaly mudstone samples from the cored interval were analysed (Fig. 10).  $T_{max}$  values from the core samples range between 443°C and 467°C with the lowest values obtained from vitrinite lenses (Fig. 28; Table 12). The vitrinite lenses show comparatively high HI values, 259 and 230, whereas the coaly mudstones give HI values between 57 and 138. An additional 13 side wall cores, 18 cuttings and 5 extracted cuttings derived from *c.* 4551–4709 m depth are shown in Figure 28 and in Table 12. Seventy-five per cent of the samples exhibit  $T_{max}$  values between 440°C and 448°C, whereas the HI values for all samples varies between 39 and 235 with the majority below 100.

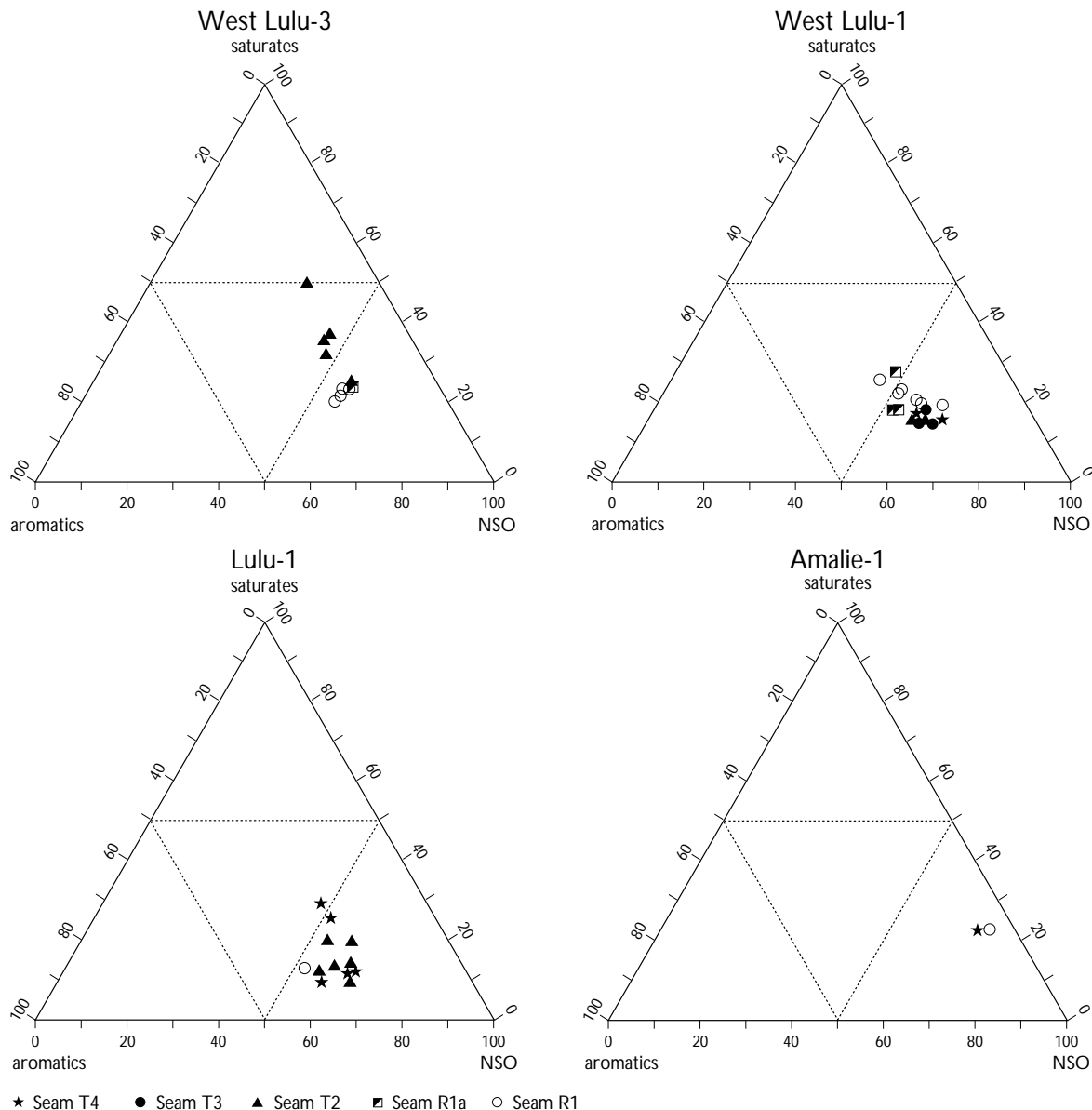


Fig. 29. Composition of the asphaltene-free solvent extract fraction from samples from coal seams R1, R1a, T2, T3 and T4 in the West Lulu-3, West Lulu-1, Lulu-1 and Amalie-1 wells. The extract fractions show dominance of NSO compounds.

### Extracts

A total of 12 samples in West Lulu-3, 18 samples in West Lulu-1, 12 samples in Lulu-1 and 6 samples in Amalie-1 were extracted for further detailed organic geochemical analyses. The extracts from both coal and coaly mudstone samples in all the wells are dominated by NSO compounds which in general exceed 50% (Fig. 29). In the West Lulu-1 and Lulu-1 wells aromatic

compounds are second and generally exceed 22%. This picture is different from the West Lulu-3 extracts where in only a few cases do the aromatic compounds exceed 22%, whereas the saturates in general constitute more than 23%. Four of the extracts from Amalie-1 likewise have a higher content of saturates, in particular in extracts from the coal samples. A single extract (4609.74 m) from Cleo-1 is dominated by NSO compounds (79.7%) followed by saturates (11.6%) and aromatics (8.7%).

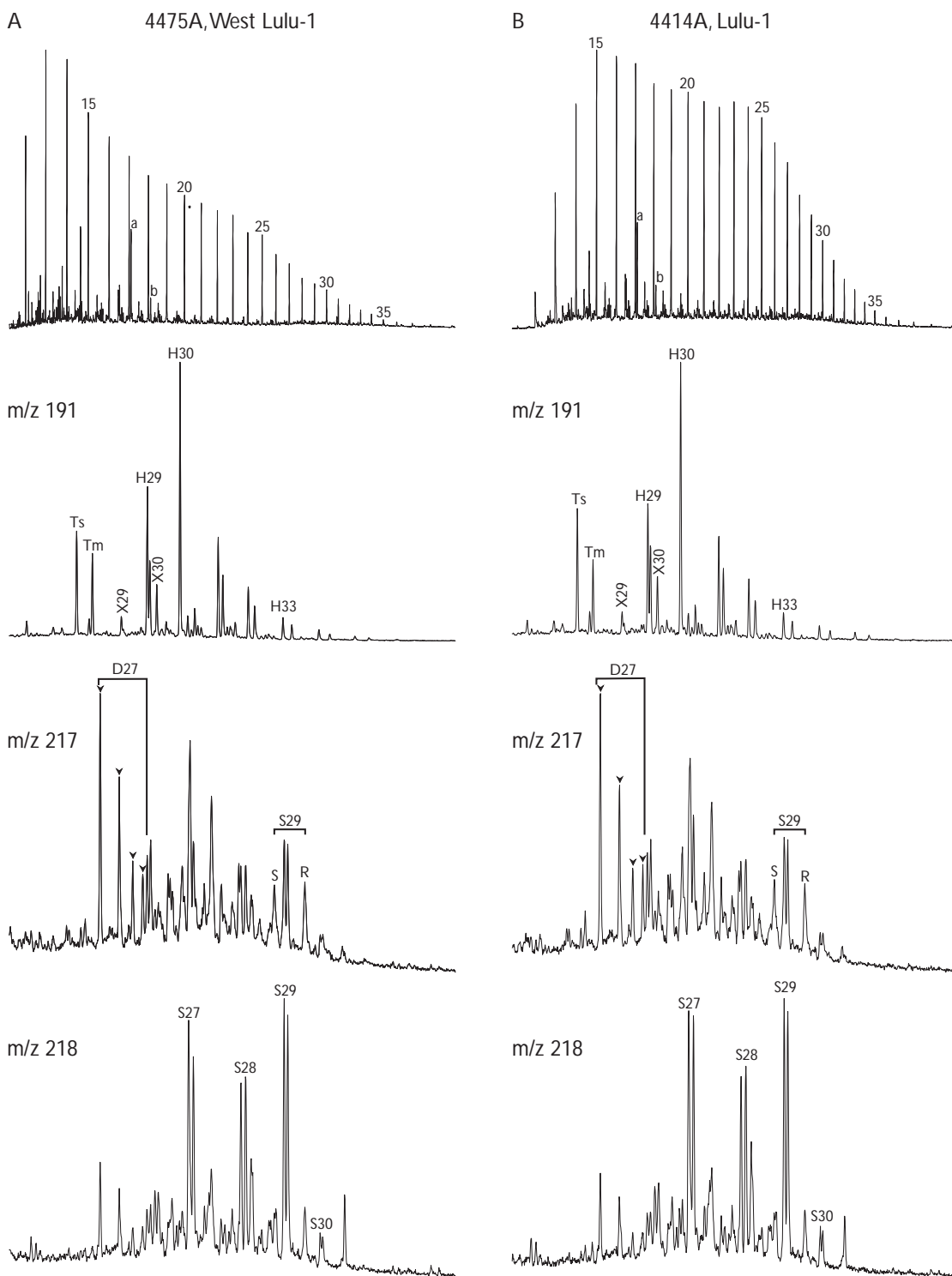


Fig. 30. Examples of gas chromatograms and  $m/z$  191,  $m/z$  217 and  $m/z$  218 ion fragmentograms from saturated fractions of solvent extracts of Bryne Formation coals. **A:** sample 4475A, seam T3, West Lulu-1 well; **B:** sample 4414A, seam T2, Lulu-1 well. Annotation: numbers on GC-traces refer to  $n$ -alkane carbon numbers, a: pristane, b: phytane; Ts: trisnorhopane, Tm: trisnorhopane, H29: norhopane, H30: hopane, H33, trishomohopane, X29: dianorhopane, X30: diahopane; D27:  $C_{27}$  diasteranes (4 isomers), S27, S28, S29 and S30:  $C_{27-30}\alpha\beta\beta$  regular steranes, S:  $C_{29}\alpha\alpha\alpha(20S)$ , R:  $C_{29}\alpha\alpha\alpha(20R)$ . Note the high proportions of  $C_{27}$  steranes and the presence of  $C_{30}$  steranes indicative of marine influence during deposition.

## Gas chromatography

The typical GC trace of the saturated fraction is characterised by a light-end-biased *n*-alkane distribution and a predominance of the  $nC_{14}$  to  $nC_{17}$  range (Fig. 30). The pristane/phytane ratios (Pr/Ph) are in general higher than 2.5 for all samples, but differences between wells are observed. The highest Pr/Ph ratios are present in the West Lulu-3 well, where the ratios range between 5.19 and 7.77, averaging 5.98, with the highest values occurring in the coaly mudstones (Tables 7–10). These high values are comparable to the values obtained in seams R1 and R2 in West Lulu-2 (Petersen *et al.* 1996). The Pr/Ph ratios decrease in a seaward direction and average 3.47 in West Lulu-1, 2.88 in Lulu-1 and 2.55 in Amalie-1. The carbon preference index (CPI) calculated from  $2(C_{23}+C_{25}+C_{27}+C_{29})/[C_{22}+2(C_{24}+C_{26}+C_{28})+C_{30}]$  in any sample never exceeds 1.15 and is close to 1 for all samples from the wells (Tables 7–10).

In the Cleo-1 well, the Pr/Ph ratio is 1.57 and the CPI is 1.07 (Table 13).

## Gas chromatography/mass spectrometry

**Pentacyclic triterpanes.** The distribution of the hopanes is dominated by the regular hopanes, with a maximum at  $C_{30}$ , and with the concentration of extended hopanes decreasing with increasing carbon number (Fig. 30). The 22S/(22S+22R) epimer ratios of the 17 $\alpha$ (H),21 $\beta$ (H)  $C_{31}$ – $C_{35}$  extended hopanes range between 0.57 and 0.67, with the majority around 0.60. The ‘ $C_{35}$ -homohopane index’, defined as  $C_{35}/\sum C_{31-35}$  (Peters & Moldowan 1991), varies between wells and seams and laterally within seams (Table 14). Even though these differences are rather small a consistent landward–seaward trend is present in the data. The most landward wells, West Lulu-3 and West Lulu-1, relative to the palaeo-shoreline, have average indices (coal seams and mudstones) of 0.013 and 0.017 respectively, whereas the Lulu-1 and Amalie-1 wells situated seaward have average indices of 0.034 and 0.044 respectively. Individual seams likewise show increasing ratio in a seaward direction, e.g. the index increases from 0.011 to 0.045 in seam R1. Except for Amalie-1, seams T2, T3 and T4 have higher indices than seams R1 and R1a.

In the Lulu-1 and Amalie-1 wells 28,30-bisnorhopane is present.

Epimer ratios of  $C_{31}$ – $C_{35}$  extended hopanes lie between 0.56 and 0.63 in the single sample from the Cleo-1 well, and the  $C_{35}$ -homohopane index is 0.028.

Table 13. Cleo-1 well: GC data and composition of solvent extract fraction (asphaltene-free)

Depth (m)	Pr/Ph	CPI	EOM	Sat (%)	Aro (%)	Polars (%)
4609.74	1.57	1.07	25	12	9	79

Table 14. Average of  $C_{35}$ -homohopane index

Well Seam	W. Lulu-3	W. Lulu-1	Lulu-1	Amalie-1
T4	-	0.023	0.037	0.034
T3	-	0.021	-	-
T2	0.016	0.020	0.034	-
R1a	0.012	0.016	-	-
R1	0.011	0.013	0.020	0.045
Mudstones	0.010	0.013	-	0.047
Average*	0.013	0.017	0.034	0.044

\*average of coals and mudstones

**Steranes.** With the exception of an outlier of 0.25, the  $\alpha\alpha\alpha 20S/(20S+20R)$  epimer ratios of the  $C_{29}$  steranes range between 0.36 and 0.51, with the majority lying between 0.45 and 0.50 (Tables 7–10). The range of the  $\alpha\beta\beta 20(S+R)/[\alpha\beta\beta 20(S+R)+\alpha\alpha\alpha 20(S+R)]$  ratio is between 0.44 and 0.66, except for an outlier of 0.37, but the majority (73%) lie between 0.50 and 0.64 (Tables 7–10).

The relative proportions of  $C_{27}\alpha\beta\beta$ ,  $C_{28}\alpha\beta\beta$  and  $C_{29}\alpha\beta\beta$  compared to the total amounts of the three steranes are shown in Figure 31 and Tables 7–10. The coals of the West Lulu-3 well are characterised by the highest contents of  $C_{29}$  sterane and the lowest contents of  $C_{27}$  sterane averaging 59.2% and 15.0% respectively. In the coals of the West Lulu-1 well the  $C_{29}$  sterane content has fallen to an average of 45.2% and the  $C_{27}$  sterane content has increased to an average of 27.0% (Fig. 31). These trends are continued in the coals of the Lulu-1 and Amalie-1 wells where the average  $C_{29}$  sterane content has decreased to 38.0% and 35.8% respectively and the average  $C_{27}$  sterane content has increased to 33.5% and 35.8% respectively (Fig. 31). Thus, generally the average content of  $C_{29}$  steranes in a well decrease and that of  $C_{27}$  steranes increase in a seaward direction, and this is also valid within a seam if it is followed laterally in a landward–seaward direction (e.g. seam R1, Fig. 31; Tables 7–10). Furthermore, it is evident that T-seams (seams T2, T3 or T4) compared to R-seams (seams R1 and R1a) in a well generally have a higher content of

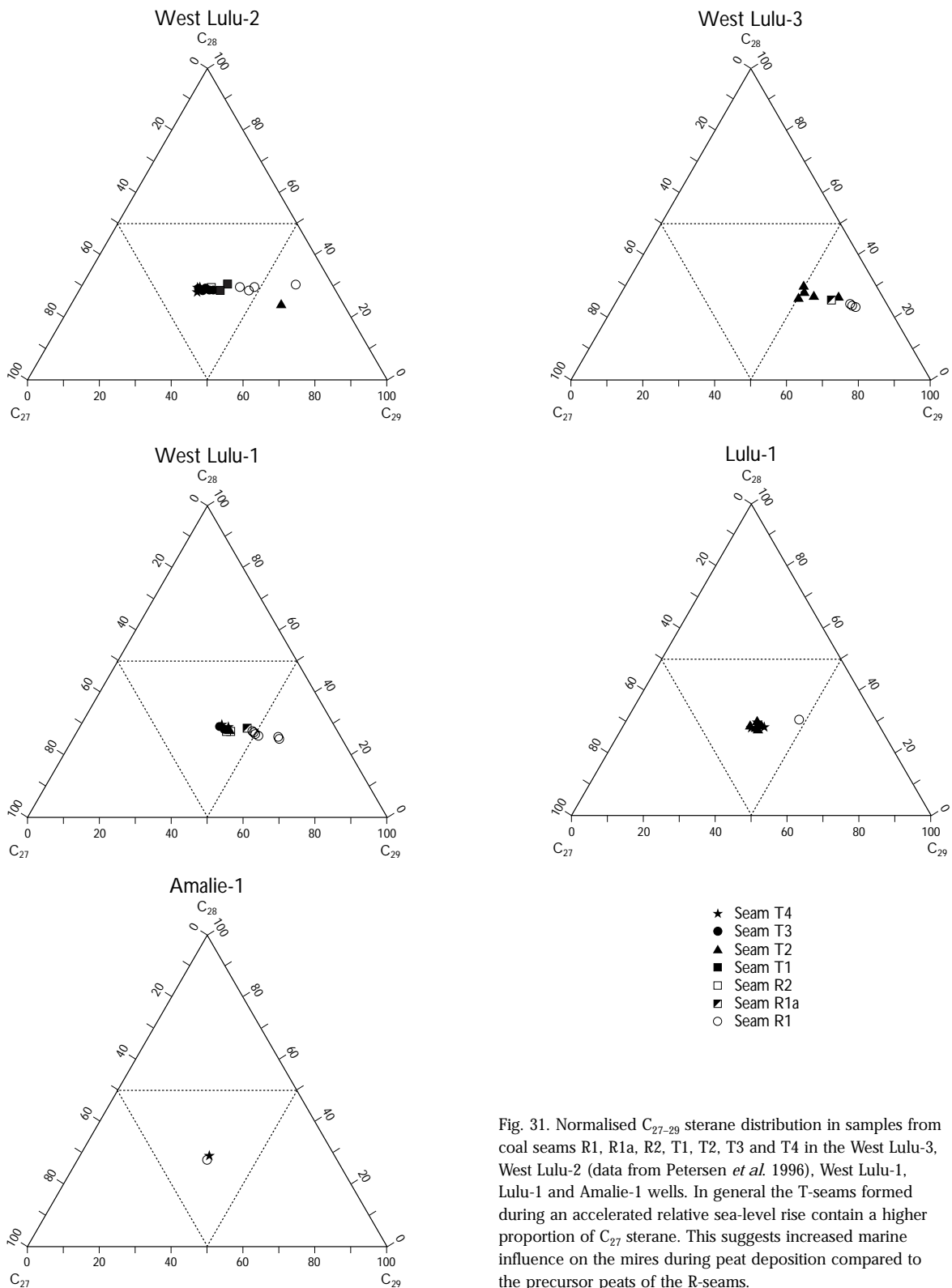


Fig. 31. Normalised C<sub>27-29</sub> sterane distribution in samples from coal seams R1, R1a, R2, T1, T2, T3 and T4 in the West Lulu-3, West Lulu-2 (data from Petersen *et al.* 1996), West Lulu-1, Lulu-1 and Amalie-1 wells. In general the T-seams formed during an accelerated relative sea-level rise contain a higher proportion of C<sub>27</sub> sterane. This suggests increased marine influence on the mires during peat deposition compared to the precursor peats of the R-seams.

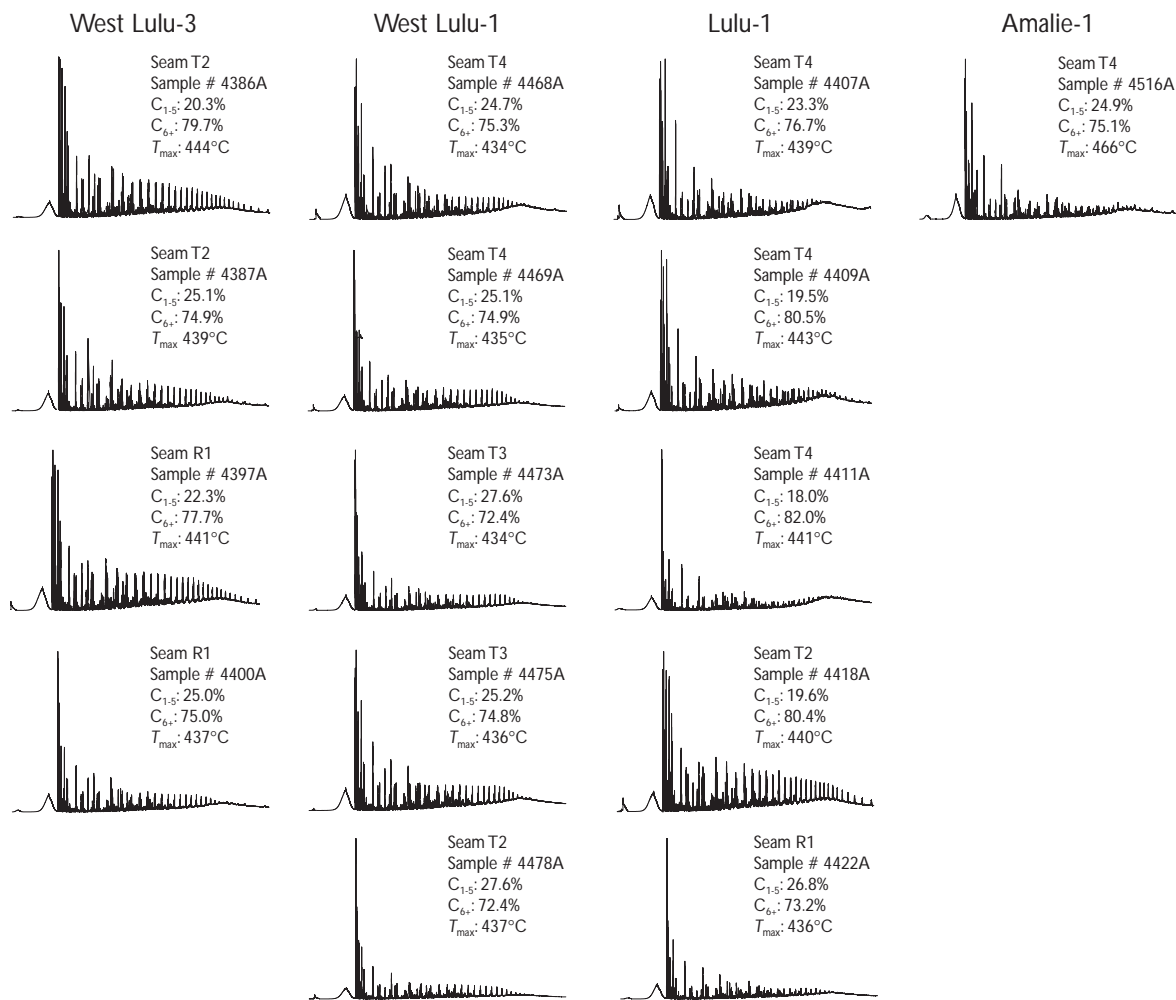


Fig. 32. Pyrograms of the 15 solvent-extracted coal samples from four wells in the Søgne Basin. The pyrolysates are characterised by low molecular weight aromatic/phenolic compounds and normal alkanes/alkenes.

C<sub>27</sub> steranes. However, this difference diminishes in a seaward direction as shown in the Amalie-1 well (Fig. 31; Table 10).

The  $\alpha\alpha\alpha 20S/(20S+20R)$  epimer ratio of the C<sub>29</sub> steranes in the Cleo-1 well sample is 0.44, while the  $\alpha\beta\beta 20(S+R)/[\alpha\beta\beta 20(S+R)+\alpha\alpha\alpha 20(S+R)]$  ratio is 0.53. The distribution of the C<sub>27</sub>, C<sub>28</sub> and C<sub>29</sub> regular steranes are 11%, 23% and 66% respectively.

### Pyrolysis-gas chromatography

A total of 15 coal samples were selected from the West Lulu-3, West Lulu-1, Lulu-1 and Amalie-1 wells. The

sample set thus represents a landward (West Lulu-3) to seaward (Amalie-1) transect with respect to the palaeo-shoreline. The samples were selected from seams R1 (West Lulu-3 and Lulu-1 wells), T2 (West Lulu-3, West Lulu-1, Lulu-1 wells), T3 (West Lulu-1 well), and T4 (West Lulu-1, Lulu-1, and Amalie-1 wells). Pyrograms of the samples are shown in Figure 32. Generally, the overall pyrolysate composition is very similar for all samples, but minor differences between individual seams may be detected in the detailed pyrolysate compositions. Except for sample 4397A from West Lulu-3, pyrolysates of seam R1 show very modest proportions of unresolved components, and prominence of a number of low molecular weight aromatic/phenolic com-

pounds, notably benzene, alkyl-benzenes, phenol, alkyl-phenols, naphthalene, alkyl-naphthalenes, and 'unknowns' compared to normal alkanes/alkenes. Normal alkanes/alkenes are present at least up to chain-lengths of 26 carbon atoms. Sample 4397A, which was collected close to the top of seam R1, shows some resemblance to samples of the overlying seam T2. T2 samples generally yield higher proportions of *n*-alkanes/alkenes, which may be present up to chain lengths of at least 35 carbon atoms, and a minor envelope of unresolved components centred around *n*C<sub>25</sub>. Aromatic and phenolic moieties are of minor importance compared to *n*-alkyl moieties. Samples of seam T3, which was sampled only in the West Lulu-1 well, are somewhat depleted in *n*-alkyl moieties compared to the T2 samples discussed above, both with respect to abundance relative to other resolved components, and with respect to maximum chain-length. This is even more pronounced in samples of seam T4.

Although *n*-alkyl components are prominent in a number of samples, aromatic/phenolic moieties and 'unknowns' tend to predominate. In particular, this is observed in the sample collected from the Amalie-1 well, which is of higher rank or maturity compared to the remainder of the samples. Higher rank/maturity will tend to increase the proportion of aromatic and phenolic moieties.

## Results of the multivariate regression analysis

The multivariate regression analysis was carried out in order to create a model explaining as high a proportion of the variation of  $S_2$  as possible. A model explaining 87% of the variation of  $S_2$  was created, but includes only 51 out of 94 samples (= objects) (Fig. 33, class A). The following 19 variables are regarded as important to the variation of  $S_2$ : TOC, vitrinite (Vit), vitrite (V), clarite (Cl), duroclarite (DC), clarodurite (CD), carbominerite (CM), telinite (Tel), collotelinite (Collotel), collodetrinite (Collodetr), corpogelinite (Corpo), sporinite (Sp), cutinite (Cu), liptodetrinite (Lipto), resinite (Res), fusinite (Fus), semifusinite (Semif), inertodetrinite (Inerto) and macrinite (Mac). In contrast to an earlier model based only on data from West Lulu-2 (Petersen *et al.* 1996), the  $T_{max}$  values can be deleted from the model without any loss of information. Petersen *et al.* (1996) drew attention to the uncertainty by correlating  $T_{max}$  due to the small variance in maturity, and this fact may also be valid for the present data set which only shows limited variance in  $T_{max}$ . With a correlation coefficient of 0.94 and an average prediction error on  $S_2$  of 11, the predictive ability of the model is good (Fig. 33, class A). The relatively low slope of 0.88 indicates, however, a lack in the model's response, which implies that the petrographic composition together with the TOC values cannot fully explain the variation in  $S_2$ .

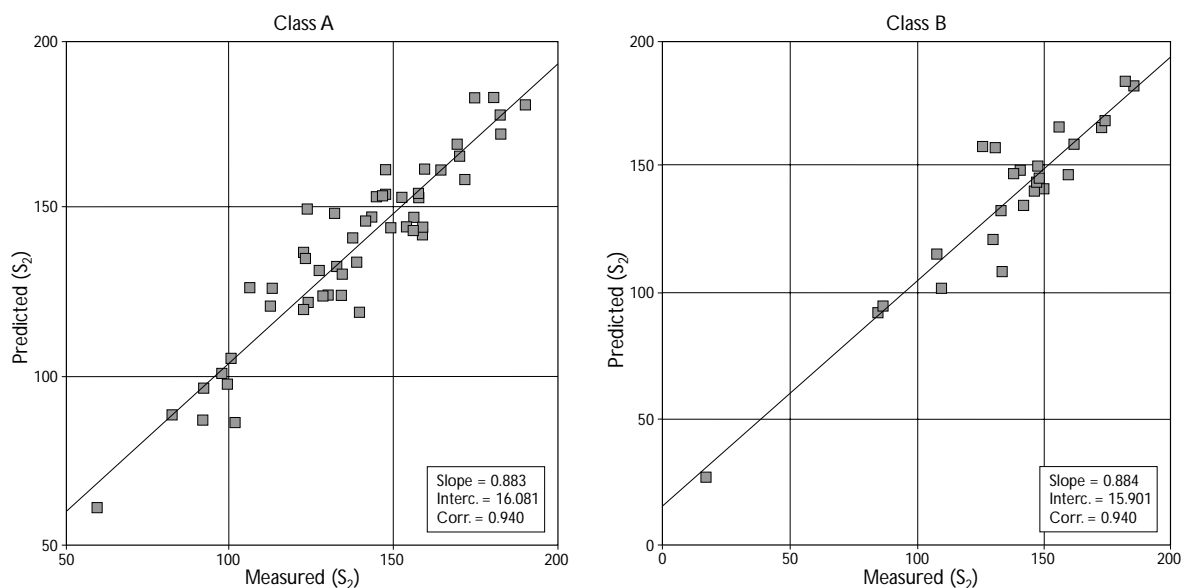


Fig. 33. Predicted vs. measured  $S_2$  for classes A and B. The predicted values are responses from the partial least squares regression (PLSR) model. Correlations of 0.94 are considered to be reasonable, though slopes of 0.88 indicate a lack in the model's response.

Another model, comprising the same variables as the first model, was formed. This model included 26 of the remaining 43 samples. The predictive ability of this model is in the same order as the previous model (Fig. 33, class B), but with a somewhat higher (16) average prediction error. The difference between the two models was studied using SIMCA. The discrimination power of the individual variables indicates that the separation into two classes is primarily caused by duroclarite together with minor contributions from clarite, coropogonite, cutinite and fusinite. Examination of the raw data did not reveal a clear trend in the dataset, which could satisfactorily explain the separation into two classes. The bar graph shows the membership of individual samples to either class A or class B (Fig. 34). The samples exhibit a slightly higher membership to their own class than to the other class. The separation is however weak, and the separation into two classes cannot be justified from these results.

Consequently a third group was formed comprising the samples from classes A and B, with the same variables as used above. A few extra samples could be added to the combined group, ending with 81 of the 94 samples included in the model. The consequence of including more samples in the model is a weaker correlation, and only 71% of the variation in  $S_2$  can be explained. The response is much weaker with a correlation coefficient of 0.85 and a slope of 0.73 (Fig. 35). The average prediction error is satisfactory at 14, but the variation in the prediction error is high. The general applicability of the model is, however much higher than for the previous two models, since more samples covering a wider span of variance are included. The low slope in the response line emphasises that other factors than the petrographic composition and the TOC values have significant influence on the  $S_2$  value. Although the model appears to be relatively weak, it is possible to study the relations between the remaining petroleum generative potential and the petrographic characteristics, and it is possible to identify individual parameters with major influence on  $S_2$ , and those with little or no influence.

Samples not fitting the model were regarded as outliers. The raw data for the outliers were studied in order to explain why they did not fit the model. The outliers fell into two major groups: those having very high  $S_2$  values and those having very low  $S_2$  values. The first group comprises samples 291941, 291943, 291997 (Petersen & Andsbjerg 1996) and 4400A which all have  $S_2$  values above 200. The second group comprises samples 291945, 291969, 291974, 4515A, 4516A and 4521A which have  $S_2$  values around 100 or very low values.

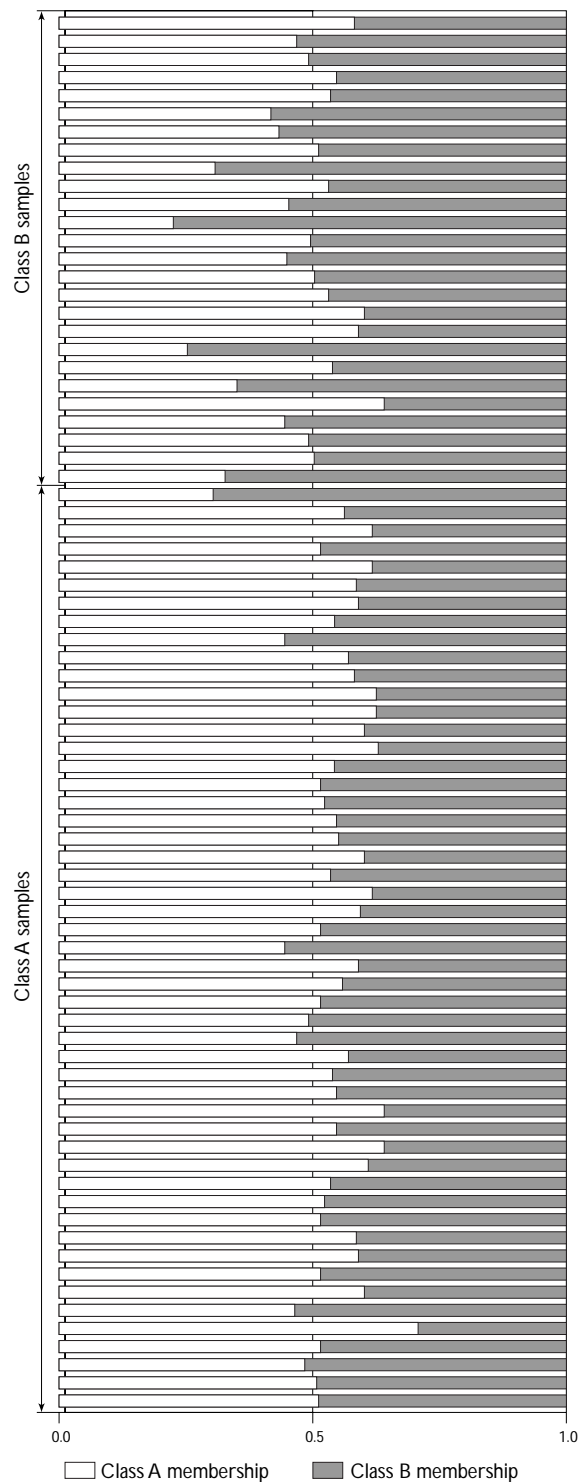


Fig. 34. Bar graph showing the individual sample's membership to either class A or class B. The samples exhibit a slightly higher membership to their own class; however, the separation is weak.



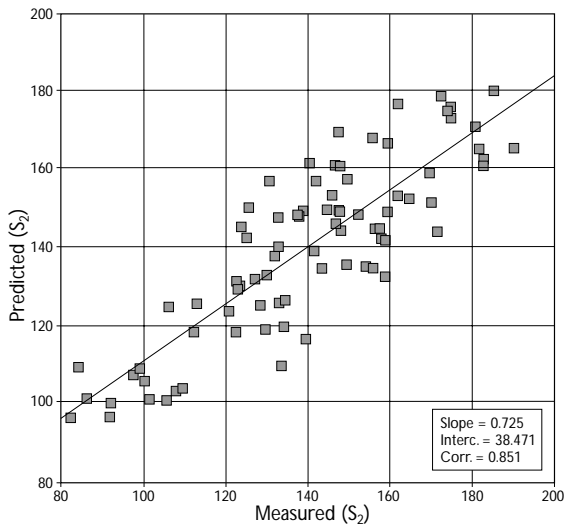


Fig. 35. Predicted vs. measured  $S_2$  for the combined class comprising 81 samples of the 94 samples included in the model. The model explains 71% of the variation in  $S_2$ . Compared to class A and class B a weaker response is shown by a correlation coefficient of 0.85 and a slope of 0.73. The low slope of the response line emphasises that other factors than the petrographic composition and the TOC values have significant influence on  $S_2$ . However, the general applicability of the model is higher than for models A and B since more samples covering a wider span of variance are included.

It is likely that the inclusion of more samples with  $S_2$  values in the low and high end would result in inclusion of the outliers in the model due to broadening of the models 'tolerance'.

Three other samples that do not fit the model are 4407A, 4487A and 4504A. Extreme  $S_2$  values cannot explain these outliers, but some other 'extraordinary' characteristics compared to the samples fitting the model could be the reason: sample 4407A has an unusually low TOC value (48.24 wt%), sample 4487A has a relatively high clarite content (14 vol.%) together with a low inertinite content (9 vol.%), and finally 4504A has a high TOC value (80.1 wt%) combined with a relatively low  $S_2$  value (101.4 mg HC/g rock).

## Discussion

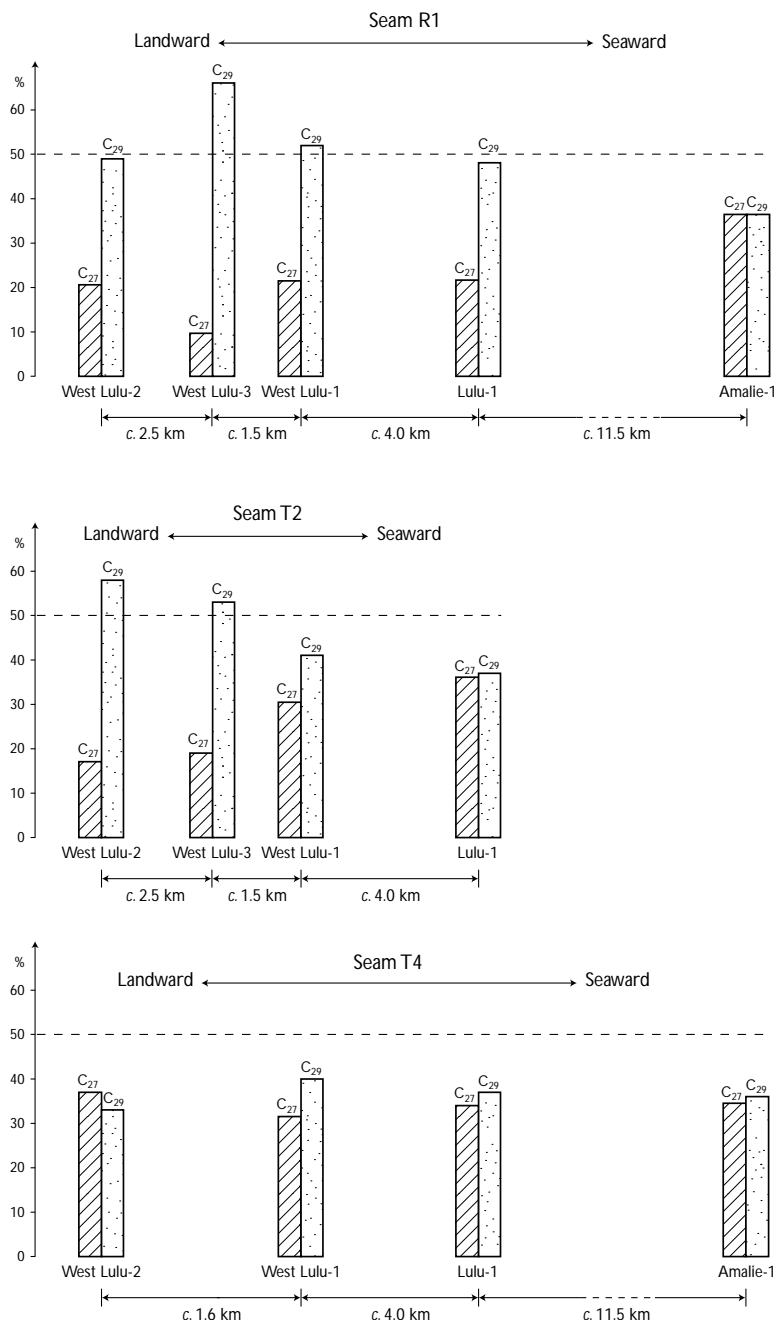
### *Peat-forming mires and depositional development of the coal-bearing succession*

The types of mire environments indicated to the right on each coal seam log (Figs 18, 20, 21, 24, 26) is based

on Petersen (1994). Type 1 is a wet, open mire represented by a limnic coal facies characterised by allochthonous organic components and a high content of allochthonous inorganic components (> 20 vol.%). Type 2 is a low-lying, wet and generally anoxic mire, commonly isolated from active siliciclastic depositional systems, and represented by a vitrinite-rich coal facies formed by autochthonous peat accumulation. The vitrinite content is > 50 vol.%, the inertinite < 40 vol.% and the mineral content < 20 vol.%. The Type 2 mire is called Type 2(I) if considerable amounts of allochthonous, hypalochthonous or *in situ* formed pyroinertinite is present. The Type 3 mire environment is the driest of the three types and can be divided into two subenvironments, Type 3a and 3b. Both are represented by inertinite-rich coal facies: in Type 3a the vitrinite content is < 30 vol.% and the inertinite content > 60 vol.%, and in Type 3b the vitrinite content is between 30 and 50 vol.% and the inertinite content between 40 and 60 vol.%. These coal facies were formed due to a fluctuating watertable in the precursor mires, maybe associated with doming of the peat surface, which favoured periodic oxidation of the organic matter.

The siliciclastic sediments encasing the coal seams in the wells indicate that peat accumulation occurred in the vicinity of the palaeo-coastline in a coastal plain setting, and peat formation thus took place in coastal mires occasionally influenced by saline water (see below; Figs 6–9). The laterally extensive seam R1 is in the most landward position relative to the ancient shoreline overlying fluvial channel (West Lulu-3) and fluvial or tidal channel (West Lulu-2; Petersen & Andsbjerg 1996) deposits, and in a seaward direction shoreface or strandplain (West Lulu-1) and lagoonal (Lulu-1, Amalie-1) deposits. The seam represents in the four wells a wet type 2 mire environment characterised by high contents of vitrinite and fluctuating but generally high contents of vitrinite+clarite (Fig. 18). However, although part of the inertinite in R1 in West Lulu-1 is composed of allochthonous inertodetrinite, a tendency to a decrease in the amount of vitrinite-rich microlithotypes coupled with an increase in inertinite-rich microlithotypes towards the top of the seam may suggest an incipient evolution towards drier conditions. The peat mire evolution at this location would thus be similar to the evolution observed in the West Lulu-2 well (Petersen & Andsbjerg 1996). Varying proportions of inertinite and inertinite-rich microlithotypes in R1 in West Lulu-3 may likewise be attributed to temporarily drier conditions, probably caused by an unstable watertable in the precursor mire. This is further supported by the

Fig. 36. Evolution in the proportion of steranes  $C_{27}$  and  $C_{29}$  in seams R1, T2 and T4 from a landward to a seaward position relative to the palaeo-coastline. A general decrease in the proportion of  $C_{29}$  sterane and associated increase in the proportion of  $C_{27}$  sterane towards the palaeo-shoreline in all three seams suggests stronger brackish-marine influence on the coastal reaches of the ancient mires. In addition, seams T2 and in particular T4 contain a higher proportion of  $C_{27}$  sterane than seam R1, indicating stronger brackish-marine influence on the precursor peat mires of seams T2 and T4.



presence of unsorted possibly oxidation-derived in-  
ertodetrinite and macrinite in the seam together with  
pyrolytic carbon, which may record ignition by light-  
ning strikes, possibly exacerbated during drier periods.  
Pyrite, which may indicate a marine influence during  
peat formation (e.g. Cohen *et al.* 1984; Brown & Cohen  
1995), is only present in low amounts or is absent indi-  
cating a mainly freshwater precursor mire of seam R1.

This is also indicated by the predominance of  $C_{29}$  ster-  
ane (particularly in West Lulu-3), which is often attrib-  
uted to terrestrial contributions to the organic matter  
(Huang & Meinschein 1979; Philp 1994), over  $C_{27}$  ster-  
ane, which is mainly related to marine algae (e.g. Hunt  
1996; Figs 31, 36; Tables 7–10). Seaward, equal amounts  
are achieved in Amalie-1 (Fig. 36), although the higher  
maturity of the Amalie-1 coals may have influenced the

sterane distribution (Dzou *et al.* 1995). Similarly the seam is, with the exception of Amalie-1, characterised by relatively lower  $C_{35}$ -homohopane indices than the other seams, in particular the T-seams (Table 14). The highest index is present in Amalie-1, i.e. in a seaward position. A high homohopane index is believed to indicate highly reducing marine conditions (Peters & Moldowan 1991). In a basinward direction, 28,30-bisnorhopane in seam R1 in Lulu-1 and Amalie-1 may also indicate marine-influenced anoxic conditions during peat deposition in this part of the precursor mire (e.g. Peters & Moldowan 1993).

Although a slight marine influence may be observed in a basinward direction the limited marine signature and prevailing 'terrestrial' nature of the seam composition is in good agreement with the interpretation of the depositional conditions for seam R1 in West Lulu-2 (Petersen & Andsbjerg 1996; Petersen *et al.* 1996). The seam marks the boundary between a lowstand systems tract or early transgressive systems tract and a transgressive systems tract, and peat-formation occurred during early relative sea-level rise and accordingly a low rate of base-level rise. In a landward direction a generally lower regional watertable may have favoured watertable fluctuations promoting both oxidation of the organic matter and wildfires. Seaward a continuously higher-standing watertable caused by a larger influence from the rise in relative sea-level diminished the influence from watertable fluctuations thereby reducing the amount of coal facies recorded in seam R1 in that area.

Continued watertable rise outpaced peat accumulation and in the location of Lulu-1 and Amalie-1 lagoonal conditions were established, whereas open-water mire and lake conditions were established more landward (Figs 6–9). However, presumably a restricted watertable rise was not able to outpace the rate of peat accumulation at the position of West Lulu-2, where the precursor peat of seam R1 continued to accumulate peat. Peat formation was resumed in part of the previously flooded areas when conditions suitable for peat formation were re-established. This resulted in the split of seam R1, and the formation of seam R1a. Seam R1a carries many of the petrographic characteristics of seam R1, and in the position of West Lulu-1 the uppermost part of the seam accumulated in a type 3a mire environment characterised by an inertinite-rich coal facies (Fig. 20). Char particles derived from heat-affected, degassed humified organic matter (peat) and pyrolytic carbon, both indicative of wildfire, have been observed in R1a. In its organic geochemical composition R1a however, records an increased marine influence on the mire envi-

ronment by having higher  $C_{27}$  sterane contents and  $C_{35}$ -homohopane indices than seam R1 (Fig. 31; Tables 7, 8, 14).

Following deposition of the laterally restricted seam R1a continued relative sea-level rise caused a regional rise in the watertable level resulting in formation of open-water mires and lakes, occasionally with deposition of splay sediments, in an area from West Lulu-2 seaward to Lulu-1 (Figs 6–9). Possibly a relative sea-level fall exposed the coastal plain, and a renewed base-level rise linked to a rise in relative sea-level created once again favourable conditions for peat accumulation due to a stagnant high standing watertable and sediment starvation over a large area. However, the transgressive sea hindered peat accumulation in the Amalie-1 area where lagoonal, estuarine channel, tidal flat, possibly lacustrine, shoreface and offshore deposition prevailed after deposition of seam R1 (Fig. 9). An open-water mire may, however, have been established temporarily (carbonaceous mudstone and thin coal, c. 5062 m on Fig. 9). It is possible that this level may be correlatable landward to one of the coal seams, but a correlation is not attempted on the basis of the available data.

According to Petersen & Andsbjerg (1996) the precursor peat of seam T2 accumulated during an accelerated rate of relative sea-level rise which resulted in a more 'wet' coal seam composition. Seam T2 in West Lulu-2 has a variable coal facies composition representing a rather complex succession of mire environment types, including the drier type 3b. This pattern is also seen in West Lulu-3 and West Lulu-1 (Fig. 21). In West Lulu-3 an increase in the content of inertinite and inertinite-rich microlithotypes up through the major part of the seam and a decrease in pyrite content towards the top suggests a freshwater mire with an unstable watertable, at least during deposition of the middle part (type 3b → type 2 → type 3b) of the coal seam. Char and oxidised cutinite and resinite are additional evidence for temporarily drier conditions. Likewise T2 in West Lulu-1 shows an evolution from a wet type 2 mire environment towards a dry type 3a mire characterised by a pronounced content of inertite. Allochthonous fine-grained and occasionally micrograded inertodetrinite, which may be associated with detrital liptinite, may characterise the coal facies of the type 2 mire environment. Such a coal facies with abundant inertodetrinite (well-sorted, rounded, micrograded, microlaminated) also characterises the inertinite-rich interval in T2 in Lulu-1 (Fig. 21), and represents a type 2(I) mire environment. The presence of char, fusinite and pyrolytic carbon

points to an *in situ* wildfire-derivation of part of the inertinite. Wildfires may lower the peat surface down to the groundwater table, which may promote redeposition of inertodetrinite and possibly the introduction of saline water (pyrite peak between 0.33–0.38 m in Lulu-1).

Despite the petrographic evidence for temporarily drier peat-forming conditions the nearly constant presence of pyrite, including framboidal forms, suggests that the T2 precursor mire was generally wetter and more strongly influenced by the nearby sea than the precursor mires of both seams R1 and R1a. This would be in agreement with recent studies on the Changuinola peat deposit in Panama which suggests that coals with a distinct transgressive signature are likely to have a significant content of pyrite (Phillips & Bustin 1996). A more severe saline water influence on the T2 precursor mire is further indicated by the sterane distribution and the homohopane index (Fig. 31; Tables 7–9, 14). The relative proportion of  $C_{29}$  sterane is generally lower than in seams R1 and R1a and that of  $C_{27}$  sterane generally higher, and equal proportions are present in the Lulu-1 well (Fig. 36). Likewise, in a landward–seaward transect the homohopane index of seam T2 increases and in the wells it shows higher values than recorded in seams R1 and R1a. In the Lulu-1 position 28,30-bisnorhopane is also present in the coal.

A continued rise in relative sea-level caused drowning and transgression of the T2 precursor mire. The coastal reaches of the mire in the Lulu-1 area was transgressed by the sea and shoreface and offshore environments were established followed by shoreface and foreshore environments (Fig. 8). Landward, in the West Lulu-1 area, estuarine channels were established after peat mire termination (Fig. 7). Later lagoonal and flood tidal delta systems were formed. Further landward fluvial or tidal channels and bay-head deltas dominated (Fig. 6). The siliciclastic depositional systems thus reflect a marine transgression which reached the Lulu-1 area during maximum extent, whereas a diminished marine influence is recorded west of this area (West Lulu-1, West Lulu-2 and West Lulu-3) by sediments of marginal marine and paralic depositional systems.

In West Lulu-2, a *c.* 2 m thick coal bed was divided into two seams, R2 and T3, on the basis of organic petrography and geochemistry (Petersen & Andsbjerg 1996; Petersen *et al.* 1996). The R2 seam presumably has a very restricted areal extent and it has not been observed in the other wells. In West Lulu-2 seam T3 is characterised by a significant content of sulphur (average: 4.5%) which must reflect prolonged infiltration of saline water (Phillips *et al.* 1994). Seam T3 is present in West

Lulu-1 and represents a wet type 2 mire environment (Fig. 24). The transgressive signature of T3 in this well is demonstrated by the presence of pyrite combined with high  $C_{27}$  sterane contents and a comparatively high homohopane index (Figs 24, 31; Tables 8, 14).

Peat accumulation in the precursor mire of seam T3 was terminated by deposition of siliciclastic sediments. Re-establishment of peat-forming conditions favoured deposition of seam T4 over a large area. The seam is present in all wells except West Lulu-3 (Fig. 12). In a landward–seaward transect from West Lulu-2 to Amalie-1 the seam is vitrinite- and vitrite+clarite-rich, and it represents a wet type 2 mire, occasionally enriched in fine-grained, allochthonous inertodetrinite or high-reflecting pyrofusinite (type 2(I) mire; Fig. 26). The pyrofusinite and char observed in Lulu-1 and Amalie-1, and in the latter also pyrolytic carbon, indicate that wildfires were active in the mire, probably mainly crown fires burning aerial plant tissues due to the generally high watertable suggested by the petrography. Framboidal and minute pyrite indicates marine influence during peat formation as does relatively high proportions of  $C_{27}$  sterane and homohopane indices (Fig. 31; Tables 8–10, 14). Approximately equal proportions of  $C_{29}$  and  $C_{27}$  steranes occur in T4 seaward in Lulu-1 and Amalie-1 (Fig. 36), where 28,30-bisnorhopane is also recorded, in particular in the latter well. In addition, the T4 seam exhibits the highest homohopane index of all seams in the West Lulu-1 and Lulu-1 wells. Seam T4 marks the last extensive peat accumulation in the Søgne Basin before the sea transgressed over the area. Above seam T4, lagoonal deposits overlain by transgressive shoreface and shelf deposits are preserved in Amalie-1, whereas transgressive shoreface and shelf deposits directly overlie seam T4 in Lulu-1 (Figs 7–9). The most landward part of seam T4 in the West Lulu-2 well is overlain by tidal channel and delta sediments followed by beach and outer shelf and offshore deposits.

Varying, but commonly high inertinite contents are a general feature of the Bryne Formation coals. Periods with comparatively slow watertable rises, possibly occasionally combined with doming of the peat surface, may have promoted watertable fluctuations, which may have favoured the formation of oxidation-derived inertinite as recently demonstrated in the Palangkaraya peat deposit, Kalimantan Tengah, Indonesia (Moore *et al.* 1996). However, the presence of char and pyrolytic carbon and the occurrence of pyroinertinite in all seams also imply a generally high frequency of wildfires in the mire systems. Thus, a seasonal climate with temporarily drier periods would enhance the possibility for drops

in the watertable level below the peat surface and the ignition of fires. Reconstruction of precipitation suggests a seasonal wet climate for the region during the Early–Mid Jurassic (Parrish *et al.* 1982; Hallam 1985), and this is corroborated by annual rings in Lower–Middle Jurassic wood from Jameson Land in East Greenland and the island of Bornholm in the Baltic Sea (Fig. 1; Höhne 1933; Harris 1937; Nielsen 1995; Surlyk *et al.* 1995). Additionally, Cope (1993) observed an abundance of charcoalfied material in cores from deltaic sediments of the Middle Jurassic Brent Group in the North Sea. Inertinite in mid-Cretaceous coals in the Gates Formation, Canada, was likewise interpreted to be exclusively fire-derived; formation occurred during periodic drought in the wetland settings (Lamberson *et al.* 1996). The somewhat uneven distribution of the inertinite in the Bryne Formation coals is probably to some degree related to the level of the watertable (wetness of the peat), but investigations of recent mire systems show that wildfires also may be related to the vegetation (Cohen & Stack 1996).

### *Influence of relative sea-level changes on coal composition*

Siliciclastic deposits suggest a progressive southward transgression of the deeper eastern part of the Søgne Basin during the Bathonian–Callovian which during the Callovian gradually flooded the western part of the basin (Johannessen & Andsbjerg 1993; Andsbjerg 1997). Peat mires were established on the coastal plains west-south-west off the palaeo-shoreline. In particular the organic geochemistry of the coal seams support this interpretation. Increased proportions of C<sub>27</sub> sterane and higher homohopane indices towards the palaeo-coastline is strong evidence for prolonged infiltration of saline water into the peat mires from a sea lying to the east. The coal seams in the West Lulu-3 well generally exhibit the strongest terrestrial signature by having the highest relative proportion of C<sub>29</sub> sterane and the lowest homohopane indices of all samples. This area of the mire systems was thus least influenced by the marine environment to the east. Likewise the landward stepping nature and overall transgressive trend of the coal-bearing succession is reflected in the vertical succession of the coal seams which shows an increased saline influence in the organic geochemical composition from seam R1 to T4. These observations support the assumption that relative sea-level changes may exert an important control on peat accumulation in coastal mires. This

is caused by the hydrological contact between sea water and groundwater in coastal settings, where the level of groundwater table and sea level more or less coincide (Diessel 1994). A relative sea-level rise will raise the watertable or base level on the coastal plain creating the necessary accommodation space for peat accumulation in a large, low-lying area with stagnant water and sedimentary bypass or ponding upstream, conditions very suitable for peat formation (e.g. Arditto 1991; Hartley 1993; Kusters & Suter 1993; Aitken 1994; Flint *et al.* 1995; Petersen & Andsbjerg 1996). The part of the precursor mires located closest to the palaeo-shoreline was most strongly influenced by base-level rise and the rate of peat accumulation was therefore more rapidly outpaced by the rate of watertable rise than in mire areas situated landward. This is reflected in the thinning of the coal seams in a seaward direction (Table 6). Thus, the rate of base-level rise and the position of the coal seams in the sequence stratigraphic framework may be reflected in their organic petrographic and geochemical composition (e.g. Diessel 1992; Banerjee *et al.* 1996; Petersen *et al.* 1996, 1998), which may have implications for the petroleum generative potential. For example, coal facies cycles formed by watertable rises or inundations linked to relative sea-level changes on Hochstetter Forland, North-East Greenland, are characterised by liptinite-enrichment towards the top of each cycle (Petersen *et al.* 1998). This has resulted in coal facies (dull lithotype) with extraordinarily high HI values (average: 464), and thin intercalated carbonaceous mudstones have an average HI of 459. Furthermore, Petersen *et al.* (1996) noticed a tendency to higher HI values and thermally extracted and generated hydrocarbon contents, S<sub>1</sub>+S<sub>2</sub>, in the T1–T4 seams compared to seams R1–R2 in the West Lulu-2 well. The highest average HI values in West Lulu-1 are likewise recorded in seams T2–T4, and the highest S<sub>1</sub>+S<sub>2</sub> contents were obtained from seam T3. In the Lulu-1 seam T4 has the highest average HI value and seam T2 gives the highest S<sub>1</sub>+S<sub>2</sub> contents.

### *Organic maturity*

The majority of the vitrinite reflectance values obtained from the coal seams in West Lulu-3, West Lulu-1, Lulu-1 and West Lulu-2 (West Lulu-2 data from Petersen *et al.* 1996) range between 0.81 %R<sub>m</sub> and 0.89 %R<sub>m</sub>, while a minor proportion yields slightly lower values, 0.75–0.78 %R<sub>m</sub> (Fig. 37). The latter values are measured in samples from coal seams T1, T3 and T4 and except for one outlier these coal samples are characterised by high vit-

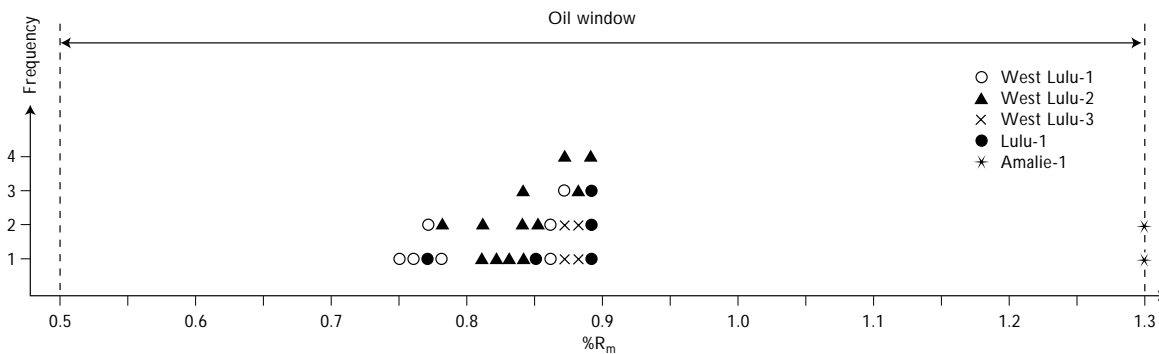


Fig. 37. Vitrinite reflectance values ( $\%R_m$ ) indicate that the coals in the West Lulu-1, -2, -3 and Lulu-1 wells with respect to thermal maturity are situated within the range of peak oil generation in the oil window (early catagenesis maturation stage). The much higher vitrinite reflectance values from the coals in the Amalie-1 well indicate that the organic matter with respect to thermal maturity is at the end of the oil window and is close to the late catagenesis maturation stage. West Lulu-2 data are from Petersen *et al.* (1996).

ritrite contents (up to c. 84 vol.%) or high pyrite contents (up to c. 3 vol.%), or both. The retarded reflectance values are primarily related to hydrogen-enriched vitrinite, which has matured at a reduced rate (Petersen & Rosenberg 1998). The vitrinite precursor material was hydrogen-enriched during early diagenesis due to anoxic and occasionally marine-influenced conditions in the ancient mires.  $T_{max}$  values obtained from extracted coal samples, representing the total vitrinite reflectance range shown by the coals, do not indicate  $T_{max}$  suppression. However,  $T_{max}$  values obtained from hydrogen-enriched vitrinite concentrates show a slight  $T_{max}$  suppression compared to  $T_{max}$  values obtained from concentrates of 'normal' vitrinite (Petersen & Rosenberg 1998).

All reflectance values correspond to high volatile bituminous B/A rank and with respect to thermal maturity the coals are situated within the maturity range of peak oil generation in the 'oil window' (early catagenesis maturation stage) (Fig. 37). The oil window is situated between vitrinite reflectances of c. 0.5  $\%R_m$  and 1.3  $\%R_m$  with peak oil generation occurring between c. 0.8–1.0  $\%R_m$  (Hunt 1996). The average  $T_{max}$  values, ranging from 440°C to 444°C in the West Lulu-3, West Lulu-1 and Lulu-1 wells, are compatible with the reflectance values and confirm the coals to be in the early catagenesis stage of maturation (Hunt 1996, fig. 10-38, p. 389).

$T_{max}$  values obtained from vitrinite lenses in Cleo-1 are comparable to the above results, while coaly mudstones yield higher pyrolysis temperatures. These latter samples are, however, also characterised by lower HI values possibly suggesting the presence of oxidised (inert) organic matter which may increase  $T_{max}$  (Peters 1986). The approximately 1000 m deeper burial depth of the organic matter in the Cleo-1 well compared to

coals in the West Lulu-1, -2 and -3 wells and in Lulu-1 may on the other hand render a higher maturity. Excluding the two vitrinite lenses, the average  $T_{max}$  value is 456°C, i.e. approximately equivalent to a vitrinite reflectance of 1.1  $\%R_m$  (cf. Hunt 1996, fig. 10-38, p. 389), which may seem to be a reliable value compared to the Amalie-1 well (discussed below). A reflectance of 1.1  $\%R_m$  suggests a level of maturity in the late oil window.

The reflectance values of 1.3  $\%R_m$  obtained from seam T4 in Amalie-1 indicate that the organic matter with respect to thermal maturity is at the end of the oil window and is entering the late catagenesis maturation stage where mainly condensates and wet gas are formed. The coals are thus post-mature for oil generation. An average  $T_{max}$  value of 468°C is in very good agreement with the reflectance values. The high level of thermal maturity of the coals in the studied Amalie-1 succession is related to burial of c. 5000 m. The proposed reflectance value of 1.1  $\%R_m$  for the organic matter in Cleo-1 and the reflectance value of 1.3  $\%R_m$  in Amalie-1 would thus be in agreement with the c. 400 m deeper burial of the Amalie-1 well coals. According to the vitrinite reflectance values obtained from Amalie-1 and suggested for Cleo-1, a significant vitrinite reflectance increase is observed from c. 3500–5000 m burial depth. The higher rate of reflectance increase is a function of the exponential nature of vitrinite reflectance, in particular caused by the formation of polycyclic aromatic units above a reflectance value of 0.7  $\%R_o$  (Carr & Williamson 1990; Levine 1993).

The homohopane  $C_{31}$ – $C_{35}$  epimer ratios between 0.57 and 0.67, with the majority of  $C_{29}$  sterane ratios between 0.45 and 0.50, and the majority of the  $\alpha\beta\beta 20(S+R)/[\alpha\beta\beta 20(S+R)+\alpha\alpha\alpha 20(S+R)]$  ratios between 0.50 and 0.64 indicate that the transformation ratios of

these organic geochemical parameters have reached equilibrium (cf. Waples & Machihara 1991; Peters & Moldowan 1993) in the West Lulu-1, West Lulu-2, West Lulu-3, Lulu-1, Cleo-1 and Amalie-1 wells. The ratios are thus consistent with the level of maturity yielded by the vitrinite reflectance and  $T_{max}$  values. CPI values close to 1 indicate the absence of odd carbon-numbered  $n$ -alkane predominance in the heavy-end range, which is related to cleavage reactions at this level of maturity (Radke *et al.* 1980a).

### *Petroleum generative potential*

The coals of the West Lulu-1 and -3 wells and the Lulu-1 well with respect to thermal maturity are in the phase of peak oil generation within the oil window. Despite the fact that the level of maturity indicates the coals have been depleted in hydrogen, they yield HI values above 200. Total average HI values for all coal samples within each of the wells West Lulu-1, West Lulu-3 and Lulu-1 are 180, 178 and 200, respectively, suggesting the coals are still capable of generating liquid and gaseous petroleum (Fig. 27). The coaly mudstones have HI values within the same range as the coals. This is related to the composition of the disseminated organic material, which is composed of macerals similar to the coals. Therefore, no evidence for a higher generative potential of the intercalated coaly mudstones can be demonstrated, a result in agreement with observations by Cook & Struckmeyer (1986).

Based on rank data, coals in the Amalie-1 well are post-mature with respect to liquid petroleum generation, but gas potential may still be present. The high rank of the coals results in generally low HI values and  $S_1+S_2$  yields caused by exhaustion of the petroleum potential. However, HI values at *c.* 130 at the present level of maturity suggest that the coals may have generated liquid petroleum at a lower level of maturity.

With the exception of the vitrinite-lens samples and four sidewall core samples, HI values of samples from Cleo-1 are below 130 (Fig. 28; Table 12). This indicates a generally poor generative potential of the organic matter. Core samples represent floodplain and possibly tidally-influenced fluvial channel environments. Both environments may be well-drained, with the possibility for the disseminated organic debris to be redistributed and oxidised. This would account for gas-prone kero-gen types III and IV with a small generative potential.

Seams T3 and T4 generally yield the highest average HI values and average thermal extracted and gen-

erated petroleum content,  $S_1+S_2$ , in West Lulu-3, West Lulu-1 and Lulu-1 (Table 11). Thus, generally the T-seams in individual wells show the higher HI values and  $S_1+S_2$  yields and the R-seams the lower values. The extraordinary high value of HI=331 in West Lulu-3 contributes to the high average values of seam R1 in this well. In addition, for individual seams an increase in the average HI values is generally recorded in a seaward direction. These observations strongly suggest an influence of the depositional setting on the generative potential of the seams. The T-seams are interpreted to have formed during a comparatively fast rise in relative sea-level promoting a continuously high-standing watertable in the precursor mires and favouring prolonged influence of saline water, particularly in the low-lying reaches of the mires towards the palaeo-shoreline. Such conditions would, in general, create an anoxic peat mire with high activity of anaerobic bacteria, which favours the preservation of hydrogen-enriched vitrinitic precursor material and lipid substances (e.g. Khorasani 1987; Hunt 1996). Hydrogen-enriched (per-hydrous) vitrinite or vitrinite impregnated with absorbed bitumen may in particular be important progenitors of petroleum generation (Petersen & Rosenberg 1998), the formation of which is shown by development of secondary fluorescence. The general fluorescence of both collotelinite and collodetrinite thus suggests petroleum generative capability of the vitrinite, which may partly compensate for the low content of liptinite macerals in the coals (Fig. 25). Comparison of the seams in all wells reveals that the coal seams have the strongest terrestrial signature (highest Pr/Ph ratios, highest proportion of  $C_{29}$  steranes, lowest average homohopane index) in West Lulu-3. Thus, the landward position of West Lulu-3 and the general isolation from marine influence in this area during peat formation are not ideal conditions for the formation of hydrogen-enriched vitrinite, and this may explain why low or the lowest HI values and  $S_1+S_2$  yields are recorded in this location.

These findings are corroborated by the multivariate regression analysis. The influence of the variables on  $S_2$  is illustrated by the target coefficients, where the explained variances of the variables are projected on  $S_2$  (Fig. 38). The target projection can be used to study the relation of each variable to  $S_2$ , that is a large bar in a negative direction indicates a variable with strong negative correlation to  $S_2$ , whereas a positive bar indicates a positive correlation to  $S_2$ . Intercorrelation between the variables is introduced by the closed data set, and the target projection can thus only be interpreted with an understanding of this limitation. The TOC content

has a strong positive influence on the generative potential, as have vitrinite-rich components, in particular vitrinite, clarite, duroclarite, collotelinite, telinite and the vitrinite maceral group (Fig. 38). Generally collodetrinite is considered to be more oil-prone than collotelinite due to its close association with liptinite and because of the lower reflecting, commonly fluorescent vitrinite particles hinting the presence of absorbed hydrocarbons. However, in this study and also in the earlier study by Petersen *et al.* (1996) the significance of collodetrinite alone on the remaining generative potential is nil, whereas the structured, frequently fluorescent telinite and in particular collotelinite macerals seem to be very important components. The absolute effect of telinite may, however, be limited due to the generally low content of this maceral. The combined effect of all the different vitrinite macerals on the generative potential is significant, and this is also stressed by the positive correlation between  $S_2$  and the vitrinite-rich microlithotypes. These results emphasise the importance of the vitrinite components on the petroleum generative potential of coal-bearing strata.

Of the liptinite macerals only resinite shows an important influence on the remaining generative potential (Fig. 38). Sporinite exhibits a weak positive correlation, but surprisingly cutinite shows a strong negative correlation to the remaining  $S_2$ . The absolute effect of cutinite is small as 48% of the samples only contain from 0 to 0.3 vol.% of cutinite. Due to the wide range of acti-

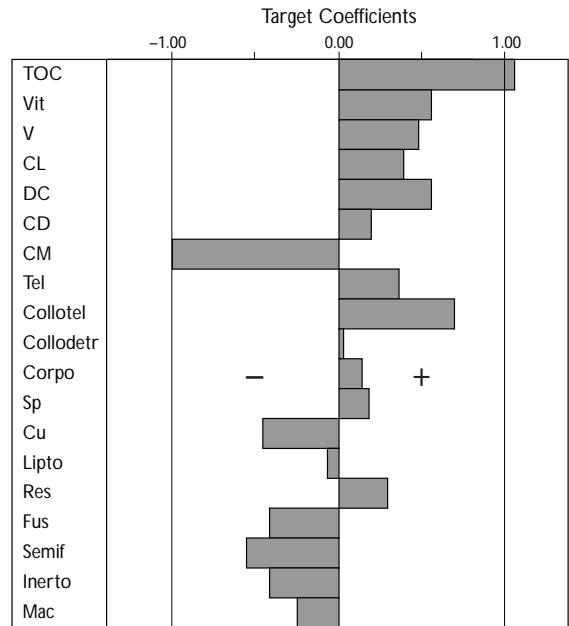
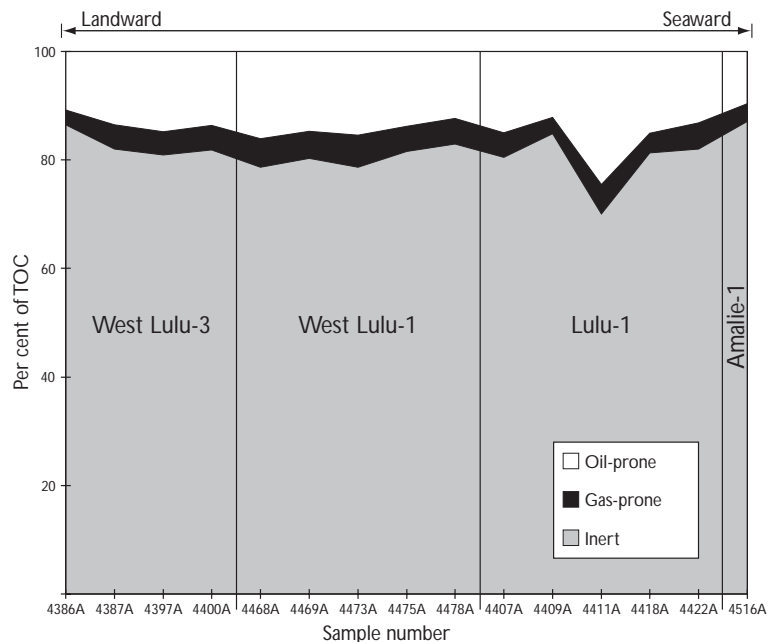


Fig. 38. Target projection of the partial least squares regression (PLSR) model, which gives a measure of the correlation between individual variables and  $S_2$ . The TOC content, vitrinite, vitrinite, clarite, duroclarite, collotelinite and telinite are in particular positively correlated to the remaining generative potential  $S_2$ . TOC = total organic carbon; Vit = vitrinite maceral group; V = vitrinite; CL = clarite; DC = duroclarite; CD = clarodurite; CM = carbominerite; Tel = telinite; Collotel = collotelinite; Collodetr = collodetrinite; Corpo = corpogelinite; Sp = sporinite; Cu = cutinite; Lipto = liptodetrinite; Res = resinite; Fus = fusinite; Semif = semifusinite; Inerto = inertodetrinite; Mac = macrinite.

Fig. 39. The proportion of oil-prone, gas-prone and chemically inert carbon in the coals from West Lulu-3, West Lulu-1 and Lulu-1 wells computed by combining Rock-Eval and Py-GC data. The majority of the carbon in the coals is chemically inert with respect to petroleum generation. However, the graph shows that between 13% and 30% of the carbon will contribute to the formation of petroleum during maturation. Note the high proportion of oil-range components ( $C_{6+}$ ) which constitute between 72.4% and 82.0% of the total pyrolysate, whereas gas-range components ( $C_{1-5}$ ) only constitute between 18.0% and 27.6% of the pyrolysate.





Harald Field oil: West Lulu-3, test 1

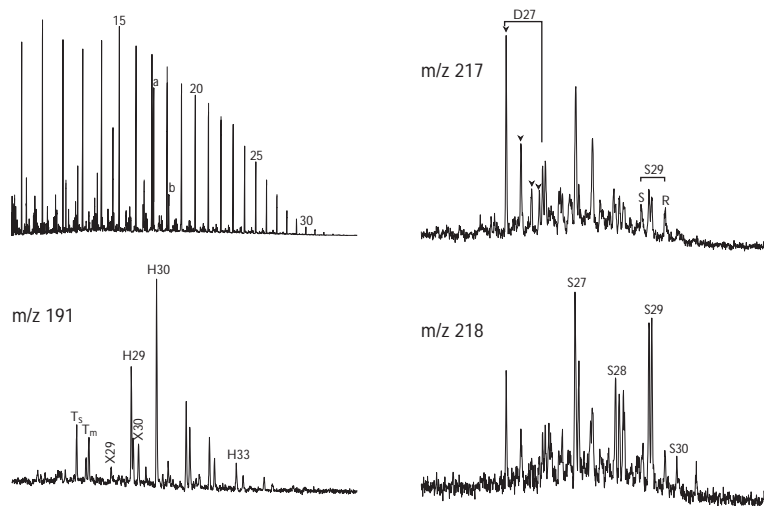


Fig. 40. An example of an oil/condensate derived from the Bryne Formation in the West Lulu-3 well. A typical terrestrial composition is shown by a Pr/Ph ratio of 4.24, a hopane distribution which maximises at C<sub>30</sub>, and a C<sub>27-29</sub> sterane distribution dominated by the C<sub>29</sub> sterane (44%). The compositional similarity to the coal extracts shown in Fig. 30 is evident. Annotation: numbers on GC-trace refer to *n*-alkane carbon numbers, a: pristane, b: phytane; T<sub>s</sub>: trisnorhopane, T<sub>m</sub>: trisnorhopane, H<sub>29</sub>: norhopane, H<sub>30</sub>: hopane, H<sub>33</sub>, trishomohopane, X<sub>29</sub>: dianorhopane, X<sub>30</sub>: diahopane; D<sub>27</sub>: C<sub>27</sub> diasteranes (4 isomers), S<sub>27</sub>, S<sub>28</sub>, S<sub>29</sub> and S<sub>30</sub>: C<sub>27-30</sub>αββ regular steranes, S: C<sub>29</sub>ααα(20S), R: C<sub>29</sub>ααα(20R).

vation energies of the different macerals in coals they do not release petroleum simultaneously, but generation of individual components is dependent on the thermal history of the coal (Boreham & Powell 1993). It may tentatively be suggested that the generative capacity of cutinite at the present level of maturity is limited, resulting in a negative correlation to S<sub>2</sub>.

As expected the carbon-rich and hydrogen-poor inertinite macerals exhibit a negative correlation to S<sub>2</sub> (Fig. 38). Likewise the mineral-rich microlithotype carbominerite has a negative impact on the generative potential.

Using the classification scheme of Larter (1985), which is based on Py-GC, the pyrolysates from the 15 solvent-extracted Bryne Formation coals closely resemble the "II/IIIpp type" kerogen. This kerogen type is recognised by the presence of abundant aliphatic as well as aromatic/phenolic moieties in the pyrolysate, and is held to be present mainly in marine deposits containing high proportions of predominantly vitrinitic and liptinitic terrestrial organic debris. The abundance of aliphatic moieties is generally accounted for by the presence of highly aliphatic liptinite macerals such as cutinite and alginite, whereas the aromatic phenolic moieties are assumed to originate from vitrinite and sporinite. However, in the present case, none of the coal samples contain notable proportions of liptinite macerals, and the abundance of aliphatic moieties may thus also point to the presence of hydrogen-enriched (perhydrous) vitrinite or submicroscopical liptinite.

The oil-prone nature of the Bryne Formation coals discussed in previous paragraphs is strongly supported

by evidence from Py-GC. An estimate of the fractions of TOC of oil-prone, gas-prone and chemically inert carbon may be computed by combining Rock-Eval and Py-GC data (Pepper & Corvi 1995). This calculation shows that although most carbon contained in the coals is chemically inert in the sense that it will not contribute to the petroleum product potentially generated during thermal maturation, between 13 and 30% of the carbon may, at the present level of maturity, potentially participate in the formation of petroleum products, i.e. oil and gas (Fig. 39). All pyrograms show the presence of very high proportions of oil-range components (C<sub>6+</sub>), which constitute from 72.4% to 82.0% of the total pyrolysate (Figs 32, 39). Gas-range components (C<sub>1-5</sub>) are but minor constituents, which constitute from 18.0% to 27.6% of the pyrolysate.

There is a tendency towards increased proportions of oil-like components in pyrolysates from the more marine-influenced Lulu-1 well coals. Furthermore, the fractions found for the partitioning of 'gas' and 'oil' components correspond well to the results of Pepper & Corvi (1995), which show 'gas' fractions of 0.2 to 0.3 for samples with HI values similar to those of the samples analysed in this study. With respect to petroleum generation, the maturity of the samples is comparatively high. However the data indicate that considerable generation of petroleum remains to take place before the full potential is eventually realised. This observation corroborates the idea of progressive generation over a wide span of thermal maturities from rocks dominated by terrestrial kerogen (e.g. Bordenave *et al.* 1993).

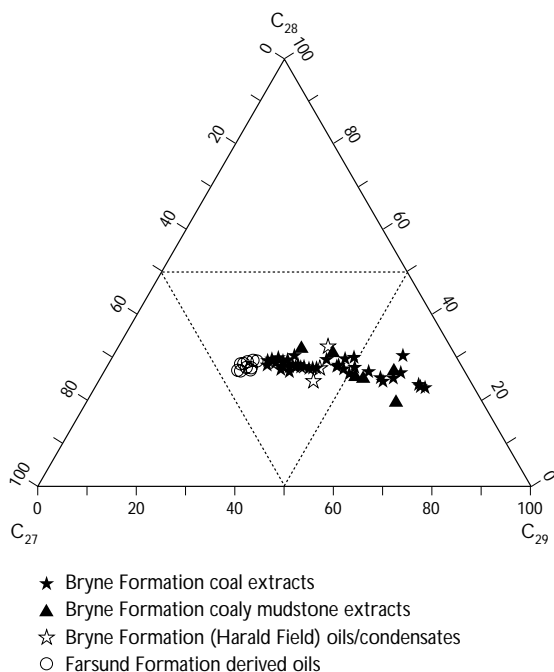


Fig. 41. Normalised  $C_{27-29}$  sterane distribution in 58 Bryne Formation coal extracts (including West Lulu-2 data from Petersen *et al.* 1996), 8 Bryne Formation coaly mudstone extracts, 3 Harald Field derived oils/condensates and 19 Farsund Formation derived oils (data from Bojesen-Koefoed *et al.* 1994). Extracts from both the coals and the intercalated mudstones are dominated by  $C_{29}$  sterane, and show a sterane distribution very similar to the sterane distribution of the Harald Field oils/condensates. The sterane distribution of the Farsund Formation derived oils differ by having a higher proportion of  $C_{27}$  sterane.

The discussion on the ability of coals to expel liquid petroleum was discussed earlier, and implications for the expulsion capability of the West Lulu-2 coals was discussed in Petersen *et al.* (1996). Two commercial gas and oil accumulations in the Harald Field (expected reserves, oil: 7 million  $m^3$ , gas: 25 billion  $Nm^3$ ; Danish Energy Agency 1997) and the Lulita discovery (which contains a high-wax terrigenous oil; GEUS, unpublished data) are indirect evidence for the capability of the coals to expel petroleum. As described above no petrographic or geochemical data point to a better generative potential of the intervening carbonaceous mudstones rendering the coals the likely source rock. Three oil/condensate samples recovered from Bryne Formation sandstones in West Lulu-1 and West Lulu-3 display similar maturity as the coals and they have a typical terrestrial composition (Fig. 40), including Pr/Ph ratios between 4.09 and 4.24, a hopane distribution which max-

Table 15. Average of Migration Index,  $S_1/TOC$

Well	W. Lulu-2	W. Lulu-3	W. Lulu-1	Lulu-1	Amalie-1
Seam					
T4	0.25	-	0.19	0.21	0.13
T3	0.25	-	0.21	-	-
R2	0.25	-	-	-	-
T2	0.24	0.19	0.19	0.20	-
R1a	-	0.15	0.19	-	-
R1	0.23	0.16	0.18	0.19	0.13
T1	0.27	-	-	-	-
Mudstones	0.17	0.16	0.19	0.23	0.16

imises at  $C_{30}$ , and bulk isotope  $\delta^{13}C$  ratios of up to or greater than  $-26\text{‰}$ , which is significantly heavier than the common oils generated from the marine Farsund Formation (Petersen *et al.* 1995, 1996). The Harald Field oil/condensate samples also differ from Farsund Formation derived oils by having a higher proportion of  $C_{29}$  sterane. However, the sterane distribution of the oil/condensate samples is very similar to the sterane distribution of the Bryne Formation coal extracts (Figs 30, 40, 41). Sterane distribution of intercalated coaly mudstone extracts is likewise dominated by  $C_{29}$  sterane. In Amalie-1, a condensate recovered from the Bryne Formation likely consists of a mixture of material generated from terrestrial and marine source rocks (Statoil, unpublished data; GEUS, unpublished data). The condensate has a bulk isotope  $\delta^{13}C$  ratio of  $-25.26\text{‰}$  and, based on gas from the same test, a maturation level corresponding to a vitrinite reflectance of 1.3 %R was assumed, a maturity which corresponds exactly to the vitrinite reflectance values obtained from the coals (Fig. 37). Thus, this evidence supports the contention that petroleum has been released from the coals. Hunt (1996) describes a 'migration index' (MI) defined as  $S_1/TOC$  and suggests MI values between 0.1 and 0.2 for oil expulsion. According to this index all coal seams and carbonaceous mudstones are able to expel liquid petroleum (Table 15). The West Lulu-2 coals show MI values from 0.23 to 0.27, whereas the MI values of the coals in the West Lulu-3, West Lulu-1 and Lulu-1 wells range from 0.15 to 0.21. The West Lulu-3 well exhibits the lowest values, which is in agreement with generally lower HI values and  $S_1+S_2$  yields of the seams in this well (Table 11). Seams R1 and T4 in Amalie-1 show lower MI values which are related to the high thermal maturity. MI values of the mudstones are lower or similar to the MI values of the coals, which again reject the intercalated carbonaceous mudstones as a more significant source rock than the coals.

# Middle Jurassic (Central Graben Group) strata outside the Søgne Basin

## Sedimentological description and interpretation of the measured core-intervals

### *Alma-1x well*

The deepest part of the measured succession consists of light grey, homogeneous silty mudstone with a single coaly horizon (Fig. 42B). Upwards the silty mudstone becomes faintly parallel-laminated, and sediment disturbances are occasionally present. Coal particles and streaks are common together with coalified leaves and twigs. The silt content gradually decreases, and the silty mudstone is overlain by a homogeneous, dark grey mudstone. This is followed by a light grey, slightly more silty, homogeneous mudstone with rare sediment disruption.

The shallower part of the cored interval starts with a dark grey, homogeneous mudstone, which upwards changes to a faintly parallel-laminated heterolithic mud- and siltstone (Fig. 42A). The heterolith is increasingly dominated by silt, and gradually changes to a siltstone, followed by a weakly parallel-laminated very fine-grained sandstone. Small-scale faults and sediment disruptions are common. Towards the top the very fine-grained sandstone again changes to a parallel-laminated, heterolithic mudstone and siltstone. The uppermost heterolith contains coal particles and streaks, and plant fossils as coalified leaves and twigs. The sedimentary succession is interpreted to have been deposited in a floodplain environment.

### *Anne-3a well*

Only cuttings have been investigated from this well.

### *Elly-3 well*

The succession starts with a dark grey, homogeneous to very faintly parallel-laminated mudstone with rare small pyrite concretions (Fig. 43). Towards the top the mudstone becomes black and carbonaceous and finally turns into a coaly interval with visible vitrinitic organic matter. Thin light grey beds of homogeneous siltstone

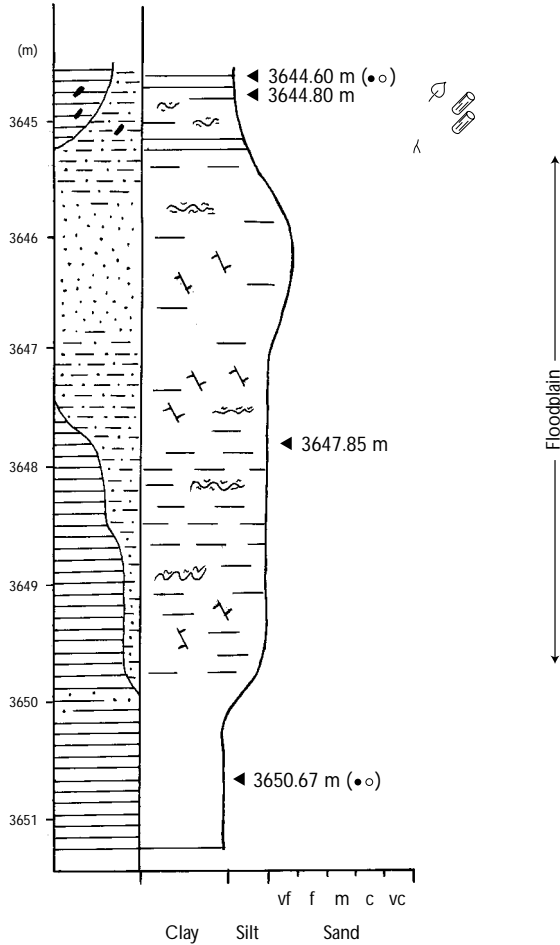
and very fine-grained sandstone overlie the coaly level. These are followed by a new homogeneous mudstone interval, which in the lower part is black and carbonaceous. Coal particles and streaks are common, and coalified leaves (probably from ferns) and twigs are present in a narrow interval. The mudstone is overlain by a light grey, generally homogeneous clayey siltstone unit with abundant coal particles, coalified twigs, and probably rootlets. Towards the top of the clayey siltstone the abundance of coal particles increases, possibly associated with an increase in rootlets, and it gradually turns into a black, carbonaceous mudstone.

A succession consisting of more or less homogeneous heterolithic mudstone and siltstone, commonly with coal particles and coalified wood fragments, overlies the carbonaceous mudstone. The sediments were deposited in a low-energy coastal plain setting dominated by floodplain, lakes and lagoons. A mire environment is represented by the coaly level at about 4088 m.

### *Falk-1 well*

The lower part of the succession consists of homogeneous brownish, dark grey mudstone and black, dull carbonaceous mudstone (Fig. 44). The latter contains vitrinite lenses and streaks, and small vertical pyrite cleats are seen in the lenses. Up to millimetre-thick horizontal and bifurcating vertical rootlets are present together with coal particles and coalified leaves and twigs in the upper part of the mudstone interval. The mudstone is succeeded by a grey heterolithic parallel- to faintly parallel-laminated siltstone and mudstone with occasional poorly developed small-scale cross-lamination and intercalated homogeneous dark grey mudstones. Sediment disruption is common. Coal particles and streaks, and coalified leaves and twigs are abundant in the heterolith, and small pyrite concretions may occur. The very fine-grained sandstone bed between 4118 and 4119 m is slumped and structureless with abundant 'floating' organic debris. A dark, carbonaceous mudstone with coal streaks and lenses, and a coal horizon overlies the heterolith. Except for the uppermost part the rest of the measured succession is composed of grey faintly parallel-laminated and homoge-

A Alma-1x well



B Alma-1x well

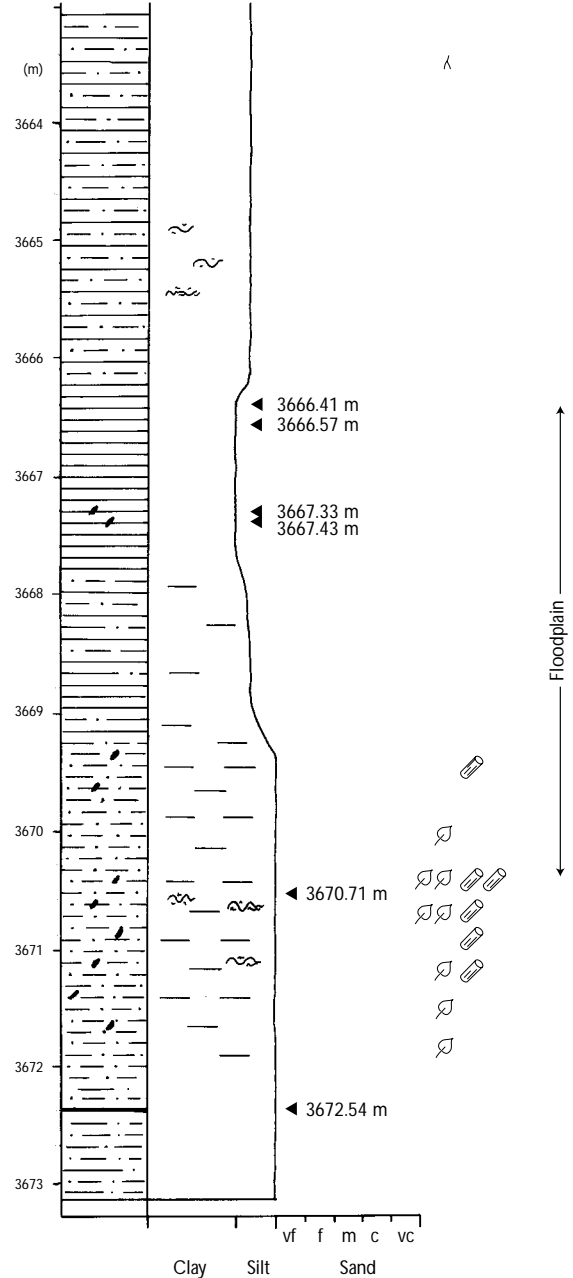


Fig. 42. A and B: Sedimentological logs of the measured parts of the Alma-1x well showing the interpreted depositional environments. Collected samples shown; ●: petrographically analysed sample; ○: sample analysed by GC and GC/MS. See Fig. 5 for legend and Fig. 1 for well location.

neous heterolithic mudstone and siltstone, and black carbonaceous mudstone. Coal particles and streaks together with plant remains are present. The uppermost carbonaceous mudstone contains silt streaks and lenses, and a coaly horizon contains a level with very

coarse-grained sand and gravel. The mudstone is erosionally overlain by a clast-supported conglomerate with grain sizes up to c. 2 cm. The deposits are interpreted as deposited in a low-energy coastal plain setting with open-water mires and lakes.

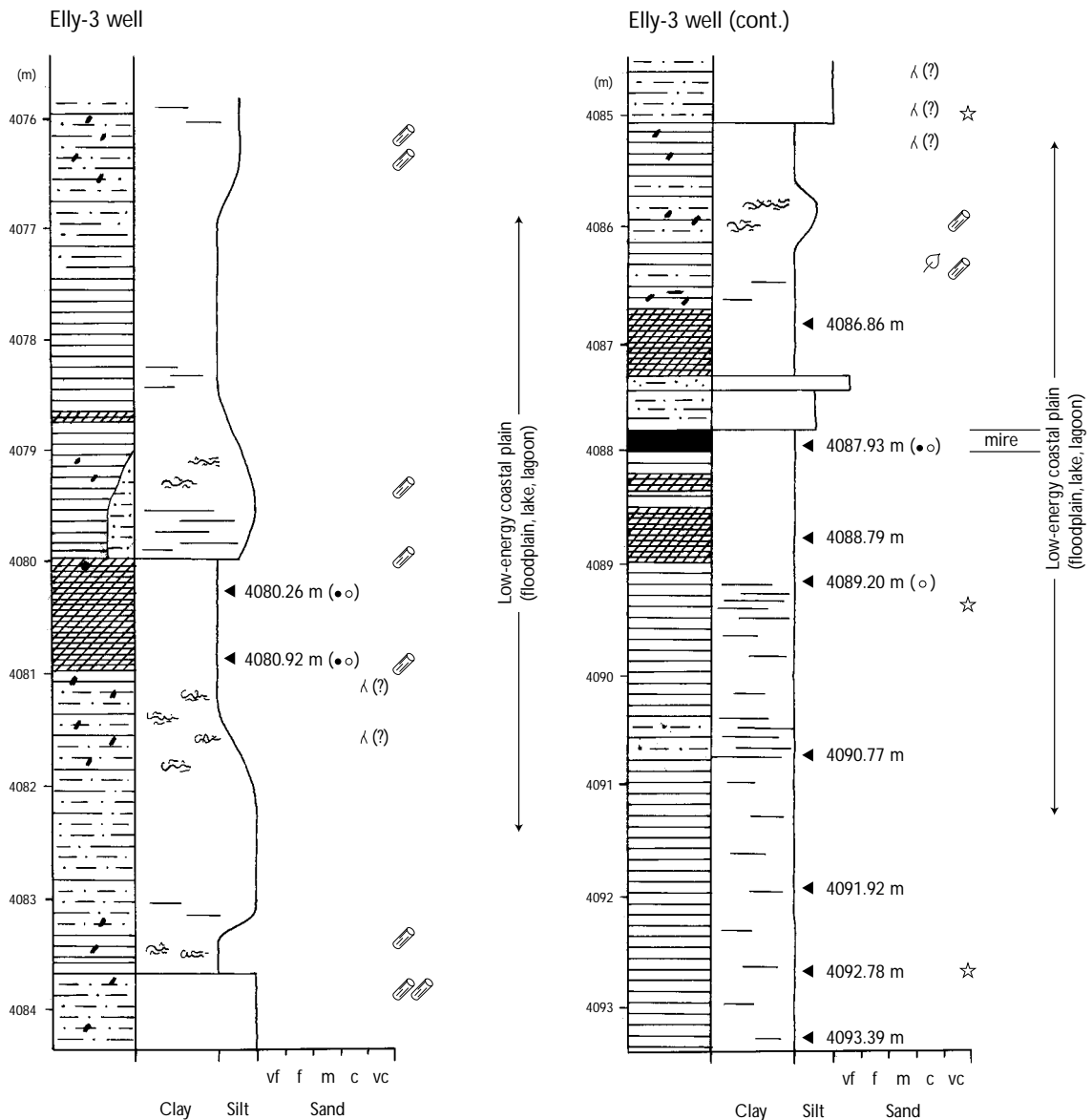


Fig. 43. Sedimentological log of the measured part of the Elly-3 well showing the interpreted depositional environments. Collected samples shown; ●: petrographically analysed sample; ○: sample analysed by GC and GC/MS. See Fig. 5 for legend and Fig. 1 for well location.

### *M-8 well*

Only cuttings have been investigated from this well.

### *Skjold Flank-1 well*

Section A consists primarily of a mainly dark grey to blackish grey, homogeneous, silty mudstone succes-

sion (Fig. 45A). The upper part is rooted by simple roots composed of one main string with small side-roots. Towards the top the mudstone is developed as 3–6 cm thick, red brown to dark grey, rhythmic bands. The silty mudstone is erosionally overlain by siltstone and sandstone beds with flaser-bedding, sediment disruption and organic matter. The uppermost part of section A is developed as a strongly bioturbated heterolithic mudstone and siltstone. The mudstone succession is

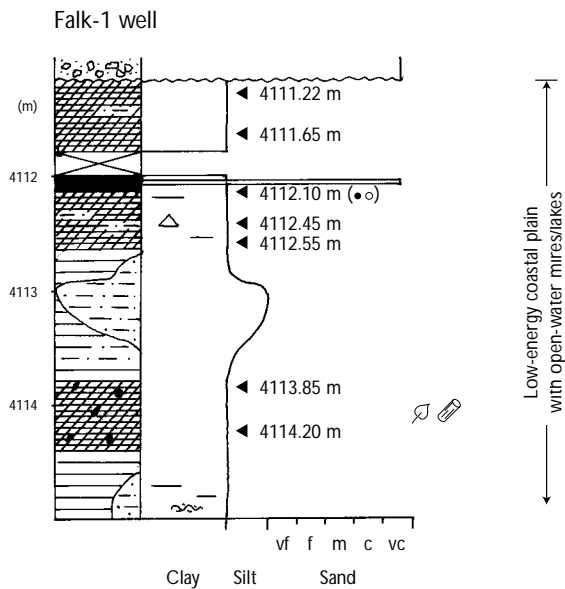
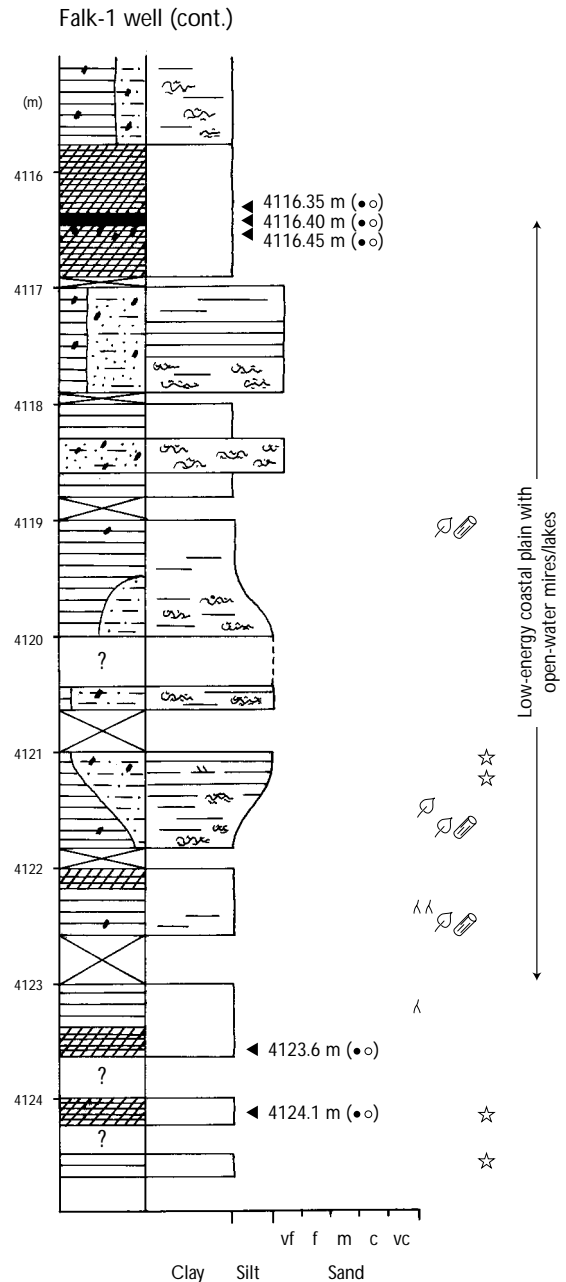


Fig. 44. Sedimentological log of the measured part of the Falk-1 well showing the interpreted depositional environments. Collected samples shown; ●: petrographically analysed sample; ○: sample analysed by GC and GC/MS. See Fig. 5 for legend and Fig. 1 for well location.

interpreted to represent lagoon or lake deposits, whereas the siltstone and sandstone beds are interpreted to have been deposited in fluvial channels which may have been tidally influenced.

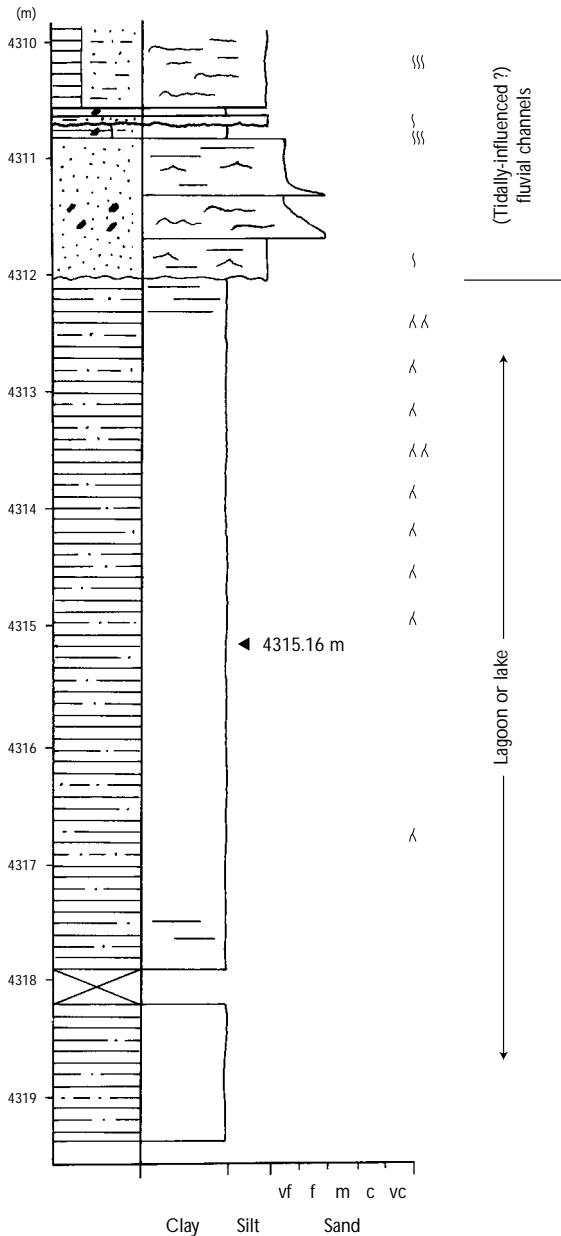
The lowermost part of section B is a homogeneous dark grey to black and occasionally carbonaceous mudstone (Fig. 45B). Small (millimetre-scale) spherical pyrite concretions have been observed in one of the carbonaceous intervals. Small-scale faults and bioturbation is present. The mudstone is erosively overlain by homogeneous and micro-flaser-bedded silty or very fine-grained to fine-grained sandstone beds with abundant organic debris and coal laminae. The sandstone beds are succeeded by a heterolithic mudstone and siltstone or very fine-grained sandstone. The lowermost part of the heterolith is weakly parallel-laminated and disturbed, whereas in general the rest is homogeneous. Organic matter in particular is present in the more sandy intervals, while bioturbation occurs where mudstone dominates. The sediments of section B are interpreted to represent lagoonal or lacustrine and ?tidally-influenced fluvial channel deposits.

Section C starts with a succession of homogeneous to faintly parallel-laminated mudstone and siltstone beds (Fig. 45C). The succession is erosively overlain



by a well-sorted, medium-grained, cross-bedded sandstone, followed by a homogeneous fine- to medium-grained sandstone. The sandstones are topped by an erosion surface characterised by carbonate particles and many shell fragments. Overlying the erosion surface is an interval of fine- to medium-grained sandstones and intraformational conglomerates of layered

A Skjold Flank-1 well



B Skjold Flank-1 well

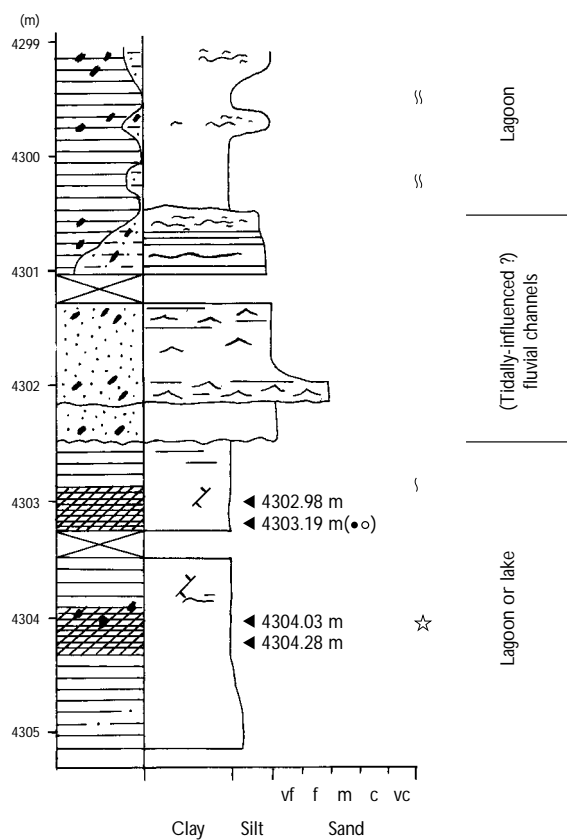
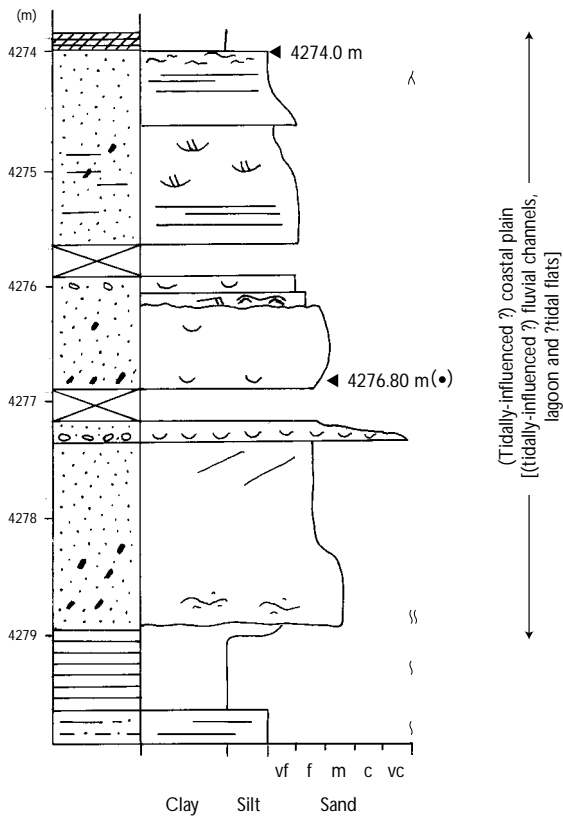


Fig. 45. A-C: Sedimentological logs of the measured parts of the Skjold Flank-1 well showing the interpreted depositional environments. Collected samples shown; ●: petrographically analysed sample; ○: sample analysed by GC and GC/MS. See Fig. 5 for legend and Fig. 1 for well location.

rip-up mudstone clasts. Coaly matter occurs in a weakly flaser-bedded interval. The succession is followed by a unit of mainly fine-grained sandstone beds showing flaser-bedding, cross-bedding, parallel-lamination and occasional herringbone-lamination and small-scale cross-lamination. Coal material may occur on foresets and as laminae. The sandstones are succeeded by siltstone and

heterolithic mudstone and siltstone showing faintly parallel-lamination, sediment disruption and small-scale faults. Bioturbation is common. The uppermost homogeneous mudstone is overlain by a poorly sorted medium-grained sandstone rich in coal particles, which in the lower part is bioturbated. This is followed by a mainly homogeneous, greyish, fine-grained sandstone, and an

C Skjold Flank-1 well



C Skjold Flank-1 well (cont.)

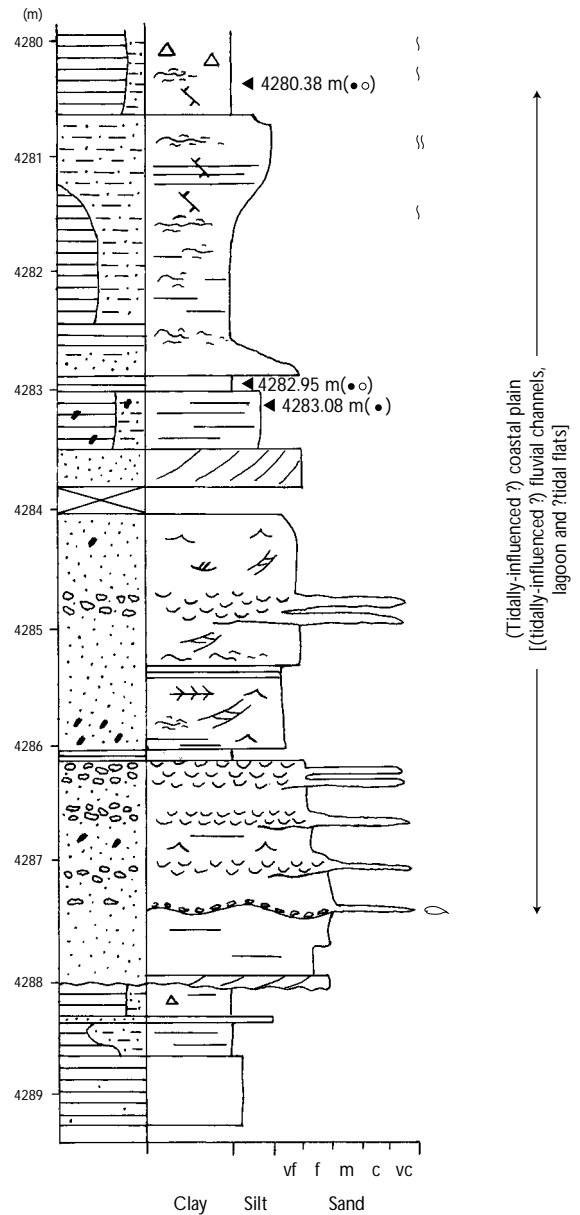


Fig. 45. cont.

intraformational conglomerate of rip-up mudstone clasts. An interval above the conglomerate is dark olive-grey, and contains abundant coal particles and mudstone clasts. A fine-grained sandstone showing interference of wave-current ripples and wavy-bedding overlies an erosion surface. The rest of section C is fining-upwards and the sandstones may show faintly parallel-lamination and

small-scale cross-lamination with concentrations of coaly material in the small-scale troughs. In the uppermost part a light grey, rooted sandstone is overlain by a black, carbonaceous mudstone. The sediments of section C are interpreted to have been deposited in a possibly tidally influenced coastal plain setting with ?tidally-influenced fluvial channels, lagoons and ?tidal flats.



Table 16. Alma-1x: kerogen compositions and vitrinite reflectance value

Depth (m)	%R <sub>m</sub>	Mineral matrix	Pyrite	Organo-mineral matrix	Liptinitic ter. OM	Terrestrial OM	Kerogen Type
3644.60	0.79	51	3	14*	3	29	111/11b
3650.67	-	92	2	1*	4	1	111

\* vitrinitic and liptinitic organo-mineral matrix; ter. = terrestrial

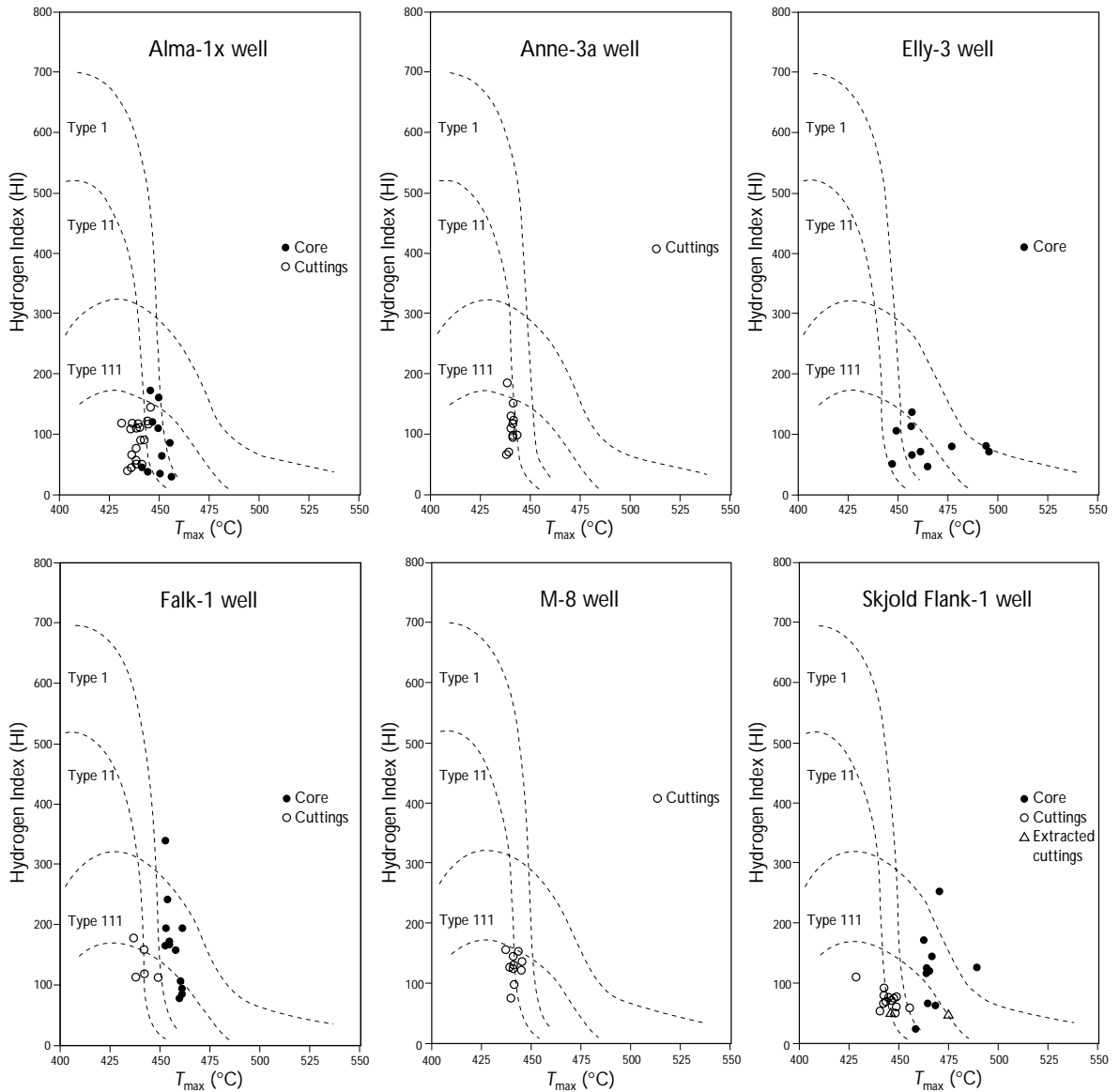


Fig. 46. Hydrogen Index vs.  $T_{max}$  plot of core samples, cuttings and extracted cuttings from the Alma-1x, Anne-3a, Elly-3, Falk-1, M-8 and Skjold Flank-1 wells.

## Organic petrographic and geochemical results

### Alma-1x well

A vitrinite reflectance from 3644.6 m depth gives a value of 0.79 %R<sub>m</sub>, inferring a rank of high volatile bituminous A for the organic matter (Table 16). The kerogen composition at the same depth is dominated by terrestrial OM and organo-mineral matrix composed of vitrinitic and liptinitic organic material intimately associated with mineral matter. Liptinic terrestrial OM amounts to 3 vol.%. The TOC is 1.85 wt% and the HI 162 (Table 17). The organic matter content in a sample from a depth of 3650.67 m is lower (TOC = 0.96 wt%). The kerogen is dominated by liptinitic terrestrial OM, and the HI is 121. Based on organic matter composition and HI values the two kerogens are classified as type III/IIB and type III respectively (cf. Mukhopadhyay *et al.* 1985).

$T_{max}$  values from core samples vary between 441°C and 456°C, averaging 449°C, while the cuttings show  $T_{max}$  values between 431°C and 445°C, averaging 439°C (Fig. 46; Table 17). TOC contents are in general below 1.5 wt%, and HI values from core samples and cuttings range between 31 and 162 with the majority below 120. Thermally extracted and generated petroleum contents, S<sub>1</sub>+S<sub>2</sub>, only occasionally exceed 2 mg HC/g rock.

Extracts from two samples (3644.6 and 3650.67 m; Table 18) show a dominance of polar components followed by saturates. The Pr/Ph ratios are 4.31 and 2.47, respectively, and CPI values 1.09 and 1.00.

Table 17. Alma-1x well: screening data

Sample type	Depth (m)	TOC (wt%)	$T_{max}$ (°C)	S <sub>1</sub> (mg HC/g rock)	S <sub>2</sub> (mg HC/g rock)	HI	PI
Core	3644.60	1.85	449	0.60	3.00	162	0.17
	3644.80	7.48	445	2.17	12.98	174	0.14
	3647.85	0.58	449	0.35	0.64	111	0.35
	3650.67	0.96	446	0.14	1.16	121	0.11
	3666.41	0.78	456	0.06	0.24	31	0.20
	3666.57	0.57	450	0.06	0.20	35	0.23
	3667.33	0.46	444	0.06	0.18	39	0.25
	3667.43	0.45	441	0.05	0.21	47	0.19
	3670.71	1.59	455	0.23	1.37	86	0.14
	3672.54	4.03	451	0.54	2.60	65	0.17
	Cuttings	3551	1.09	438	0.09	0.64	59
3554		1.03	434	0.05	0.41	40	0.11
3557		1.13	436	0.08	0.51	45	0.14
3560		1.12	438	0.07	0.64	57	0.10
3563		1.13	438	0.07	0.59	52	0.11
3566		1.12	436	0.11	0.75	67	0.13
3569		1.12	441	0.11	0.57	51	0.16
3572		1.17	438	0.17	1.30	111	0.12
3575		1.19	431	0.29	1.41	118	0.17
3578		1.18	435	0.25	1.29	109	0.16
3581		1.22	440	0.18	1.37	112	0.12
3584		1.10	436	0.23	1.31	119	0.15
3587		1.25	440	0.18	1.14	91	0.14
3591		1.25	439	0.21	1.48	118	0.12
3594		1.31	442	0.18	1.20	92	0.13
3597		1.27	436	0.23	1.51	119	0.13
3600		1.28	438	0.11	0.99	77	0.10
3603		3.28	444	0.57	3.88	118	0.13
3606		2.08	444	0.55	2.54	122	0.18
3609	3.02	445	0.75	4.37	145	0.15	

The 22S/(22S+22R) epimer ratios of the 17 $\alpha$ (H),21 $\beta$ (H) C<sub>31</sub> and C<sub>32</sub> extended hopanes range between 0.57 and 0.63. The  $\alpha\alpha$ 20S/(20S+20R) epimer ratio of the C<sub>29</sub>

Table 18. GC data and composition of solvent extract fractions (asphaltene-free) from the Alma-1x, Elly-3, Falk-1 and Skjold Flank-1 wells

Well	Depth (m)	Pr/Ph	CPI	EOM	Sat (%)	Aro (%)	Polars (%)
Alma-1x	3644.60	4.31	1.09	51	39	13	48
	3650.67	2.47	1.00	50	37	9	54
Elly-3	4080.26	2.05	1.04	17	18	12	70
	4080.92	2.08	1.05	33	19	20	61
	4087.93	1.71	0.96	10	9	18	73
	4089.20	1.14	1.00	37	17	17	66
Falk-1	4112.10	2.01	1.05	57	23	20	57
	4116.35	3.48	0.98	30	28	7	65
	4116.40	3.59	1.01	28	19	19	62
	4116.45	3.55	1.01	39	23	15	62
	4123.60	4.06	1.01	24	35	21	44
	4124.10	3.17	1.03	30	28	11	61
Skjold Flank-1	4280.38	2.27	1.00	46	18	24	58
	4282.95	2.03	1.20	37	33	5	62
	4303.19	1.96	1.03	34	31	11	58

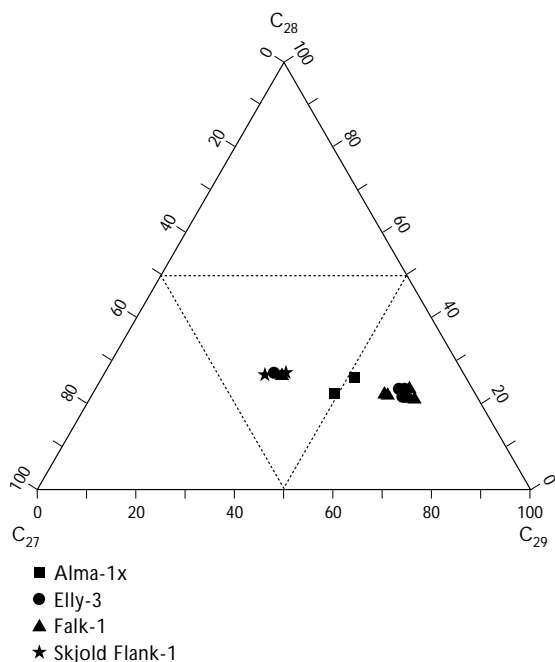


Fig. 47. Normalised  $C_{27-29}$  sterane distribution in extracts from the Alma-1x, Elly-3, Falk-1 and Skjold Flank-1 wells. The majority of the samples are dominated by sterane  $C_{29}$  suggesting a high content of terrestrial organic matter.

sterane lies between 0.45 and 0.48, while the  $\alpha\beta\beta 20(S+R)/[\alpha\beta\beta 20(S+R)+\alpha\alpha\alpha 20(S+R)]$  ratio is 0.55 (Table 19). The relative proportion of the  $C_{27}\alpha\beta\beta$ ,  $C_{28}\alpha\beta\beta$  and  $C_{29}\alpha\beta\beta$  steranes is characterised by high contents of the  $C_{29}$  sterane (Fig. 47).

### Anne-3a well

Only cuttings are available from this well. TOC contents are within 1.09–11.51 wt%, and the  $T_{max}$  values range between 438°C and 443°C (Table 20). HI values range between 68 and 186 (Fig. 46), averaging 114, and thermally extracted and generated petroleum contents,  $S_1+S_2$ , are within the range 0.77–23.42 mg HC/g rock, but with the majority < 4 mg HC/g rock.

### Elly-3 well

A single vitrinite reflectance measurement carried out on a sample from 4087.93 m depth shows a reflectance value of 1.13 % $R_m$  indicating that the organic matter has just entered the medium volatile bituminous coalifica-

Table 19. Alma-1x, Elly-3, Falk-1 and Skjold Flank-1 wells: sterane isomerisation ratios

Well	Depth (m)	Steranes	
		29 $\alpha\alpha\alpha$ S	29 $\alpha\beta\beta$ (S+R)
		29 $\alpha\alpha\alpha$ (S+R)	29 $\alpha\beta\beta$ (S+R)+29 $\alpha\alpha\alpha$ (S+R)
Alma-1x	3644.60	0.45	0.55
	3650.67	0.48	0.55
Elly-3	4080.26	0.47	0.60
	4080.92	0.45	0.60
	4087.93	0.46	0.59
	4089.20	0.46	0.57
Falk-1	4112.10	0.52	0.63
	4116.35	0.45	0.63
	4116.40	0.48	0.60
	4116.45	0.48	0.61
	4123.60	0.46	0.63
	4124.10	0.46	0.60
Skjold Flank-1	4280.38	0.26	0.41
	4282.95	0.40	0.53
	4303.19	0.43	0.57

Table 20. Anne-3a well: screening data

Sample type	Depth (m)	TOC (wt%)	$T_{max}$ (°C)	$S_1$ (mg HC/g rock)	$S_2$ (mg HC/g rock)	HI	PI
Cuttings	3441	2.38	440	0.24	3.11	131	0.07
	3450	2.20	441	0.33	2.10	95	0.14
	3460	3.98	443	0.26	3.98	100	0.06
	3469	3.20	441	0.24	3.16	99	0.07
	3478	2.75	440	0.17	3.06	111	0.05
	3487	4.23	441	0.44	6.47	153	0.06
	3496	3.07	441	0.25	3.61	118	0.06
	3505	11.51	438	2.02	21.40	186	0.09
	3519	4.80	441	0.24	5.99	125	0.04
	3530	1.46	439	0.05	1.05	72	0.05
	3533	1.09	438	0.03	0.74	68	0.04

tion stage (Table 21). The sample has a TOC content of 32.92 wt% and the kerogen is composed of terrestrial OM and vitrinitic organo-mineral matrix, occasionally associated with framboidal pyrite (Fig. 48; Tables 21, 22). Two other kerogen samples (4080.26 and 4080.92 m) have TOC contents of 8.58 wt% and 4.24 wt% respectively, and show dominance of terrestrial OM and minor contents of liptinitic OM. Kerogen typing is difficult due to the rank of the organic matter. However, based on the present kerogen composition and HI values between 107 and 137, the kerogen is classified as type III and possibly IIb.

The TOC contents of the core samples vary between 0.56 wt% and 32.92 wt% and  $T_{max}$  values range from 447°C to 495°C (Fig. 46; Table 22). Except for the three

Table 21. Elly-3 well: kerogen compositions and vitrinite reflectance value

Depth (m)	%R <sub>m</sub>	Mineral matrix	Pyrite	Organo-mineral matrix			Terrestrial OM	Kerogen Type
				(vol.%)				
4080.26	-	82	0	0	2	16	111/(11b?)	
4080.92	-	84	1	0	3	12	111/(11b?)	
4087.93	1.13	30	1	10*	0	59	111/(11b?)	

\* vitrinitic

investigated kerogen samples thermally extracted and generated petroleum contents, S<sub>1</sub>+S<sub>2</sub>, are below 1 mg HC/g rock.

Extracts are dominated by polar compounds followed by a tendency to dominance of aromatics over

saturates (Table 18). The Pr/Ph ratios are between 1.14 and 2.08, and CPI ratios close to 1.

The range of the 22S/(22S+22R) epimer ratios of the 17α(H),21β(H) C<sub>31</sub> and C<sub>32</sub> extended hopanes is between 0.56 and 0.64. The ααα20S/(20S+20R) epimer

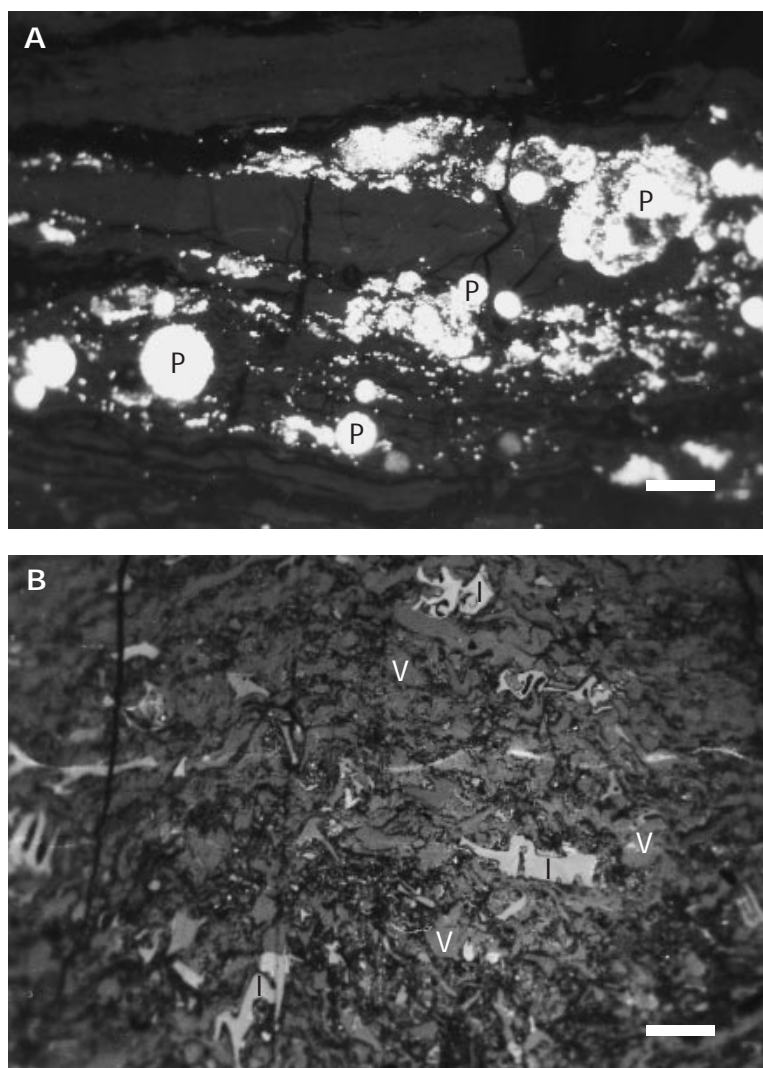


Fig. 48. Photomicrographs of kerogen from the Elly-3 well (sample 4300A, 4087.93 m). **A:** Framboidal pyrite (P) in vitrinite. **B:** Detrital vitrinite groundmass (V) with few inertodetrinite (I) particles and mineral matter. Black and white photographs in reflected white light and oil immersion. Scale bar ~ 35μm.

Table 22. Elly-3 well: screening data

Sample type	Depth (m)	TOC (wt%)	T <sub>max</sub> (°C)	S <sub>1</sub> (mg HC/g rock)	S <sub>2</sub> (mg HC/g rock)	HI	PI
Core	4080.26	8.58	456	1.03	9.63	112	0.10
	4080.92	4.24	449	0.45	4.54	107	0.09
	4086.86	1.94	465	0.15	0.91	47	0.14
	4087.93	32.92	457	4.08	45.12	137	0.08
	4088.79	1.04	447	0.17	0.52	50	0.25
	4089.20	0.56	477	0.13	0.45	80	0.22
	4090.77	1.01	457	0.23	0.67	66	0.26
	4091.92	0.90	494	0.21	0.71	79	0.23
	4092.78	1.08	461	0.23	0.77	72	0.23
	4093.39	1.02	495	0.25	0.72	71	0.26

ratio of the C<sub>29</sub> sterane is around 0.46, while the  $\alpha\beta\beta 20(S+R)/[\alpha\beta\beta 20(S+R)+\alpha\alpha\alpha 20(S+R)]$  ratio ranges from 0.57–0.60 (Table 19). With the exception of a single sample with about equal relative proportions of the C<sub>27</sub> $\alpha\beta\beta$  and C<sub>29</sub> $\alpha\beta\beta$  steranes, the C<sub>29</sub> is the dominant sterane (Fig. 47).

### Falk-1 well

Vitrinite reflectance values range between 1.05 %R<sub>m</sub> and 1.11 %R<sub>m</sub>, inferring a rank of late high volatile bituminous A (Table 23). Microscopically investigated kerogens, having TOC contents from 7.98 to 69.90 wt % (Table 24), are dominated by vitrinitic OM (Fig. 49), of which the majority in the sample from 4116.40 m depth is fluorescent (Table 23). The samples have varying amounts of inertinitic OM, liptinitic OM and organo-mineral matrix (Fig. 49), which may be mainly vitrinitic or liptinitic. The samples contain from 2 to 5 vol.% pyrite. The HI values of the 4 petrographic investigated samples range between 167 and 243 (Table 24). The samples are accordingly classified as kerogen type III. However, the two samples from depths of 4112.10 m

Table 24. Falk-1 well: screening data

Sample type	Depth (m)	TOC (wt%)	T <sub>max</sub> (°C)	S <sub>1</sub> (mg HC/g rock)	S <sub>2</sub> (mg HC/g rock)	HI	PI
Core	4111.22	6.31	461	2.19	6.12	97	0.26
	4111.65	7.32	460	2.26	8.00	109	0.22
	4112.10	69.90	453	12.35	116.76	167	0.10
	4112.45	5.23	460	1.33	4.18	80	0.24
	4112.55	5.79	461	1.66	5.08	88	0.25
	4113.85	6.16	458	1.52	9.82	160	0.13
	4114.20	15.92	455	3.79	26.82	168	0.12
	4116.35	27.75	453	5.00	54.46	196	0.08
	4116.40	51.37	454	9.78	124.82	243	0.07
	4116.45	35.24	455	5.89	61.86	176	0.09
	4123.60	7.98	461	2.45	15.66	196	0.14
	4124.10	22.40	453	7.52	76.38	341	0.09
Cuttings	4051	2.36	437	1.50	4.27	181	0.26
	4081	2.45	438	1.21	2.82	115	0.30
	4111	2.87	442	1.79	3.47	121	0.34
	4141	6.65	449	2.69	7.65	115	0.26
	4171	2.46	442	1.46	3.96	161	0.27

and 4116.40 m can, based on petrography and TOC content, be classified as humic coal.

The T<sub>max</sub> values from the core samples vary between 453°C and 461°C, averaging 457°C, while 5 cuttings only average 442°C (Fig. 46; Table 24). HI values range between 80 and 341 with more than 50% having values greater than 160. Thermally extracted and generated petroleum contents, S<sub>1</sub>+S<sub>2</sub>, are highest for the organic-rich samples (Table 24).

Extracts are dominated by polar compounds followed by saturates (Table 18), and Pr/Ph ratios range between 2.01 and 4.06. CPI ratios are close to 1.

Five of the six investigated samples yield 22S/(22S+22R) epimer ratios of the 17 $\alpha$ (H),21 $\beta$ (H) C<sub>31</sub> and C<sub>32</sub> extended hopanes in the range 0.52–0.68, whereas an outlier yields 0.47 and 0.87. The  $\alpha\alpha\alpha 20S/(20S+20R)$  epimer ratios and the  $\alpha\beta\beta 20(S+R)/[\alpha\beta\beta 20(S+R)+\alpha\alpha\alpha 20(S+R)]$  ratios of the C<sub>29</sub> sterane range from 0.45–0.52 and

Table 23. Falk-1 well: kerogen compositions and vitrinite reflectance values

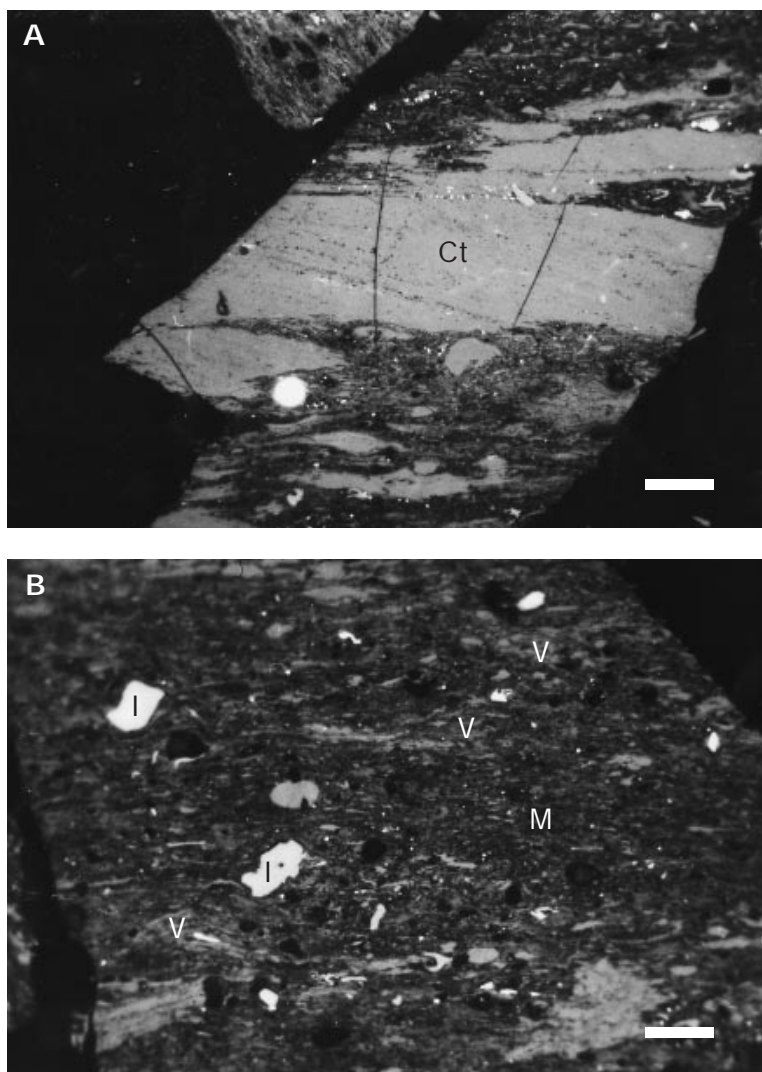
Depth (m)	%R <sub>m</sub>	Mineral matrix	Pyrite	Organo-mineral matrix	Liptinitic ter. OM	Vitrinitic OM	Inertinitic OM	Kerogen type
4112.10	-	2	5	0	1	51	41	111
4116.35	-	30	2	13*	0	52	3	111
4116.40	1.05	1	2	0	4	93#	4	111
4116.45	1.11	-	-	-	-	-	-	-
4123.60	-	78	2	5**	2	9	4	111
4124.10	1.07	-	-	-	-	-	-	-

\* vitrinitic organo-mineral matrix; \*\*mainly liptinitic organo-mineral matrix; # mainly fluorescing; ter. = terrestrial

Fig. 49. Photomicrographs of kerogen in the Falk-1 well (sample 4334A, 4116.35 m).

**A:** Collotelinite band (Ct) surrounded by detrital vitrinite and mineral matter.

**B:** Detrital vitrinite (V) intimately associated with mineral matter (M) and a few inertodetrinite (I) particles. Black and white photographs in reflected white light and oil immersion. Scale bar ~ 35 $\mu$ m.



0.60–0.63 respectively (Table 19). With the exception of a single sample with about equal relative proportions of the  $C_{27}\alpha\beta\beta$  and  $C_{29}\alpha\beta\beta$  steranes, the  $C_{29}$  constitutes above 59% of the steranes in the remainder of the samples (Fig. 47).

### *M-8 well*

Only cuttings are available, and they have TOC contents between 1.27 wt% and 11.27 wt% (Table 25).  $T_{\max}$  values range from 437–445°C. HI values and thermally extracted and generated petroleum contents,  $S_1+S_2$ , are

in the ranges 76–156 and 1.46–20.14 mg HC/g rock, respectively (Fig. 46; Table 25). The majority of the  $S_1+S_2$  contents are, however, < 3 mg HC/g rock.

### *Skjold Flank-1 well*

Two reflectance measurements both yield the value of 1.22 % $R_m$  indicating a medium volatile bituminous rank (Table 26). Microscopic kerogen analyses of three samples, having TOC contents between 0.84 wt% and 1.53 wt% (Table 27), reveal a dominance of terrestrial OM and small proportions of organo-mineral matrix (Table 26).

Table 25. M-8 well: screening data

Sample type	Depth (m)	TOC (wt%)	$T_{\max}$ (°C)	$S_1$ (mg HC/g rock)	$S_2$ (mg HC/g rock)	HI	PI
Cuttings	3100	1.48	439	0.52	1.88	127	0.22
	3109	1.52	441	0.54	1.92	126	0.22
	3118	1.72	441	0.63	2.22	129	0.22
	3127	11.27	443	2.88	17.26	153	0.14
	3136	5.57	445	1.99	7.58	136	0.21
	3146	2.63	445	0.88	3.24	123	0.21
	3155	1.80	441	0.61	1.76	98	0.26
	3164	1.38	440	0.42	1.04	76	0.29
	3173	1.27	437	0.77	1.98	156	0.28
	3182	1.39	441	0.63	2.02	145	0.24

The pyrite content ranges from 1 to 5 vol.%. Kerogen composition and HI values in the range 127–225 for the three samples suggest the kerogen should be classified as type III and possibly also type IIb for the sample from 4280.38 m depth.

$T_{\max}$  values from core samples range between 458°C and 489°C; the majority are in the range 462–468°C (Fig. 46; Table 27). Cuttings with TOC contents between 1.23 wt% and 11.89 wt% show, except for two samples, significantly lower  $T_{\max}$  values (Fig. 46; Table 27). HI values are also generally lower, while thermally extracted and generated petroleum contents,  $S_1+S_2$ , vary between 1.21 and 6.38 mg HC/g rock.

Three core extracts are dominated by polar compounds (Table 18). In the two samples containing kerogen type III saturates are second, whereas aromatics are second in the sample (4280.38 m) containing kerogen type III and possibly type IIb. The Pr/Ph ratios lie between 1.96 and 2.27 and the CPI ratios close to 1.

The 22S/(22S+22R) epimer ratios of the 17 $\alpha$ (H),21 $\beta$ (H)  $C_{31}$  and  $C_{32}$  extended hopanes yield, except for a

Table 27. Skjold Flank-1 well: screening data

Sample type	Depth (m)	TOC (wt%)	$T_{\max}$ (°C)	$S_1$ (mg HC/g rock)	$S_2$ (mg HC/g rock)	HI	PI	
Core	4274.01	7.21	468	1.61	4.70	65	0.26	
	4276.80	40.96	464	3.75	50.86	124	0.07	
	4280.38	0.84	470	0.36	2.14	255	0.14	
	4282.95	1.18	462	0.33	2.06	174	0.14	
	4283.08	60.98	466	5.79	89.42	147	0.06	
	4302.99	1.99	463	0.36	2.38	120	0.13	
	4303.19	1.53	463	0.38	1.94	127	0.16	
	4304.03	7.48	464	1.01	5.14	69	0.16	
	4304.28	1.98	458	0.51	0.52	26	0.50	
	4315.16	0.90	489	0.22	1.16	128	0.16	
	Cuttings	4173	1.37	446	0.81	1.00	73	0.45
		4188	1.32	442	0.92	0.90	68	0.51
		4218	2.59	440	1.34	1.42	55	0.49
		4234	2.25	443	1.33	1.57	70	0.46
		4249	2.32	445	1.44	1.80	78	0.44
4264		5.68	447	2.04	2.95	52	0.41	
4279		4.04	455	1.35	2.55	63	0.35	
4295		4.90	448	1.53	3.92	80	0.28	
4310		2.58	442	1.71	2.43	94	0.41	
4325		2.59	428	1.97	2.95	114	0.40	
4340		1.45	446	0.85	1.10	76	0.44	
4356		1.23	442	0.48	1.01	82	0.32	
4371	2.16	448	0.94	1.37	63	0.41		
Extracted cuttings	4203	1.96	446	0.16	1.05	54	0.13	
	4389	11.89	475	0.21	6.17	52	0.03	

single outlier (0.28), values between 0.55 and 0.62. The ranges of the  $\alpha\alpha\alpha 20S/(20S+20R)$  epimer ratios and the  $\alpha\beta\beta 20(S+R)/[\alpha\beta\beta 20(S+R)+\alpha\alpha\alpha 20(S+R)]$  ratios of the  $C_{29}$  sterane are, with the exception of a single outlier (0.26 and 0.41, respectively), from 0.40–0.43 and 0.53–0.57 respectively (Table 19). The relative proportions of the  $C_{27}\alpha\beta\beta$ ,  $C_{28}\alpha\beta\beta$  and  $C_{29}\alpha\beta\beta$  steranes show a general dominance of  $C_{27}$  sterane followed by  $C_{29}$  sterane (Fig. 47).

Table 26. Skjold Flank-1 well: kerogen compositions and vitrinite reflectance values

Depth (m)	%R <sub>m</sub>	Mineral matrix	Pyrite	Organo-mineral matrix (vol.%)	Liptinitic ter. OM	Terrestrial OM	Kerogen type
4276.80	1.22	-	-	-	-	-	-
4280.38	-	81	5	1	0	13	111/(11b?)
4282.95	-	90	1	0	0	9*	111
4283.08	1.22	-	-	-	-	-	-
4303.19	-	87	1	2	0	10*	111

\* mainly vitrinitic; ter. = terrestrial

## Discussion

### *Organic maturity*

The two wells from the Heno Plateau, Elly-3 and Falk-1, yield vitrinite reflectance values between 1.05 %R<sub>m</sub> and 1.13 %R<sub>m</sub> from a depth of about 4 kilometres (Tables 21, 23). The  $T_{\max}$  values from the Elly-3 well show a wide range. However, the three most organic-rich samples show values from 449 to 457°C. This range and the comparatively narrow range of  $T_{\max}$  values (average 457°C) from core samples of the Falk-1 well, are in good agreement with the vitrinite reflectances (Table 24). Higher  $T_{\max}$  values may be related to interference by mineral matrix or the nature of the organic matter (inertinite) (Peters 1986). The lower temperatures obtained from cuttings from the Falk-1 well may be caused by lignite added to the drilling mud. Biomarker ratios are, as expected at this level of maturity, close to equilibrium (Table 19). Thus, with respect to thermal maturity the organic matter has passed the peak of oil generation (approximately between 0.8 and 1.0 %R, cf. Hunt 1996), and is found in the late oil window.

The remaining wells are situated in the Salt Dome Province in the southern part of the Danish Central Graben. The Skjold Flank-1 well yields two vitrinite reflectance values of 1.22 %R<sub>m</sub> at approximately 4280 m depth, and the majority of the  $T_{\max}$  values derived from core samples range from 462 to 468°C indicating a level of maturity of the organic matter close to the end of the oil window and the start of condensate generation (Tables 26, 27). The measured vitrinite reflectance values match perfectly the modelled reflectance values from a depth of about 4300 m (GEUS, unpublished data). Cuttings yield lower  $T_{\max}$  values which may be caused by drilling mud additives like lignite. Biomarker ratios are slightly below equilibrium and show lower values than modelled epimerisation ratios (Table 19). This may imply influence from migrated products.

The Alma-1x, Anne-3a and M-8 wells exhibit lower maturities. A vitrinite reflectance value from a depth of about 3645 m in Alma-1x yields a value of 0.79 %R<sub>m</sub> (Table 16). This value is in good agreement with the average  $T_{\max}$  value (439°C) of the cuttings, and to some degree also with modelled vitrinite reflectance values for this depth (GEUS, unpublished data). However, core samples show higher values (average 449°C; Table 17), and core samples with comparatively high TOC contents (1.85 and 7.48 wt%) and HI values (162 and 174) probably give reliable  $T_{\max}$  values of 449°C and 445°C suggesting that the vitrinite reflectance value may be

too low. A vitrinite reflectance value corresponding to these  $T_{\max}$  values would be between 0.9 and 1.0 %R<sub>m</sub>. The highest  $T_{\max}$  values are commonly associated with low HI values implying interference from inert organic matter. In the Alma-1x well the biomarker ratios have nearly reached equilibrium (Table 19).

Cuttings from approximately 3440–3530 m depth in Anne-3a show similar  $T_{\max}$  values as the cuttings from Alma-1x (Table 20), thus corresponding to a vitrinite reflectance between 0.7 %R<sub>m</sub> and 0.8 %R<sub>m</sub>. This is slightly more than measured and modelled vitrinite reflectance values from a depth of about 3500 m in the Anne-3a well (Thomsen *et al.* 1995). Cuttings from the interval 3100–3182 m in M-8 also yield similar  $T_{\max}$  values (Table 25), but here measured vitrinite reflectance values (%R<sub>m</sub> about 0.77; Thomsen *et al.* 1995) match the pyrolysis temperatures.

The maturity parameters indicate that the organic matter in the Alma-1x, Anne-3a and M-8 wells is within the early catagenesis stage of maturation and is close to or within the peak oil generation range in the oil window.

### *Petroleum generative potential*

Organic maturity parameters from the Elly-3 well indicate a level of thermal maturity corresponding to the late oil window. Some core samples from the Elly-3 well still have HI values above 100 and give high S<sub>2</sub> yields, but generally the organic matter is depleted in hydrogen and only a limited generative potential remains (Table 22). The  $T_{\max}$  versus HI diagram suggests the core samples follow the pathway of kerogen type II (Fig. 46), and petrographic investigations of the organic material suggest a composition of kerogen type III and possibly IIb (Table 21). The high relative proportion of C<sub>29</sub> sterane in the majority of the samples from Elly-3 indicates a strong input of terrestrial organic matter from higher land plants (Huang & Meinschein 1979; Philp 1994; Fig. 47). Influence from kerogen type II material is however suggested by the comparatively low Pr/Ph ratios (Table 18), in particular in the sample from 4089.20 m depth which has a Pr/Ph ratio of 1.14 and furthermore exhibits a slight dominance of C<sub>27</sub> sterane, which is considered to be a marine indicator (e.g. Hunt 1996). These observations could imply an initially good generative potential of the organic matter in Elly-3. In that context it is notable that a terrigenous oil has been recovered in the nearby Elly-2 well: the Pr/Ph ratio is 2.06 and relative proportions of C<sub>27</sub> and C<sub>29</sub> steranes are 24% and 52% respectively (GEUS, unpublished data).



The Elly discovery, expected to be set in production in 1999, contains primarily gas (expected reserve: 5 billion Nm<sup>3</sup>) and minor oil (expected reserve: 1 million m<sup>3</sup>; Danish Energy Agency 1997).

The organic matter in the Falk-1 well has a similar level of thermal maturity as that observed in Elly-3. The maturity level infers exhaustion of the petroleum generative potential. However, high S<sub>2</sub> yields indicate that generative potential still remains (Table 24), and several HI values close to or above 200 indicate a good generative capacity (Fig. 46). Although petrography and Pr/Ph ratios generally above 3 support a classification of the organic matter as kerogen type III, the deposition in low-energy, open-water mires or lakes with restricted oxygen availability, as shown by the carbonaceous mudstones, and the presence of organo-mineral matrix and liptinitic terrestrial organic matter may account for the comparatively high HI values and the ability to generate petroleum at this level of maturity (Fig. 44; Tables 18, 23).

Several HI values between 100 and 200 obtained from core samples from Skjold Flank-1 and relatively high S<sub>2</sub> yields imply that the organic matter, constituted by kerogen type III and possibly type IIb, may possess the capability to generate condensate and gas even at the present level of thermal maturity (Fig. 46; Table 27). This is corroborated by computed petroleum genera-

tion depth trends for kerogen types II and III which show that in the Central Graben Group these kerogen types are within the condensate/gas window (GEUS, unpublished data). It is likely that the marine influenced coastal plain (as shown by dominance of C<sub>27</sub> sterane, Fig. 47) with a variety of depositional environments, like lakes and lagoons, in places favoured the sedimentation and preservation of petroleum-prone organic matter.

The petrographic composition of the organic matter in the Alma-1x well is composed mainly of kerogen type III and some type IIb. However, although the organic matter with respect to thermal maturity is within the peak oil generation range the generally low HI values and S<sub>2</sub> yields suggest a rather poor petroleum generative potential (Fig. 46; Table 17). The overall floodplain environment seems in general to have been unfavourable for deposition of oil-prone organic matter.

The HI values from the Anne-3a and M-8 wells only in a few cases exceed 140 implying a limited petroleum generative capacity of the organic matter (Fig. 46; Tables 20, 25). The position of the cuttings in the HI versus T<sub>max</sub> diagrams does not indicate a depth trend, but the presence of kerogen type II could be implicated. The comparatively low generative capacity, however, is probably related to a dominance of kerogen type III in the cuttings.

## Conclusions

### The coal seams of the Bryne Formation in the Søgne Basin

1. Peat accumulation occurred in coastal mires. Increased marine influence is observed in the Lulu-1 and Amalie-1 wells, where lagoonal, estuarine channel, shoreface and offshore siliciclastic sediments dominate.
2. The cumulative coal seam thickness decreases in a seaward direction from 5.05 m in the West Lulu-2 well, to 3.27 m in West Lulu-1 and 1.57 m in West Lulu-3, decreasing to 0.98 m in the Lulu-1 well, and to 0.60 m in the Amalie-1 well. This thinning of the seams towards the palaeo-shoreline is related to a more rapid outpacing of the rate of peat accumulation by the water-table rise linked to a relative sea-level rise.
3. A spatial coal seam distribution shows that the seams R1 and T4 are the most extensive; the precursor mires occupied the majority of the Danish part of the Søgne Basin. A seam split of seam R1, named R1a, is only present in the West Lulu-1 and West Lulu-3 wells. The precursor mire of seam T2 was also extensive, but did not reach the southern part (Amalie-1 well) of the basin. The mires represented by seams T1 and T3 had a limited extent and were restricted to the north-western part of the Danish Søgne Basin.

4. Petrographically the seams are characterised by low contents of liptinite (R-seams: 0.8–4.4 vol.%, T-seams: 1.6–7.8 vol.%), fluctuating but frequently important amounts of either allochthonous or *in situ* derived inertinite, and significant amounts of generally fluorescent vitrinite. The intimate association of the macerals creates a complex microlithotype composition. Towards the palaeo-coastline the coal facies generally represents a wet peat-forming environment due to a continuously high-standing watertable, whereas coal composition implies that the precursor peats may have been more subjected to a fluctuating watertable and desiccation landward of the palaeo-coastline. The presence of pyroinertinite, char and pyrolytic carbon in the seams is evidence for wildfires in the ancient mires, probably ignited by lightning. A stronger prolonged marine influence on the coastal reaches of the ancient mire systems is reflected by increased proportions of sterane  $C_{27}$  compared to sterane  $C_{29}$  and increased  $C_{35}$ -homohopane indices in all seams towards the palaeo-shoreline. This is supported by the recording of 28,30-bisnorhopane in seams R1, T2 and T4 in Lulu-1 and Amalie-1, which suggests marine-influenced anoxic conditions. In contrast, the seams in West Lulu-3 have the highest proportions of  $C_{29}$  sterane and the highest Pr/Ph ratios (average: 5.98) implying that this area of the precursor mires were least effected by the marine environment. Compared to the seams formed during a comparatively slow relative sea-level rise (seams R1, R1a and R2) the seams formed during an accelerated relative sea-level rise (seams T2, T3 and T4), which favours waterlogged, anoxic conditions due to a continuously high-standing watertable, have several characteristics suggesting an overall stronger marine influence on the precursor mires. These characteristics are: a) in general a higher content of pyrite in the T-seams, b) in general a higher proportion of  $C_{27}$  sterane in the T-seams in all well-sites, c) in a landward–seaward direction equal proportions of  $C_{27}$  and  $C_{29}$  steranes are obtained earlier (Lulu-1 well, seams T2 and T4, compared to Amalie-1 well, seam R1), and d) higher  $C_{35}$ -homohopane indices in the T-seams. Additionally, the  $C_{35}$ -homohopane index shows a vertical increase from the lowermost to the uppermost seam in each well reflecting the backstepping nature and overall transgressive trend of the coal-bearing succession. The depositional environment, in particular watertable (base-level) rise in the mires linked to relative sea-level rise, is thus recorded by the organic petrographic and geochemical composition of the coal seams.
5. The composition (macerals) of the organic matter in the coaly mudstones is similar to the composition of the coal seams.
6. Vitrinite reflectance values from the coals in the West Lulu-1, West Lulu-3 and Lulu-1 wells are in the range 0.75–0.89 % $R_m$  indicating a high volatile bituminous B/A rank. Average  $T_{max}$  values in the wells range between 440°C and 444°C. Thus with respect to thermal maturity the coals are situated within the maturity range of peak oil generation in the oil window. The coals in the Amalie-1 well yield a vitrinite reflectance value of 1.3 % $R_m$  indicating a medium volatile bituminous rank. The average  $T_{max}$  value is 468°C, and the coals with respect to thermal maturity are at the end of the oil window and are entering the late catagenesis maturation stage where mainly condensates and wet gas are formed. The organic matter in the Cleo-1 well has likewise a maturity level corresponding to the late oil window. The homohopane  $C_{31}$ – $C_{35}$  epimer ratios between 0.57 and 0.67, the majority of the  $C_{29}$  sterane ratios between 0.45 and 0.50, and the majority of the  $\alpha\beta\beta 20(S+R)/[\alpha\beta\beta 20(S+R)+\alpha\alpha\alpha 20(S+R)]$  ratios between 0.50 and 0.64, indicate that the transformation ratios of these organic geochemical parameters have reached equilibrium.
7. The average HI values from the coals in the West Lulu-3, West Lulu-1 and Lulu-1 wells are 178, 180 and 200 respectively; coaly mudstones yield average HI values of 172, 168 and 145 respectively. The highest average HI values (on seam basis) are generally obtained from the T-seams (in particular seams T3 and T4) as are the highest average  $S_1+S_2$  contents, and for individual seams an increase in the average HI values is generally recorded in a seaward direction. The tendency to higher HI values and  $S_1+S_2$  contents in the T-seams implies an influence of the depositional environment on the generative potential of the seams. The deposition of the precursor peats of the T-seams during a comparatively faster relative sea-level rise may have: a) promoted a continuously high-standing watertable and the creation of an anoxic peat mire, b) favoured prolonged influence of saline water, particularly in the low-lying reaches of the mires towards the palaeo-coastline, and c) increased microbic activity of anaer-

obic bacteria. Such conditions will favour the preservation of hydrogen-enriched vitrinitic precursor material and lipid substances, which are important in petroleum generation. Thus, the general isolation from marine influence on the mire systems in the West Lulu-3 area may explain why low or the lowest HI values and  $S_1+S_2$  yields are recorded in this location.

The coaly mudstones exhibit a lower generative potential or a similar potential as the coals. The organic matter in the Cleo-1 well has a general small generative potential, and is mainly gas-prone.

8. The coals are, despite their level of thermal maturity, capable of generating liquid and gaseous petroleum. About 13–30% of the carbon in the coals will participate in petroleum formation during maturation, and Py-GC data from the coals indicate that the generated petroleum will consist of 72.4–82.0% liquid petroleum and only 18.0–27.6% gas. Lower HI values and  $S_1+S_2$  contents for the coals in Amalie-1 are caused by the significantly higher level of maturity, but Py-GC derived pyrolysates reveal that the coals are still capable of generating oil.
9. Multivariate statistical modelling of the data yielded a model explaining 71% of the variation in the remaining generative potential represented by  $S_2$ . The correlation coefficient is 0.85. However the low slope of 0.73 of the response line emphasises that other factors than petrographic composition and the TOC content influence  $S_2$ . Components with a significant positive influence on  $S_2$  are the TOC content, the vitrinite maceral group, the vitrinite macerals collotelinite and telinite, the vitrinite-rich microlithotypes vitrite, clarite and duroclarite, and the liptinite maceral resinite. The small amount of liptinite macerals in the coals restricts the absolute importance of this maceral group in the model. Components with a negative influence on the generative potential are the fusinite, semifusinite, inertodetrinite and macrinite macerals, and the mineral-rich microlithotype carbominerite.
10. The coals from the West Lulu-3, West Lulu-1 and Lulu-1 wells yield migration index ( $S_1/TOC$ , cf. Hunt, 1996) values between 0.15 and 0.21, whereas the West Lulu-2 coals yield indices between 0.23 and 0.27. These values are very favourable according to the suggested 0.1–0.2 range for oil expulsion. The coaly mudstones yield lower or similar values.
11. The  $C_{27-29}$  sterane distribution of three oil/condensate samples recovered from Bryne Formation sandstones in the West Lulu-1 and West Lulu-3 wells is typically terrestrial (dominance of  $C_{29}$  sterane) and it is very similar to the sterane distribution of the coal extracts. The oil/condensate samples are also of similar maturity and display typical terrestrial signatures like Pr/Ph ratios between 4.09 and 4.24 and bulk isotope  $\delta^{13}C$  ratios of up to or greater than  $-26\text{‰}$ . A condensate from the Amalie-1 well has a bulk isotope  $\delta^{13}C$  ratio of  $-25.26\text{‰}$ , and a maturation level corresponding to a vitrinite reflectance of 1.3 %R, which is similar to the vitrinite reflectance of the Amalie-1 coals.
12. The sum of the evidence implies that the Bryne Formation coals may act, and have acted, as a source for liquid and gaseous petroleum. No data support a better generative potential for the intervening carbonaceous mudstones.

### Central Graben Group deposits

1. The examined deposits from the wells were generally deposited in a low-energy coastal plain environment with floodplains, lakes, lagoons and fluvial channels, which occasionally may have been tidally influenced.
2. The organic matter in the deposits is predominantly terrestrially derived and can be classified as kerogen type III or IIb. Pr/Ph ratios are typically greater than 2, with the highest ratio of 4.31. Except for Skjold Flank-1, where the distribution of  $C_{27-29}$  steranes show a general dominance of  $C_{27}$ , the steranes are dominated by the  $C_{29}$  steranes.
3. Maturity parameters indicate that the kerogen in Alma-1x, Anne-3a and M-8 (Salt Dome Province) is close to or within the peak oil generation range in the oil window. With respect to thermal maturity the kerogen in Elly-3 and Falk-1 (Heno Plateau) is in the late oil window, whereas the kerogen in Skjold Flank-1 (Salt Dome Province) is close to the end of the oil window.
4. *Heno Plateau wells.* The kerogen in Elly-3 is depleted in hydrogen and only a limited generative potential remains. However, an initially good petroleum potential may have been present. A terrigenous oil

has been recovered from the nearby Elly-2 well. The organic matter in the Falk-1 well gives high  $S_2$  yields and several HI values close to or above 200, implying that generative potential still remains.

*Salt Dome Province wells:* HI values between 100 and 200 and relatively high  $S_2$  yields obtained from Skjold Flank-1 samples suggest that the kerogen may possess the capability to generate condensate and gas even at the present level of thermal maturity. The kerogen in the Alma-1x, Anne-3a and M-8 wells exhibits a generally poor petroleum generative capacity.

## References

- Aitken, J.F. 1994: Coal in a sequence stratigraphic framework. *Geoscientist* **4**(5), 9–12.
- Andsbjerg, J. 1997: Sedimentology and sequence stratigraphy of the Bryne Formation, Middle Jurassic, Danish Central Graben. In: Andsbjerg, J.: Sedimentology and sequence stratigraphy of Middle Jurassic deposits. Danish and Norwegian Central Graben. Danmarks og Grønlands Geologiske Undersøgelse Rapport **1997/68**(2), 60 pp.
- Andsbjerg, J. & Dybkjær, K. 1997: Jurassic sequence stratigraphy of the Danish Central Graben. In: Andsbjerg, J.: Sedimentology and sequence stratigraphy of Middle Jurassic deposits. Danish and Norwegian Central Graben. Danmarks og Grønlands Geologiske Undersøgelse Rapport **1997/68**(1), 31 pp.
- Arditto, P.A. 1991: A sequence stratigraphic analysis of the Late Permian succession in the Southern Coalfield, Sydney Basin, New South Wales. *Australian Journal of Earth Sciences* **38**, 125–137.
- Bagge, M.A. & Keeley, M.L. 1994: The oil potential of Mid-Jurassic coals in northern Egypt. In: Scott, A.C. & Fleet, A.J. (eds): Coal and coal-bearing strata as oil-prone source rocks? Geological Society Special Publication (London) **77**, 183–200.
- Banerjee, I., Kalkreuth, W. & Davies, E.H. 1996: Coal seam splits and transgressive-regressive coal couplets: a key to stratigraphy of high-frequency sequences. *Geology* **24**(11), 1001–1004.
- Bertrand, P.R. 1989: Microfacies and petroleum properties of coals as revealed by a study of North Sea Jurassic coals. *International Journal of Coal Geology* **13**, 575–595.
- Bojesen-Koefoed, J.A., Nytoft, H.P. & Thomsen, E. 1994: Organic geochemistry of oils and source rocks, southern Danish North Sea sector. DGU Datadokumentation **1**, 99 pp. Copenhagen: Geological Survey of Denmark.
- Bojesen-Koefoed, J.A., Christiansen, F.G., Petersen, H.I., Piasecki, S., Stemmerik, L. & Nytoft, H.P. 1996: Resinite-rich coals of north-east Greenland - a hitherto unrecognized, highly oil-prone Jurassic source rock. *Bulletin of Canadian Petroleum Geology* **44**(3), 458–473.
- Bordenave, M.L., Espitalié, J., Leplat, P., Oudin, J.L. & Vandembroucke, M. 1993: Screening techniques for source rock evaluation. In: Bordenave, M.L. (ed.): Applied petroleum geochemistry, 219–278. Paris: Technip.
- Boreham, C.J. & Powell, T.G. 1993: Petroleum source rock potential of coals and associated sediments: qualitative and quantitative aspects. In: Law, B.E. & Rice, D.D. (eds): Hydrocarbons from coal. American Association of Petroleum Geologists Studies in Geology **38**, 133–157.
- Brown, K.E. & Cohen, A.D. 1995: Stratigraphic and micropetrographic occurrences of pyrite in sediments at the confluence of carbonate and peat-forming depositional systems, southern Florida. *Organic Geochemistry* **22**(1), 105–126.
- Bustin, R.M. 1988: Sedimentology and characteristics of dispersed organic matter in Tertiary Niger Delta: origin of source rocks in a deltaic environment. American Association of Petroleum Geologists Bulletin **72**(3), 277–298.
- Carr, A.D. & Williamson, J.E. 1990: The relationship between aromaticity, vitrinite reflectance and maceral composition of coals: implications for the use of vitrinite reflectance as a maturation parameter. *Organic Geochemistry* **16**(1–3), 313–323.
- Cartwright, J.A. 1991: The kinematic evolution of the Coffee Soil Fault. In: Roberts, A.M., Yielding, G. & Freeman, B. (eds): The geometry of normal faults. Geological Society Special Publication (London) **56**, 29–40.
- Christiansen, F.G., Bojesen-Koefoed, J.A., Dam, G., Nytoft, H.P., Larsen, L.M., Pedersen, A.K. & Pulvertaft, T.C.R. 1996: The Marraat oil discovery on Nuussuaq, West Greenland: evidence for a latest Cretaceous – earliest Tertiary oil prone source rock in the Labrador Sea - Melville Bay region. *Bulletin of Canadian Petroleum Geology* **44**(1), 39–54.
- Clayton, J.L., Rice, D.D. & Michael, G.E. 1991: Oil-generating coals of the San Juan Basin, New Mexico and Colorado, U.S.A. *Organic Geochemistry* **17**(6), 735–742.

- Close, J.C. 1993: Natural fractures in coal. In: Law, B.E. & Rice, D.D. (eds): Hydrocarbons from coal. American Association of Petroleum Geologists Studies in Geology **38**, 119–132.
- Cohen, A.D. & Stack, E.M. 1996: Some observations regarding the potential effects of doming of tropical peat deposits on the composition of coal beds. *International Journal of Coal Geology* **29**, 39–65.
- Cohen, A.D., Spackman, W. & Dolsen, P. 1984: Occurrence and distribution of sulfur in peat-forming environments of southern Florida. *International Journal of Coal Geology* **4**, 73–96.
- Collinson, M.E., van Bergen, P.F., Scott, A.C. & De Leeuw, J.W. 1994: The oil-generating potential of plants from coal and coal-bearing strata through time: a review with new evidence from Carboniferous plants. In: Scott, A.C. & Fleet, A.J. (eds): Coal and coal-bearing strata as oil-prone source rocks? Geological Society Special Publication (London) **77**, 31–70.
- Cook, A.C. & Struckmeyer, H. 1986: The role of coal as a source rock for oil. In: Glenie, R. (ed.): Second South-Eastern Australia Oil Exploration Symposium, 419–429. Petroleum Exploration Society of Australia.
- Cope, M.J. 1993: A preliminary study of charcoalfied plant fossils from the Middle Jurassic Scalby Formation of North Yorkshire. *Special Papers in Palaeontology* **49**, 101–111.
- Damtoft, K., Nielsen, L.H., Johannessen, P.N., Thomsen, E. & Andersen, P.R. 1992: Hydrocarbon plays of the Danish Central Trough. In: Spencer, A.M. (ed.): Generation, accumulations and production of Europe's hydrocarbons II. Special Publications of the European Association of Petroleum Geoscientists **2**, 35–58. Berlin Heidelberg: Springer-Verlag.
- Danish Energy Agency 1997: Oil and gas production in Denmark 1996, 69 pp. Copenhagen: Danish Energy Agency, Ministry of Environment and Energy.
- Diessel, C.F.K. 1992: Coal-bearing depositional systems, 721 pp. Berlin Heidelberg: Springer Verlag.
- Diessel, C.F.K. 1994: Part B - The application of sequence stratigraphy to coal geology. In: Boyd, R. & Diessel, C.F.K.: Short course: sequence stratigraphy and its application to coal geology. 28th Newcastle Symposium, 1–65. University of Newcastle, N.S.W., Australia.
- Durand, B. & Oudin, J.L. 1979: Exemple de migration des hydrocarbures dans une serie deltaïque - la delta Mahakham, Kalimantan, Indonésie. Proceedings of the 10th World Petroleum Conference **2**, 3–12.
- Durand, B. & Paratte, M. 1983: Oil potential of coals: a geochemical approach. In: Brooks, J. (ed.): Petroleum geochemistry and exploration of Europe. Geological Society Special Publication (London) **12**, 255–264.
- Dzou, L.I.P., Noble, R.A. & Senftle, J.T. 1995: Maturation effects on absolute biomarker concentration in a suite of coals and associated vitrinite concentrates. *Organic Geochemistry* **23**(7), 681–697.
- Flint, S., Aitken, J. & Hampson, G. 1995: Application of sequence stratigraphy to coal-bearing coastal plain successions: implications for the UK Coal Measures. In: Whateley, M.K.G. & Spears, D.A. (eds): European coal geology. Geological Society Special Publication (London) **82**, 1–16.
- Frandsen, N. 1986: Middle Jurassic deltaic and coastal deposits in the Lulu-1 well of the Danish Central Trough. *Danmarks Geologiske Undersøgelse Serie A* **9**, 23 pp.
- García-González, M., Surdam, R.C. & Lee, M.L. 1997: Generation and expulsion of petroleum and gas from Almond Formation coal, Greater Green River Basin, Wyoming. *American Association of Petroleum Geologists Bulletin* **81**(1), 62–81.
- Gowers, M.B. & Sæbøe, A. 1985: On the structural evolution of the Central Trough in the Norwegian and Danish sectors of the North Sea. *Marine and Petroleum Geology* **2**, 298–318.
- Hallam, A. 1985: A review of Mesozoic climates. *Journal of the Geological Society (London)* **142**, 433–445.
- Harris, T. 1937: The fossil flora of Scoresbysund, East Greenland. Part 5: Stratigraphic relations of the Plant Beds. *Meddelelser om Grønland* **112**(2), 78–104.
- Hartley, A.J. 1993: A depositional model for the Mid-Westphalian A to late Westphalian B Coal Measures of South Wales. *Journal of the Geological Society (London)* **150**, 1121–1136.
- Höhne, R. 1933: Beiträge zur Stratigraphie, Tektonik und Paläogeographie des Südbaltischen Rhät-Lias, insbesondere auf Bornholm. *Abhandlungen aus dem geologisch-palaeontologischen Institut Greifswald* **12**, 31–70.
- Huang, D., Zhang, D., Li, J. & Huang, X. 1991: Hydrocarbon genesis of Jurassic coal measures in the Turpan Basin, China. *Organic Geochemistry* **17**(6), 827–837.
- Huang, W.-Y. & Meinschein, W.G. 1979: Sterols as ecological indicators. *Geochimica et Cosmochimica Acta* **43**, 739–745.
- Huc, A.Y., Durand, B., Roucachet, M., Vandenbroucke, M. & Pittion, J.L. 1986: Comparison of three series of organic matter of continental origin. *Organic Geochemistry* **10**(1–3), 65–72.
- Hunt, J.M. 1991: Generation of gas and oil from coal and other terrestrial organic matter. *Organic Geochemistry* **17**(6), 673–680.
- Hunt, J.M. 1996: *Petroleum geochemistry and geology*, 743 pp. New York: W.H. Freeman and Company.
- Hutton, A., Bharati, S. & Robl, T. 1994: Chemical and petrographic classification of kerogen/macerals. *Energy and Fuels* **8**, 1478–1488.
- ICCP 1998: The new vitrinite classification (ICCP System 1994). *Fuel* **77**(5), 349–358 (International Committee for Coal and Organic Petrology).
- Issler, D.R. & Snowdon, L.R. 1990: Hydrocarbon generation kinetics and thermal modelling, Beaufort-Mackenzie Basin. *Bulletin of Canadian Petroleum Geology* **38**, 1–16.
- Jensen, T.F., Holm, L., Frandsen, N. & Michelsen, O. 1986: Jurassic – Lower Cretaceous lithostratigraphic nomenclature for the Danish Central Trough. *Danmarks Geologiske Undersøgelse Serie A* **12**, 65 pp.
- Johannessen, P.N. & Andsbjerg, J. 1993: Middle to Late Jurassic basin evolution and sandstone reservoir distribution in the Danish Central Trough. In: Parker, J.R. (ed.): Petroleum geology of Northwest Europe: Proceedings of the 4th conference, 271–283. London: Geological Society.
- Johnston, J.H., Collier, R.J. & Maidment, A.I. 1991: Coals as source rocks for hydrocarbon generation in the Taranaki Basin, New Zealand: a geochemical biomarker study. *Journal of Southeast Asian Earth Sciences* **5**(1–4), 283–289.
- Katz, B.J., Kelley, P.A., Royle, R.A. & Jorjorian, T. 1991: Hydrocarbon products of coals as revealed by pyrolysis-gas chromatography. *Organic Geochemistry* **17**(6), 711–722.
- Khorasani, G.K. 1987: Oil-prone coals of the Walloon Coal Measures, Surat Basin, Australia. In: Scott, A.C. (ed.): Coal and

- coal-bearing strata: recent advances. Geological Society Special Publication (London) **32**, 303–310.
- Koch, J.-O. 1983: Sedimentology of Middle and Upper Jurassic sandstone reservoirs of Denmark. In: Kaasschieter, J.P.H. & Reigers, T.J.A. (eds): Petroleum geology of the southeastern North Sea and the adjacent onshore areas. *Geologie en Mijnbouw* **62**, 115–129.
- Korstgård, J.A., Lerche, I., Mogensen, T.E. & Thomsen, R.O. 1993: Salt and fault interactions in the northeastern Danish Central Graben: observations and inferences. *Bulletin of the Geological Society of Denmark* **40**(3–4), 197–255.
- Kosters, E.C. & Suter, J.R. 1993: Facies relationships and systems tracts in the late Holocene Mississippi delta plain. *Journal of Sedimentary Petrology* **63**(4), 727–733.
- Kvalheim, O.M. & Karstang, T.V. 1987: A general-purpose program for multivariate data analysis. *Chemometrics and Intelligent Laboratory Systems* **2**, 235–237.
- Kvalheim, O.M. & Karstang, T.V. 1992: SIMCA - classification by means of disjoint cross validated principal components models. In: Brereton, R.G. (ed.): *Multivariate pattern recognition in chemometrics*, 209–244. New York: Elsevier.
- Lamberson, M.N., Bustin, R.M., Kalkreuth, W.D. & Pratt, K.C. 1996: The formation of inertinite-rich peats in the mid-Cretaceous Gates Formation: implications for the interpretation of mid-Albian history of paleowildfire. *Palaeogeography, Palaeoclimatology, Palaeoecology* **120**, 235–260.
- Larter, S.R. 1985: Integrated kerogen typing in the recognition and quantitative assessment of petroleum source rocks. In: Thomas *et al.* (eds): *Petroleum geochemistry in exploration of the Norwegian Shelf*, 269–286. Norwegian Petroleum Society and Graham and Trotman.
- Levine, J.R. 1993: Coalification: the evolution of coal as source rock and reservoir rock for oil and gas. In: Law, B.E. & Rice, D.D. (eds): *Hydrocarbons from coal*. American Association of Petroleum Geology Studies in Geology **38**, 39–77.
- Liu, S.Y. & Taylor, G.H. 1991: TEM observations on Type III kerogen, with special reference to coal as a source rock. *Journal of Southeast Asian Earth Sciences* **5**(1–4), 43–52.
- Martens, H. & Næs, T. 1991: *Multivariate calibration*, 419 pp. New York: John Wiley.
- Mogensen, T.E., Korstgård, J.A. & Geil, K. 1992: Salt tectonics and faulting in the NE Danish Central Graben. In: Spencer, A.M. (ed.): *Generation, accumulations and production of Europe's hydrocarbons II*. Special Publications of the European Association of Petroleum Geoscientists **2**, 163–173. Berlin Heidelberg: Springer-Verlag.
- Møller, J.J. 1986: Seismic structural mapping of the Middle and Upper Jurassic in the Danish Central Trough. *Danmarks Geologiske Undersøgelse Serie A* **13**, 37 pp.
- Moore, T.A., Shearer, J.C. & Miller, S.L. 1996: Fungal origin of oxidised plant material in the Palangkaraya peat deposit, Kalimantan Tengah, Indonesia: implications for "inertinite" formation in coal. *International Journal of Coal Geology* **30**, 1–23.
- Mukhopadhyay, P.K., Hagemann, H.W. & Gormly, J.R. 1985: Characterization of kerogens as seen under the aspect of maturation and hydrocarbon generation. *Erdöl und Kohle-Erdgas-Petrochemie vereinigt mit Brennstoff-Chemie* **38**, 7–18.
- Murchison, D.G. 1987: Recent advances in organic petrology and organic geochemistry: an overview with some reference to "oil from coal". In: Scott, A.C. (ed.): *Coal and coal-bearing strata: recent advances*. Geological Society Special Publication (London) **32**, 257–302.
- NAM & RGD 1980: Stratigraphic nomenclature of the Netherlands. *Verhandelingen van het Koninklijk Nederlands Geologisch Mijnbouwkundig Genootschap* **32**, 77 pp.
- Nielsen, L.H. 1995: Genetic stratigraphy of Upper Triassic – Middle Jurassic deposits of the Danish Basin and Fennoscandian Border Zone **1, 2, 3**, 162 pp. Unpublished Ph.D. thesis, University of Copenhagen, Denmark.
- Noble, R.A., Wu, C.H. & Atkinson, C.D. 1991: Petroleum generation and migration from Talang Akar coals and shales offshore N.W. Java, Indonesia. *Organic Geochemistry* **17**(3), 363–374.
- Parrish, J.T., Ziegler, A.M. & Scotese, C.R. 1982: Rainfall patterns and the distribution of coals and evaporites in the Mesozoic and Cenozoic. *Palaeogeography, Palaeoclimatology, Palaeoecology* **40**, 67–101.
- Pepper, A.S. & Corvi, P.J. 1995: Simple kinetic models of petroleum formation. Part 1: oil and gas generation from kerogen. *Marine and Petroleum Geology* **12**, 291–319.
- Peters, K.E. 1986: Guidelines for evaluating petroleum source rock using programmed pyrolysis. *American Association of Petroleum Geologists Bulletin* **70**(3), 318–329.
- Peters, K.E. & Moldowan, J.M. 1991: Effects of source, thermal maturity, and biodegradation on the distribution and isomerization of homohopanes in petroleum. *Organic Geochemistry* **17**(1), 47–61.
- Peters, K.E. & Moldowan, J.M. 1993: *The biomarker guide - interpreting molecular fossils in petroleum and ancient sediments*, 363 pp. New Jersey: Prentice Hall.
- Petersen, H.I. 1994: Depositional environments of coals and associated siliciclastic sediments in the Lower and Middle Jurassic of Denmark. The Øresund-5, -7, -13, -15 and -18 wells. *Danmarks Geologiske Undersøgelse Serie A* **33**, 55 pp.
- Petersen, H.I. 1998: Morphology, formation and palaeo-environmental implications of naturally formed char particles in coals and carbonaceous mudstones. *Fuel* **77**(11), 1177–1183.
- Petersen, H.I. & Andsbjerg, J. 1996: Organic facies development within Middle Jurassic coal seams, Danish Central Graben, and evidence for relative sea-level control on peat accumulation in a coastal plain environment. *Sedimentary Geology* **106**, 259–277.
- Petersen, H.I. & Rosenberg, P. 1998: Reflectance retardation (suppression) and source rock properties related to hydrogen-enriched vitrinite in Middle Jurassic coals, Danish North Sea. *Journal of Petroleum Geology* **21**(3), 247–263.
- Petersen, H.I., Bojesen-Koefoed, J.A. & Thomsen, E. 1995: Coal-derived petroleum in the Middle Jurassic Bryne Formation in the Danish North Sea - a new type of play. In: Grimalt, J.O. & Dorronsoro, C. (eds): *Organic geochemistry: developments and applications to energy, climate, environments and human history*. Selected papers from the 17th International Meeting on Organic Geochemistry, Donostia-San Sebastian, Spain, 4–8 September 1995, 473–475.

- Petersen, H.I., Rosenberg, P. & Andsbjerg, J. 1996: Organic geochemistry in relation to the depositional environments of Middle Jurassic coal seams, Danish Central Graben, and implications for hydrocarbon generative potential. *American Association of Petroleum Geologists Bulletin* **80**(1), 47–62.
- Petersen, H.I., Bojesen-Koefoed, J.A., Nytoft, H.P., Surlyk, F., Therkelsen, J. & Vosgerau, H. 1998: Relative sea-level changes recorded by paralic liptinite-enriched coal facies cycles, Middle Jurassic Muslingebjerg Formation, Hochstetter Forland, Northeast Greenland. *International Journal of Coal Geology* **36**, 1–30.
- Phillips, S. & Bustin, R.M. 1996: Sulfur in the Changuinola peat deposit, Panama, as an indicator of the environments of deposition of peat and coal. *Journal of Sedimentary Research* **66**(1), 184–196.
- Phillips, S., Bustin, R.M. & Lowe, L.E. 1994: Earthquake-induced flooding of a tropical coastal peat swamp: a modern analogue for high-sulfur coals? *Geology* **22**, 929–932.
- Philp, R.P. 1994: Geochemical characteristics of oils derived predominantly from terrigenous source materials. In: Scott, A.C. & Fleet, A.J. (eds): *Coal and coal-bearing strata as oil-prone source rocks?* Geological Society Special Publication (London) **77**, 71–91.
- Radke, M., Schaefer, R.G. & Leythaeuser, D. 1980a: Composition of soluble organic matter in coals: relation to rank and liptinite fluorescence. *Geochimica et Cosmochimica Acta* **44**, 1787–1800.
- Radke, M., Willsch, H. & Welte, D.H. 1980b: Preparative hydrocarbon group type determination by automated medium pressure liquid chromatography. *Analytical Chemistry* **52**, 406–411.
- Shanmugam, G. 1985: Significance of coniferous rain forests and related organic matter in generating commercial quantities of oil, Gippsland Basin, Australia. *American Association of Petroleum Geologists Bulletin* **69**(8), 1241–1254.
- Shibaoka, M., Saxby, J.D. & Taylor, G.H. 1978: Hydrocarbon generation in Gippsland Basin, Australia - comparison with Cooper Basin, Australia. *American Association of Petroleum Geologists Bulletin* **62**(7), 1151–1158.
- Snowdon, L.R. 1980: Resinite - a potential source in the Upper Cretaceous/Tertiary of the Beaufort-Mackenzie Basin. In: Miall, A.D. (ed.): *Facts and principles of world oil occurrence*. Canadian Society of Petroleum Geologists Memoir **6**, 421–446.
- Snowdon, L.R. 1991: Oil from Type III organic matter: resinite revisited. *Organic Geochemistry* **17**(6), 743–747.
- Snowdon, L.R. & Powell, T.G. 1982: Immature oil and condensate - modification of hydrocarbon generation model for terrestrial organic matter. *American Association of Petroleum Geologists Bulletin* **66**(6), 775–788.
- Stach, E., Mackowsky, M.-Th., Teichmüller, M., Taylor, G.H., Chandra, D. & Teichmüller, R. 1982: *Stach's textbook of coal petrology*, 535 pp. Berlin-Stuttgart: Gebrüder Borntraeger.
- Stout, S.A. 1994: Chemical heterogeneity among adjacent coal microlithotypes - implications for oil generation and primary migration from humic coal. In: Scott, A.C. & Fleet, A.J. (eds): *Coal and coal-bearing strata as oil-prone source rocks?* Geological Society Special Publication (London) **77**, 93–106.
- Surlyk, F., Arndorff, L., Hamann, N.E., Hamberg, L., Johannessen, P.N., Koppelhus, E.B., Nielsen, L.H., Noe-Nygaard, N., Pedersen, G.K. & Petersen, H.I. 1995: High-resolution sequence stratigraphy of a Hettangian – Sinemurian paralic succession, Bornholm, Denmark. *Sedimentology* **42**, 323–354.
- Thomas, B.M. 1982: Land-plant source rocks for oil and their significance in Australian basins. *Journal of the Australian Petroleum Exploration Association* **22**, 164–178.
- Thomsen, E., Bidstrup, T., Mathiesen, A., Guvad, C. & Bojesen-Koefoed, J.A. 1995: Regional maturity trends and hydrocarbon generation history in the Danish Central Trough. *DGU Datadokumentation* **6**, 69 pp. Copenhagen: Geological Survey of Denmark.
- Underhill, J.R. & Partington, M.A. 1993: Jurassic thermal doming and deflation in the North Sea: implications of the sequence stratigraphic evidence. In: Parker, J.R. (ed.): *Petroleum geology of Northwest Europe: Proceedings of the 4th conference*, 337–345. London: Geological Society.
- van Krevelen, D.W. 1961: *Coal*, 514 pp. Amsterdam: Elsevier.
- Vollset, J. & Doré, A.G. 1984: A revised Triassic and Jurassic lithostratigraphic nomenclature for the Norwegian North Sea. *Norwegian Petroleum Directorate Bulletin* **3**, 53 pp.
- Waples, D.W. & Machihara, T. 1991: Biomarkers for geologists - a practical guide to the application of steranes and triterpanes in petroleum geology. *American Association of Petroleum Geologists Methods in Exploration Series* **9**, 91 pp.
- Wold, S. 1976: Pattern recognition by means of disjoint principal components model. *Pattern Recognition* **8**, 127–139.
- Wold, S. 1978: Cross-validatory estimation of the number of components in factor and principal component model. *Technometrics* **20**, 397–405.
- Ziegler, P.A. 1982: *Geological atlas of Western and Central Europe*, 130 pp. The Hague: Shell Internationale Petroleum Maatschappij BV.
- Ziegler, P.A. 1990: Tectonic and palaeogeographic development of the North Sea rift system. In: Blundell, D.J. & Gibbs, A.D. (eds): *Tectonic evolution of the North Sea rifts*, 1–36. Oxford: Oxford Science Publications.

Danmarks og Grønlands Geologiske Undersøgelse (GEUS)  
*Geological Survey of Denmark and Greenland*  
Thoravej 8, DK-2400 Copenhagen NV  
Denmark

*Danmarks Geologiske Undersøgelse Serie A*

- 1 Råstofkortlægning. Erfaringer fra en forsøgskortlægning ved Ålborg (Mapping of raw material resources. Experiences from a pilot mapping project). 1976. 24 pp. (with abstract in English).  
*By E. Stenestad.* 65.00
- 2 Den geologiske kortlægning af Danmark. Den hidtidige kortlægning – og den fremtidige (The geological mapping of Denmark. The present state of the mapping – proposals for the future mapping). 1978. 79 pp. (with summary and conclusions in English).  
*Edited by H. Sørensen & A. V. Nielsen.* 123.00
- 3 Foreløbige geologiske kort (1:25.000) over Danmark. Forklaring til kortene og vejledning i deres brug (Preliminary geological maps (1:25,000) of Denmark. Explanation to the maps). 1978. 21 pp. (with summary in English).  
*Edited by H. Sørensen & E. Heller.* 65.00
- 4 Geologi på Mols. Rapport udarbejdet for Fredningsplanudvalget for Århus amt (Geology of the Mols area. Report for the Nature Conservancy Committee of Århus Amt, Denmark). 1977. 22 pp. (with abstract in English).  
*By H.W. Rasmussen.* 50.00
- 5 No issue.
- 6 Catalogue of late- and post-glacial macrofossils of Spermatophyta from Denmark, Schleswig, Scania, Halland, and Blekinge dated 13,000 B.P. to 1536 A.D. 1985. 95 pp.  
*By H.A. Jensen.* 123.00
- 7 Dinoflagellate stratigraphy of the uppermost Danian to Ypresian in the Viborg 1 borehole, central Jylland, Denmark. 1985. 69 pp.  
*By C. Heilmann-Clausen.* 123.00
- 8 Seismic stratigraphy and tectonics of sedimentary basins around Bornholm, southern Baltic. 1985. 30 pp.  
*By O.V. Vejbæk.* 140.00
- 9 Middle Jurassic deltaic and coastal deposits in the Lulu-1 well of the Danish Central Trough. 1986. 23 pp.  
*By N. Frandsen.* 50.00
- 10 Petrography of the quartz sand deposits of the Lower Cretaceous of Bornholm, Denmark. 1986. 24 pp.  
*By P. Gravesen.* 91.00
- 11 Seismic stratigraphy and tectonic evolution of the Lower Cretaceous in the Danish Central Trough. 1986. 46 pp.  
*By O.V. Vejbæk.* 152.00
- 12 Jurassic – Lower Cretaceous lithostratigraphic nomenclature for the Danish Central Trough. 1986. 65 pp.  
*By T.F. Jensen, L. Holm, N. Frandsen & O. Michelsen.* 103.00
- 13 Seismic structural mapping of the Middle and Upper Jurassic in the Danish Central Trough. 1986. 32 pp.  
*By J.J. Møller.* 101.00
- 14 Palynology of the Middle Jurassic Lower Graben Sand Formation of the U-1 well, Danish Central Trough. 1986. 25 pp.  
*By T. Hoelstad.* 51.00
- 15 The diagenesis of the Lower Triassic Bunter Sandstone Formation, onshore Denmark. 1986. 51 pp.  
*By S. Fine.* 95.00
- 16 Jurassic – Lower Cretaceous of the Danish Central Trough; – depositional environments, tectonism, and reservoirs. 1987. 45 pp.  
*By O. Michelsen, N. Frandsen, L. Holm, T.F. Jensen, J.J. Møller & O.V. Vejbæk.* 99.00
- 17 Lower Cretaceous dinoflagellate biostratigraphy in the Danish Central Trough. 1987. 89 pp.  
*By C. Heilmann-Clausen. (With a contribution on the *gottschei* ammonite Zone (Hauterivian) in the Adda-2 well by T. Birkelund.)* 132.00
- 18 Diagenesis of the Gassum Formation, Rhaetian – Lower Jurassic, Danish Subbasin. 1987. 41 pp.  
*By H. Friis.* 152.00
- 19 Geochemical investigation of potassium-magnesium chloride mineralization of Zechstein 2 salt, Mors Dome, Denmark. Microthermometry on solid inclusions in quartz crystals. 1987. 48 pp.  
*By J. Fabricius.* 152.00
- 20 Lower Cretaceous calcareous nannofossil biostratigraphy in the Danish Central Trough. 1987. 89 pp.  
*By E. Thomsen.* 152.00



- 21 Palynological zonation and stratigraphy of the Jurassic section in the Gassum No. 1-borehole, Denmark. 1988. 73 pp.  
By K. Dybkjær. 152.00
- 22 Geology of the Søby-Fasterholt area. A paleontological and geological investigation on the Miocene browncoal bearing sequence of the Søby-Fasterholt area, central Jutland, Denmark. 1989. 171 pp. + atlas 121 pp.  
By B.E. Koch. (With contributions by E. Fjeldsø Christensen and Erik Thomsen.) 180.00
- 23 Upper Triassic – Lower Jurassic tidal deposits of the Gassum Formation on Sjælland, Denmark. 1989. 30 pp.  
By L.H. Nielsen, F. Larsen & N. Frandsen. 110.00
- 24 Revision of the Jurassic lithostratigraphy of the Danish Subbasin. 1989. 21 pp.  
By O. Michelsen. 110.00
- 25 Log-sequence analysis and environmental aspects of the Lower Jurassic Fjerritslev Formation in the Danish Subbasin. 1989. 22 pp.  
By O. Michelsen. 110.00
- 26 Stratigraphy and sedimentology of the Zechstein carbonates of southern Jylland, Denmark. 1989. 32 pp.  
By L. Stemmerik & P. Frykman. 110.00
- 27 Geochemical investigation of NaCl-KCl-MgCl<sub>2</sub>-CaCl<sub>2</sub>-FeCl<sub>2</sub> solutions in Zechstein 2 salt, Suldrup Dome, Denmark. Microthermometry on fluid inclusions in halite. 1989. 33 pp.  
By J. Fabricius. 122.00
- 28 Upper Cretaceous (Cenomanian–Santonian) inoceramid bivalve faunas from the island of Bornholm, Denmark. With a review of the Cenomanian–Santonian lithostratigraphic formations and locality details. 1991. 47 pp.  
By K.-A. Tröger & W.K. Christensen. 122.00
- 29 Well records on the Phanerozoic stratigraphy in the Fennoscandian Border Zone, Denmark. Hans-1, Sæby-1, and Terne-1 wells. 1991. 37 pp.  
By O. Michelsen & L.H. Nielsen. 122.00
- 30 Palynological zonation and palynofacies investigation of the Fjerritslev Formation (Lower Jurassic – basal Middle Jurassic) in the Danish Subbasin. 1991. 150 pp.  
By K. Dybkjær. 181.00
- 31 Deep wells in Denmark 1935–1990. Lithostratigraphic subdivision. 1991. 179 pp.  
By L.H. Nielsen & P. Japsen. 350.00
- 32 Megaspore assemblages from the Jurassic and lowermost Cretaceous of Bornholm, Denmark. 1992. 81 pp.  
By E.B. Koppelhus & D.J. Batten. 176.00
- 33 Depositional environments of coals and associated siliciclastic sediments in the Lower and Middle Jurassic of Denmark. The Øresund -5, -7, -13, -15 and -18 wells. 1994. 55 pp.  
By H.I. Petersen. 120.00
- 34 Palaeozoic tectonic and sedimentary evolution and hydrocarbon prospectivity in the Bornholm area. 1994. 23 pp.  
By O.V. Vejrbæk, S. Stouge & K.D. Poulsen. 120.00
- 35 The Hanklit glaciotectionic thrust fault complex, Mors, Denmark. 1995. 30 pp.  
By K.E.S. Klint & S.A.S. Pedersen. 120.00

### *Geology of Denmark Survey Bulletin*

- 36 Petroleum potential and depositional environments of Middle Jurassic coals and non-marine deposits, Danish Central Graben, with special reference to the Søgne Basin. 1998. 78 pp.  
By H.I. Petersen, J. Andsbjerg, J.A. Bojesen-Koefoed, H.P. Nytoft & P. Rosenberg.

Prices are in Danish kroner exclusive of local taxes, postage and handling

The series *Geology of Denmark Survey Bulletin* is a continuation of *Danmarks Geologiske Undersøgelse Serie A* and incorporates *Danmarks Geologiske Undersøgelse Serie B*. These two series were issued by the former Danmarks Geologiske Undersøgelse (DGU) which was merged in 1995 with the former Grønlands Geologiske Undersøgelse (GGU) to form a new national geological survey: Danmarks og Grønlands Geologiske Undersøgelse (The Geological Survey of Denmark and Greenland) with the pet-name GEUS. Two other scientific series are issued by GEUS: *Geology of Greenland Survey Bulletin* and *Geology of Denmark and Greenland Map Series*.